

Cre-loxP based mouse models to study prion pathogenesis in the motor nervous system



Dissertation zur Erlangung des
naturwissenschaftlichen Doktorgrades
der Bayerischen Julius-Maximilians-Universität Würzburg

vorgelegt von
Katja Hochgräfe
aus Melle

Würzburg 2009

Eingereicht am:

Mitglieder der Promotionskommission

Vorsitzender:

Gutachter: Prof. Dr. Michael A. Klein

Gutachter: Prof. Dr. Erich Buchner

Tag des Promotionskolloquiums:

Doktorurkunde ausgehändigt am:

Contents

1	Introduction	7
1.1	Transmissible spongiform encephalopathies	7
1.2	Prion disease of humans and animals	8
1.2.1	Animal prion diseases	8
1.2.2	Human prion diseases	10
1.3	The prion concept	13
1.4	The prion protein (PrP)	15
1.4.1	Primary structure and processing of PrP ^C	15
1.4.2	The physiological function of PrP ^C	16
1.4.3	Structural and biochemical properties of PrP ^C and PrP ^{Sc}	18
1.4.4	Models for prion replication	20
1.5	Prion Pathogenesis	22
1.5.1	Neuroinvasion of prions: the spread of prions from peripheral sites to the CNS	22
1.5.2	Prion-induced neurodegeneration	24
1.6	Dominant-negative effect of PrP polymorphisms	25
1.7	Cre/loxP system	27
1.8	Adeno associated virus vectors	29
2	Aim of the study	31
3	Material	32
3.1	Laboratory equipment and software	32
3.2	Buffers and chemicals	34
3.3	Enzymes and synthetic oligonucleotides	38
3.4	Antibodies	39
3.5	Kits	39
3.6	DNA and Protein molecular weight markers	40
3.7	Cells	40
3.8	Mouse strains	40
3.8.1	C57BL/6	40
3.8.2	<i>Prnp</i> ^{0/0} (Zürich I knockout)	40
3.8.3	<i>Prnp lox2</i>	41
3.8.4	Tga20	42
3.8.5	Tg(SHaPrP) (Tg(SHaPrP)3922- <i>Prnp</i> ^{0/0})	42
3.8.6	NF-L-Cre	42
3.8.7	Hb9-Cre (B6.129S1-Mnx1 ^{tm4(Cre)Tmj/J})	42
3.9	Scrapie inoculum	42

4	Methods	43
4.1	Animal methods	43
4.1.1	Generation of Tg floxed LacZ-PrP ^{Q167R} mice	43
4.1.2	Mating of Tg floxed LacZ-PrP ^{Q167R} mice to Hb9-Cre and NF-L-Cre strains	43
4.1.3	Mating of Lox2 mice to Hb9-Cre and NF-L-Cre strains	44
4.1.4	Tail biopsy and earmarks	44
4.1.5	Intramuscular application of AAV-Cre vectors	44
4.1.6	Scrapie inoculation of mice	44
4.1.7	Bioassay to determine prion infectivity	45
4.1.8	Statistics	45
4.2	Molecular biology techniques	45
4.2.1	Isolation of genomic DNA from tissue samples	45
4.2.2	Determination of the nucleic acid concentration	46
4.2.3	Polymerase chain reaction (PCR)	46
4.2.4	Copy number studies in Tg floxed LacZ-PrP ^{Q167R} mice	48
4.2.5	Restriction enzyme digestion of DNA	50
4.2.6	Agarose gel electrophoresis of DNA	50
4.2.7	Production of adeno-associated virus vectors (dsAAV2-Cre) expressing Cre-recombinase	51
4.3	Cell culture techniques	52
4.3.1	Culture conditions, passaging and seeding of cells	52
4.3.2	Transient calcium-phosphate transfection of 293T cells	52
4.3.3	Fluorescence-activated cell sorting (FACS)	52
4.3.4	X-Gal assay to detect β -galactosidase in 293T cells	53
4.3.5	293T cell lysis for western blot analysis	53
4.4	Biochemical methods	54
4.4.1	Preparation of tissue homogenates	54
4.4.2	Bradford assay to determine of protein concentrations	54
4.4.3	Proteinase-K digestion	54
4.4.4	Peptide-N-glycosidase F (PNGase F) digestion	54
4.4.5	Sodium phosphotungstic acid (NaPTA) precipitation of PrP ^{Sc}	55
4.4.6	SDS polyacrylamid gel electrophoresis	55
4.4.7	Western blotting and immunodetection of proteins	55
4.4.8	Stripping and re-exposure of western blot membranes	56
4.4.9	Densitometric analysis of protein signals	56
4.5	Histological techniques	57
4.5.1	Tissue preparation for histological analysis	57
4.5.2	X-Gal assay to detect β -galactosidase (β -gal)	57

4.5.3 Immunohistochemistry (IHC)	58
5 Results	60
5.1 Transgenic mice with conditional expression of PrP ^{Q167R}	60
5.1.1 Generation and characterization of Tg floxed LacZ-PrP ^{Q167R} mice	60
5.1.2 Survival and pathology of transgenic mice upon prion infection .	77
5.2 Transfer of dsAAV2-Cre into Tg floxed LacZ-PrP ^{Q167R} mice	84
5.3 Prion accumulation in spleen of neuronal PrP deficient mice	88
5.3.1 Characterization of neuronal PrP deficient mice	88
5.3.2 Accumulation of PrP ^{Sc} in spleen and spinal cord of neuronal PrP deficient mice	90
5.3.3 Determination of prion infectivity titers in spleen of neuronal PrP deficient mice	91
6 Discussion	93
6.1 Transgenic mice with conditional expression of PrP ^{Q167R}	93
6.2 Transfer of dsAAV2-Cre into Tg floxed LacZ-PrP ^{Q167R} mice	99
6.3 Prion accumulation in spleen of neuronal PrP deficient mice	101
7 Summary	105
8 Zusammenfassung	107
References	109
9 Supplement	125
9.1 Abbreviations	125
9.2 Units	126
9.3 Resume	128
9.4 Publications	129
9.5 Erklärung	130
9.6 Danksagung	131

1 Introduction

1.1 Transmissible spongiform encephalopathies

Transmissible spongiform encephalopathies or prion diseases are neurodegenerative disorders of the central nervous system (CNS) leading to motor dysfunctions, dementia and death. Among animals the most prominent prion diseases are scrapie in sheep and bovine spongiform encephalopathy (BSE) in cattle. Human prion diseases include Creutzfeldt-Jakob disease (CJD), Kuru, Gerstmann-Sträussler-Scheinker syndrome (GSS) and fatal familial insomnia (FFI). Recently, a new variant of CJD (vCJD) attracted the interest of the public as it was ascribed to the consumption of BSE-contaminated products [Will *et al.*, 1996] and to date has claimed 164 victims until the 3rd August 2009¹.

Prion diseases show up with long incubation times and so far no therapy is available. Moreover a progressive course of the disease is observed, including a slow destruction of the brain, which is accompanied by alterations in behavior, motor impairments and cognitive decline. Beneath the characteristic neuropathological changes, such as spongiform degeneration of the CNS, astrocytic gliosis and neuronal death, the accumulation of amyloid deposits is found frequently but not necessarily in the brains of infected individuals (Fig 1). Neither humoral nor cellular immune responses have been detected in prion disease [Collinge, 2001; Prusiner, 2001].

In contrast to other disorders affecting the brain that are associated with accumulation of aggregated proteins, such as Alzheimer's or Huntington's disease, transmissibility is another hallmark of prion diseases [Tateishi *et al.*, 1996]. The transmission of prion diseases was first demonstrated in 1936, when scrapie was experimentally transmitted to healthy sheep and goats through inoculation [Cuillé and Chelle, 1936]. Thirty years later the human prion disease kuru was also shown to be transmissible [Gajdusek *et al.*, 1966] and in 1961 the infectious agent was successfully transmitted to mice [Chandler, 1961], providing an animal model for prion disease research.

To date it is known that those amyloid deposits, which are found in the brains of prion infected individuals mainly consist of an insoluble protein, designated PrP^{Sc}, which is a misfolded isoform of the endogenous cellular prion protein (PrP^C) [Prusiner, 1989]. Some decades ago most researchers postulated a "slow virus" as the cause of the disease [Sigurdsson, 1954; Gajdusek *et al.*, 1966; Gajdusek, 1977]. Then the remarkable resistance of the infectious agent to conventional sterilization techniques, like exposure to ultraviolet light, heat and even X-ray irradiation, led to the idea that the infectious agent might be devoid of nucleic acids [Alper *et al.*, 1966]. The revolutionary hypothesis that a protein could be the pathogen was first formulated by Griffith in 1967 [Griffith,

¹The National Creutzfeldt-Jakob Disease Surveillance Unit, www.cjd.ed.ac.uk

1967]. Later the protein-only hypothesis was further elaborated by Stanley B. Prusiner, who defined the infectious agent as "proteinaceous infectious particles" (prion). In 1982 he stated that prions are composed largely if not entirely of an abnormal protein [Prusiner, 1982]. Indeed a host gene, encoding for the cellular form of the prion protein (PrP^C), was discovered [Oesch *et al.*, 1985; Chesebro *et al.*, 1985; Basler *et al.*, 1986]. Over the years many studies, such as the generation of PrP knockout mice being resistant to prion infection [Büeler *et al.*, 1992, 1993], contributed to the protein-only hypothesis. In 1997 Prusiner was finally awarded for the Nobel prize in medicine "for his discovery of Prions - a new biological principle of infection".

1.2 Prion disease of humans and animals

1.2.1 Animal prion diseases

Scrapie, a prion disease of sheep and goats, has been recognized in Europe for over 200 years and is still present endemically in many countries. Scrapie was first observed in 1732 and later its experimental transmissibility was shown [McGowan, 1922; Cuillé and Chelle, 1936]. Typical symptoms of scrapie are changes in behavior, hypersensitivity to touch and noise, changes in locomotion (e. g. ataxia of hind limbs), weight loss as well as wool loss through rubbing and scratching [Gaiger, 1924].

Between 1920 and 1958 scrapie became a problem in the Suffolk breed, causing immense financial loss [Bull and Murnane, 1958]. International trade with these sheep was considered to be responsible for the worldwide spread of the disease and led to an increase in scrapie research since the 1930s [Parry, 1962, 1983]. Although scrapie is one of the best characterized prion diseases in animals, so far only little is known about its natural transmission. Today it is generally believed that scrapie is a transmissible disease, which is strongly influenced by host genetics as specific alleles provide resistance or render sheep more susceptible [Belt *et al.*, 1995; Hunter *et al.*, 1996].

Since the first case of bovine spongiform encephalopathy (BSE) was observed in the United Kingdom (UK) in 1986 [Wells *et al.*, 1987], BSE was confirmed in most European countries as well as in Canada, Scandinavia, Israel, Japan and in the USA and developed into a major epidemic. To date more than 184.000 cattle in the UK and more than 5800 cattle worldwide were affected by BSE until the 30th June 2009², provoking a severe food crisis and economic consequences. BSE may originate from sheep scrapie by feeding cattle with inadequately heat-activated meat-and-bone-meal (MBM) derived from scrapie-infected sheep [Wilesmith *et al.*, 1988]. Alternatively, BSE may have been a rare, sporadic disease of cattle, which spread extensively among

²World Organization for Animal Health, www.oie.int/eng/info/en_esbru.htm

the cattle population after the technical protocol for MBM was changed to lower temperatures in 1970 [Wilesmith *et al.*, 1991]. Independent of the source, it is very likely that MBM served as vehicle of transmission from cattle to cattle. As a consequence of these findings "The Ruminant Feed Ban of 18th July 1988" was concluded and export of cattle from the UK to other European countries was forbidden in 1989. Simultaneous to the BSE epidemic, new TSEs of ruminant species in zoos and also in domestic and captive wild cats were identified. Some of these have been confirmed to be caused by BSE-contaminated MBM [Jeffrey and Wells, 1988; Kirkwood *et al.*, 1990]. Moreover transmission of BSE to humans was described [Hill *et al.*, 1997; Collinge, 2001] and has caused about 164 cases of a new variant of CJD³. Although BSE seems to have widely spread via the food chain, prion disease have never been observed in dogs or birds [Matthews and Cooke, 2003] and feeding of pigs with BSE contaminated material did not cause the disease [Dawson *et al.*, 1990; Wells *et al.*, 2003].

Beside scrapie and BSE, several other prion diseases of animals have been described (Tab 1), including transmissible mink encephalopathy [Marsh and Hadlow, 1992], chronic wasting disease of deer and elk [Williams and Young, 1980] and feline spongiform encephalopathy in domestic cats [Wyatt *et al.*, 1991]. All these prion diseases present with alterations in behavior like enhanced aggressiveness, stereotypical scraping and motor impairments and most of them are most likely transmitted via the oral route.

Table 1: Animal prion diseases.

Disease	Species	Transmission
Scrapie	sheep goat	oral vertical, horizontal sporadic (?)
Bovine spongiform encephalopathy (BSE)	cattle other ruminants	oral sporadic (?)
Transmissible mink encephalopathy (TME)	mink	oral (cattle MBM)
Chronic wasting disease (CWD)	deer elk	possibly similar to scrapie
Feline spongiform encephalopathy (FSE)	domestic cats wild cats (zoo)	oral (cattle MBM)

³until 3rd August 2009; The National Creutzfeldt-Jakob Disease Surveillance Unit, www.cjd.ed.ac.uk

1.2.2 Human prion diseases

Human prion disease include Creutzfeldt-Jakob disease (CJD), Kuru, fatal familial insomnia (FFI) and Gerstmann-Sträussler-Scheinker syndrome (GSS). According to their etiology, they are further divided into sporadic, acquired and inherited forms (Tab 2). Although prion diseases of humans are not contagious, the transmissibility of human prion disease was proofed experimentally. Kuru was transmitted by intracerebral inoculation of infected brain homogenates into chimpanzees [Gajdusek *et al.*, 1966], later transmission studies of CJD and GSS led to the concept of "transmissible dementias" [Gibbs *et al.*, 1968; Masters *et al.*, 1981]. In addition to transmissibility and similar clinical symptoms, human and animal prion diseases also share common neuropathological features like spongiform vacuolization of the CNS, astrocytic proliferation, neuronal loss and the presence of amyloid plaques (Fig 1).

Classical or sporadic Creutzfeldt-Jakob disease (sCJD) was first described in 1920 by H. G. Creutzfeldt and A. M. Jakob [Creutzfeldt, 1920; Jakob, 1921]. sCJD is the most common human prion disease with an annual incidence of one per million [Masters *et al.*, 1979]. sCJD most frequently affects aged people of about 55-75 years, showing a disease duration of less than one year. Typical symptoms of sCJD are a rapid, progressive dementia with speech impairments, myoclonus, coordination dysfunctions and seizures. How prions spontaneously evolve in sCJD patients is so far unknown. Neither a genetic predisposition nor any signs of an infection were found [Collinge, 2001].

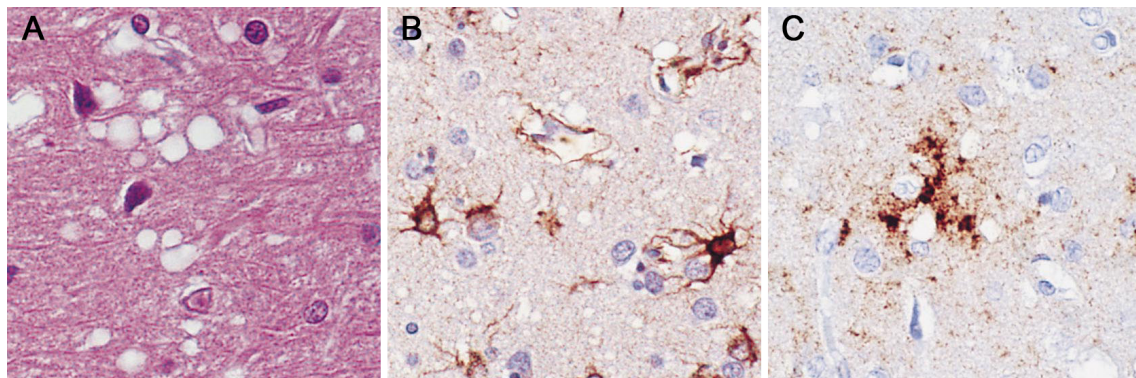


Figure 1: Characteristic neuropathological features of transmissible spongiform encephalopathies. (A) Grey matter of the brain of a CJD patient stained with hematoxylin–eosin (HE) displaying the characteristic spongiform, vacuole-like morphology. (B) Activation and proliferation of reactive, swollen astrocytes is visualized by staining with antibodies against glial fibrillary acidic protein (GFAP, brown). (C) Immunohistochemical staining using anti-PrP antibodies shows prion protein deposits (brown colour). Adapted from [Glatzel and Aguzzi, 2001].

Acquired human prion disease include Kuru, iatrogenic CJD (iCJD) and a recently described new variant of CJD (vCJD). Kuru is a neurodegenerative disease characterized by progressive ataxia and dementia and long incubation periods (>40 years) [Gajdusek and Zigas, 1957; Collinge *et al.*, 2006]. It was observed among the Fore population living in the Eastern Highlands of Papua New Guinea in the 1950s. Kuru was transmitted during cannibalistic feasts, when deceased Kuru-affected relatives were consumed by the community [Gajdusek, 1977]. Kuru is believed to have originated from a random, sporadic CJD case among the Fore [Alpers and Rail, 1971]. Consequently the recycling of prions by cannibalism among the isolated population led to a Kuru epidemic and was a major cause of death of Fore people.

Iatrogenic transmission of CJD occurred mainly from human to human via medical accidents. Most of these cases are due to injection of cadaverous human growth hormone and transplantation of dura mater [Brown, 1988; Brown *et al.*, 2000]. However, also transmission via transplantation of cornea, usage of prion-contaminated neurosurgical instruments and brain electrodes was described [Duffy *et al.*, 1974; Bernoulli *et al.*, 1977].

Variant CJD (vCJD) was first described in 1995 and 1996, when some cases of remarkably young CJD patients with an untypical clinical phenotype were identified [Will *et al.*, 1996]. In contrast to sCJD a prolonged disease duration of 13-14 month is observed. Moreover the median age of disease onset with 28 years is reduced and vCJD patients show predominantly psychiatric disturbances in comparison to sCJD. Similar to the late phase of classical CJD, all vCJD patients develop ataxia, which is followed by a progressive dementia [Zeidler *et al.*, 1997a, b].

The sudden increase in CJD cases in the UK in the early 1990s, parallel to the BSE epidemic, led to the idea that these cases might be related to BSE-exposure, in particular to ingestion of BSE-contaminated food products [Will *et al.*, 1996]. Later this hypothesis was supported by lots of studies. It was shown that mice, sheep and non-human primates can be experimentally infected by BSE-contaminated material by the oral route [Maignien *et al.*, 1999; Jeffrey *et al.*, 2001; Ridley and Baker, 1996; Bons *et al.*, 1999]. Moreover transmission characteristics, incubation times and lesion profiles as well as glycosylation pattern of vCJD and BSE in the same inbred mouse strains are similar [Hill *et al.*, 1997; Bruce *et al.*, 1997; Scott *et al.*, 1999], providing strong evidence that the agent causing vCJD is the same as the agent causing BSE. To date 164 cases of vCJD have been confirmed⁴. Although most of these cases are related to consumption of BSE-infected material at least two vCJD cases have been transmitted by blood transfusion [Llewelyn *et al.*, 2004; Peden *et al.*, 2004], leading to a debate concerning the biosafety of medical products and to efforts of developing adequate test systems.

⁴until 3rd August 2009; The National Creutzfeldt-Jakob Disease Surveillance Unit, www.cjd.ed.ac.uk

10% of all human prion diseases are inherited and related to different mutations of the *Prnp* gene, encoding for the cellular prion protein. More than 50 point- and missense mutations are known for *Prnp*, which are inherited autosomal dominantly [J. Gerstmann, 1936]. Hereditary human prion diseases have various characteristics. While GSS presents classically as a cerebellar ataxia and dementia around the age of 45 with a mean duration of about 5 years, familiar CJD (fCJD) shows a much shorter disease duration [Haltia et al., 1979]. Massive sleep disturbances, neuronal loss and gliosis in the thalamus are characteristic for FFI, a recently described inherited human prion disease [Medori et al., 1992]. Various *Prnp* mutations are described for fCJD [Kovács et al., 2002], while GSS frequently present a P102L mutation in addition to various other *Prnp* mutations [Hsiao et al., 1989]. In FFI a D178N mutation together with 129 M/M homozygosity is observed [Goldfarb et al., 1992; Medori et al., 1992].

Table 2: Human prion diseases.

Disease	Etiology	Transmission
sporadic Creutzfeldt-Jakob disease (sCJD)	sporadic	conversion of PrP ^C to PrP ^{Sc}
iatrogenic Creutzfeldt-Jakob disease (iCJD)	acquired	iatrogenic transmission (contaminated medical products and instruments)
familiar Creutzfeldt-Jakob disease (fCJD)	hereditary	various <i>Prnp</i> mutations
variant Creutzfeldt-Jakob disease (vCJD)	acquired	transmission by consumption of BSE-contaminated products or from human to human e.g. via blood transfusion
Kuru	acquired	sporadic CJD case among the Fore; transmission via endocannibalism
Gerstmann-Sträussler-Scheinker syndrome (GSS)	hereditary	various <i>Prnp</i> mutations (frequently P102L)
fatal familial insomnia (FFI)	hereditary	<i>Prnp</i> mutation D178N and 129 M/M
Protease-sensitive prionopathy (PSPr)	unknown	unknown

Even in non-hereditary human prion disease the susceptibility of humans to prion diseases is strongly influenced by the host genetics. In particular methionine / methionine (M/M) homozygosity at codon 129 of the *Prnp* gene plays an important role in prion susceptibility. 129 M/M homozygosity is found in most sCJD cases and is associated with a shorter incubation time in Kuru [Lee *et al.*, 2001; Windl *et al.*, 1996]. In addition almost all tested vCJD cases were 129 M/M homozygous [Collinge *et al.*, 1996; Hill *et al.*, 1999].

Recently a new class of prion disease, called protease-sensitive prionopathy (PSP) was described. In comparison to other human prion disease, PSP display a different histopathology and only small amounts of misfolded PrP are found in brains of affected individuals. According to the authors PSP might have been overlooked so far and classified as non-Alzheimer's dementias [Gambetti *et al.*, 2008].

1.3 The prion concept

The nature of the infectious agent, responsible for prion disease, was ambiguous for a long time. In 1936 transmission studies of the scrapie agent to healthy sheep and goats were successful but very long incubation periods were observed [Cuillé and Chelle, 1936]. This led to the conclusion that the infection might be caused by a "slow virus" with long replication cycles [Sigurdsson, 1954; Gajdusek *et al.*, 1966; Gajdusek, 1977]. On the contrary several studies proofed a remarkable resistance of the agent against conventional sterilization techniques. The infectivity of the agent was not reduced by procedures known to damage nucleic acids, such as ultraviolet light, X-ray irradiation or treatment with nucleases. Surprisingly, procedures known to modify or hydrolyze proteins, like treatment with urea, sodium hydroxide or digestion with proteinase K or trypsin, led to an inactivation of the infectious agent [Alper *et al.*, 1966, 1967; Prusiner *et al.*, 1981]. These findings led to the very unconventional hypothesis that the infectious agent might be devoid of nucleic acids [Griffith, 1967]. In 1982 S. Prusiner purified infectious material from scrapie infected hamster brain and showed that the extract was capable of forming amyloid structures *in vitro*, which were very similar to the deposits found in scrapie-infected brains [Bolton *et al.*, 1982; Prusiner, 1982; McKinley *et al.*, 1983; DeArmond *et al.*, 1985]. In order to distinguish this new class of pathogens from viruses and bacteria, he introduced the term "**proteinaceous infectious particles**" (prion) and stated that the infectious agent is composed largely if not entirely of a single protein that can replicate without the use of nucleic acids ("protein-only" hypothesis) [Prusiner, 1982].

Shortly afterwards amino acid sequencing led to the identification of the N-terminal sequence of the prion protein (PrP), which was extracted from infected brains [Prusiner *et al.*, 1984]. The usage of molecular gene probes finally led to the identification of

a host encoded single-copy chromosomal gene, which was expressed to the same extent in scrapie-affected as well as in healthy hamsters. Later the gene encoding for PrP was also discovered in mice, human and many other mammalian species [Oesch *et al.*, 1985; Chesebro *et al.*, 1985]. From these findings it was concluded that PrP might exist in two different forms. Although no differences in the primary structure of PrP, isolated from infected or healthy brains, was observed [Basler *et al.*, 1986]. It turned out that the infectious form of PrP was protease-resistant while the normal form of PrP was not [Meyer *et al.*, 1986]. Finally it became clear that the infectious form of PrP is a variant of a cellular protein. Therefore the normal, healthy form of the prion protein was called "cellular PrP" (PrP^C) and the infectious (protease-resistant) form "PrP-scrapie" (PrP^{Sc}). Furthermore it was assumed that PrP^C and PrP^{Sc} only differ in their conformation and it was proposed that PrP^{Sc} acts as a template that promotes the conversion of PrP^C to PrP^{Sc} [Pan *et al.*, 1993; Cohen *et al.*, 1994].

The generation of PrP deficient (*Prnp*^{0/0}) mice strongly supported the "protein-only" hypothesis. *Prnp*^{0/0} mice are completely resistant to prion infection, but the introduction of a PrP encoding transgene can restore their susceptibility [Büeler *et al.*, 1992, 1993; Whittington *et al.*, 1995; Fischer *et al.*, 1996]. Thus, PrP^C is required for prion propagation. Moreover polyclonal antibodies, directed against PrP were found to neutralize scrapie infectivity [Gabizon *et al.*, 1988] and the conversion of PrP^C into protease-resistant PrP^{Sc} was shown *in vitro* after co-cultivation of both forms [Kocisko *et al.*, 1994]. Recently amyloid-like fibrils, consistent of recombinant PrP, caused scrapie-typical symptoms in distinct transgenic mice. As the incubation period of these transgenic mice was extremely long and inoculation of wild-type mice did not cause a disease, it remains unclear if "de novo" infectivity was really generated [Legname *et al.*, 2004]. To date, no prion-specific nucleic acid was identified [Bellinger-Kawahara *et al.*, 1987a, b].

Although the "protein-only" hypothesis is widely accepted today, it does not explain how a single pathogenic protein can encode for a variety of strain-specific characteristics observed in prion disease. Those strain-specific characteristics include variation in incubation periods, neuropathology and lesion profiles as well as differences in transmissibility and biochemical properties such as the glycoprofile of PrP^{Sc} or inactivation behavior. Although most parameters are defined for each prion disease and species, the molecular basis of prion strains remains elusive [Aguzzi *et al.*, 2007].

1.4 The cellular prion protein (PrP^C) and its conversion into the pathological isoform PrP^{Sc}

1.4.1 Primary structure and processing of PrP^C

The cellular prion protein (PrP^C) is highly conserved in mammals and is expressed at high levels throughout adult life, predominantly in the CNS [Schätzl *et al.*, 1995; Wopfner *et al.*, 1999]. PrP^C is expressed in neurons [Kretzschmar *et al.*, 1986] but also in astrocytes and oligodendrocytes [Moser *et al.*, 1995] as well as in non-neuronal tissues including blood lymphocytes [Brown *et al.*, 1999b; Burthem *et al.*, 2001; Liu *et al.*, 2001], gastroepithelial cells [Morel *et al.*, 2004], heart, kidney and muscle [Brown *et al.*, 1998]. PrP is encoded by a single-copy gene *Prnp*, which consists of 3 exons and is located on chromosome 2 [Sparkes *et al.*, 1986]. The coding sequence of *Prnp* is restricted to exon 3. In case of murine *Prnp*, the translation of exon 3 results in a 254 amino acid (aa) protein (Fig 2) [Basler *et al.*, 1986].

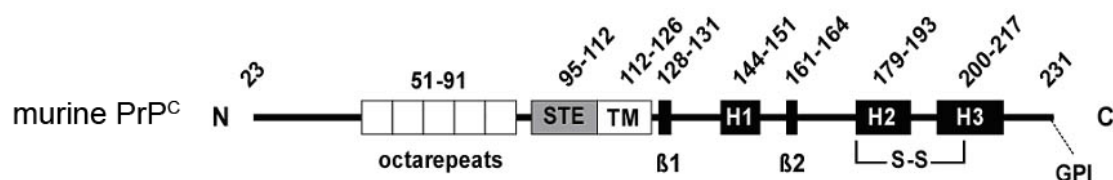


Figure 2: Primary structure of murine PrP^C. Adapted from [Flechsigg and Weissmann, 2004].

The translation of PrP^C starts at the endoplasmic reticulum (ER), from where it proceeds to the Golgi apparatus and is finally exported to the cell surface. During its biosynthesis, PrP^C undergoes several post-translational modifications [Caughey, 1991]. A leader sequence of 22 aa is cleaved off the N-terminus to translocate PrP^C into the ER [Oesch *et al.*, 1985; Basler *et al.*, 1986], where the asparagine residues 180 and 196 are glycosylated [Haraguchi *et al.*, 1989] and a disulphide bond is formed between the cysteines 178 and 213 [Hope *et al.*, 1986; Safar *et al.*, 1998]. Using the secretory pathway, PrP^C passes the Golgi apparatus and the protein reaches the plasma membrane, where 24 hydrophobic residues of the C-terminus are removed [Stahl *et al.*, 1987]. Finally, PrP^C is attached to the outer leaflet of the membrane by a glycosphosphatidylinositol anchor (GPI) [Stahl *et al.*, 1987]. On the cell surface, PrP^C is enriched in distinct microdomains (lipid rafts) [Vey *et al.*, 1996], which are characterized by a high cholesterol content [Simons and Ikonen, 1997], or is associated with clathrin-coated pits [Shyng *et al.*, 1994]. From the cell surface PrP^C is internalized by endocytosis and again recycled to the cell surface or degraded [Shyng *et al.*, 1993]. The relevance of this PrP recycling process is currently unknown and discussed controversially. Mature PrP^C exhibits a flexible, non-structured N-terminus and a globular

C-terminal domain. Another characteristic feature, located in the flexible N-terminus, is the presence of the so-called octarepeat domain (aa 51-91) [Brown *et al.*, 1997]. The octarepeat domain contains five repetitive sequences (PQGGTWGQ) and is capable of binding copper ions. In addition a stop-transfer region (STE, aa 95-112) and a hydrophobic trans-membrane sequence (TM, aa 112-126) are described [Nakahara *et al.*, 1994].

1.4.2 The physiological function of PrP^C

PrP^C is a highly conserved protein among mammals and other species. The presence of PrP^C in neuronal tissue and also in a variety of other tissues indicates an important physiological function of the protein. Many approaches have been used to understand the physiological function of PrP^C, including identification of PrP^C interaction partners, human genetic studies of the *Prnp* gene, over-expression of PrP^C in different cell types and organisms and finally *Prnp* knockout strategies in mice [Linden *et al.*, 2008].

The most strikingly phenotype of *Prnp*^{0/0} mice is their resistance to prion infection, which can be restored upon re-introduction of PrP encoding transgenes. From these studies it became clear that PrP^C expression is required for prion induced toxicity [Büeler *et al.*, 1993, 1994; Sailer *et al.*, 1994]. Apart from that, an altered circadian rhythm and sleep disturbances were documented for *Prnp*^{0/0} mice [Tobler *et al.*, 1996, 1997]. These studies suggest that PrP^C might be involved in the regulation of sleep, as sleep deficits are also observed in several human prion diseases, like sCJD and FFI [Lugaresi *et al.*, 1998; Landolt *et al.*, 2006]. Also different behavioral phenotypes of *Prnp*^{0/0} mice were described. Beside cognitive defects and memory impairment, increased locomotor and decreased anxiety were reported [Roesler *et al.*, 1999; Coitinho *et al.*, 2003; Criado *et al.*, 2005; Nico *et al.*, 2005]. Moreover differences in neuronal excitability, such as impairments in long-term potentiation (LTP) and increased susceptibility to seizures were reported in PrP deficient mice [Collinge *et al.*, 1994; Walz *et al.*, 1999]. Later it was shown that neurons of the hippocampus are disorganized and show diminished sensitivity to arriving action potentials, suggesting a role for PrP^C in calcium homeostasis [Colling *et al.*, 1996].

Recently it was demonstrated that *Prnp*^{0/0} mice show an altered behavior in olfactory tasks and a disrupted electrophysiology in the deep layers of the main olfactory bulb. As both alterations could be rescued by transgenic neuronal specific expression of PrP^C, it was suggested that PrP^C might be important in the normal processing of sensory information by the olfactory system [Pichon *et al.*, 2009].

Copper ions (Cu²⁺) are important co-factors for many enzymatic processes and many cells have evolved a special mechanisms for Cu²⁺ uptake and transport. PrP^C is known to bind Cu²⁺ at the octapeptide region (histidine 96 and 111) and facilitates Cu²⁺

endocytosis [Jackson *et al.*, 2001; Pauly and Harris, 1998]. Moreover a decreased Cu^{2+} content was measured in *Prnp*^{0/0} mice [Brown *et al.*, 1997]. Therefore it was proposed that PrP^C might play a role in copper metabolism.

A protective function of PrP^C as Cu/Zn superoxide dismutase (SOD-1) was described, suggesting that PrP^C might be involved in defense against oxidative stress [Brown *et al.*, 1999a]. The study was confirmed by another group, showing that SOD-1 activity was reduced in *Prnp*^{0/0} mice [Wong *et al.*, 2001]. However, Waggoner *et al.* were not able to reproduce the results and mouse genetic experiments argue against a SOD-like activity *in vivo* [Hutter *et al.*, 2003; Waggoner *et al.*, 2000].

As PrP^C is a GPI-anchored cell surface protein, a function of PrP^C in signal transduction was proposed [Stahl *et al.*, 1987]. Indeed, several interaction partners of PrP^C were identified. Using the yeast two-hybrid system, a direct binding of PrP^C to a precursor of the laminin receptor was shown [Rieger *et al.*, 1997; Gauczynski *et al.*, 2006]. Alternative interaction partners are caveolin-1 [Mouillet-Richard *et al.*, 2000] and the cell adhesion molecule N-CAM, showing increased activity of Fyn kinase [Schmitt-Ulms *et al.*, 2001] and leading to enhanced axonal outgrowth in cell culture [Graner *et al.*, 2000; Santuccione *et al.*, 2005]. Recently it was shown that oligomers of the Alzheimers amyloid- β peptide (A β 42) bind to PrP^C with nanomolar affinity. Moreover A β 42 inhibited PrP^C-dependent LTP, suggesting a A β 42-PrP^C signalling pathway responsible for synaptic plasticity [Laurén *et al.*, 2009].

Further interaction partner of PrP^C are the heat-shock protein STI-1 and Hsp60 [Edenhofer *et al.*, 1996; Zanata *et al.*, 2002] as well as to the anti-apoptotic factor Bcl-2 [Kurschner and Morgan, 1995]. Although a physiological relevance of these interactions seem to be marginal because PrP^C is not expressed in the same compartments *in vivo*, a neuroprotective function of PrP^C is discussed [Westergard *et al.*, 2007].

Since it was demonstrated that PrP^C is expressed on the surface of hematopoietic stem cells and a decreased proliferation of neuronal precursors was observed in *Prnp*^{0/0} mice, a role for PrP^C in stem and progenitor cell biology was proposed [Zhang *et al.*, 2006; Steele *et al.*, 2006].

1.4.3 Structural and biochemical properties of PrP^C and PrP^{Sc}

Although PrP^C and PrP^{Sc} exhibit identical primary structures and post-translational modifications, they differ in their biochemical properties and display different secondary protein structures (Tab 3). While PrP^C is a non-infectious, soluble and protease-sensitive protein of 33-35 kDa, the infectious isoform PrP^{Sc} shows a partial resistance to proteinase K (PK) and is insoluble in non-ionic detergents [Cohen and Prusiner, 1998]. The digestion of murine PrP^{Sc} with PK results in a 27-30 kDa fragment, as 90 aa are cleaved from the N-terminus [Oesch *et al.*, 1985].

According to its size and partial PK-resistance this fragment is called PrP²⁷⁻³⁰ or alternatively PrP^{res} [Bolton *et al.*, 1982]. Moreover PrP^{Sc} tends to aggregate, leading to the formation of amyloid plaques. Upon purification and enrichment of infectivity from prion infected hamster brain homogenates, the appearance of amyloid fibrils ("prion rods") is observed. Prion rods are insoluble in aqueous solutions as well as in organic or non-ionic detergents [McKinley *et al.*, 1991].

Furthermore PrP^C and PrP^{Sc} show different secondary structures. Different spectroscopic techniques, like fluorescence emission, circular dichroism and infrared spectroscopy were applied to solve the structure of PrP. The data showed that PrP^C is rich in α -helical structure [Baldwin *et al.*, 1994; Pan *et al.*, 1993; Pergami *et al.*, 1996], while PrP^{Sc} has a higher β -sheet content [Gasset *et al.*, 1993; Caughey and Raymond, 1991; Safar *et al.*, 1993]. The structure of recombinant PrP^C, produced in *Escherichia coli*, was also determined by nuclear magnetic resonance (NMR). The C-terminal region consists of 3 α -helices and 2 anti-parallel β -sheets flanking helix 1, while the flexible N-terminus of PrP^C (aa 23-120) is random coiled (Fig 3) [Hornemann *et al.*, 1997; Riek *et al.*, 1997]. It is likely that the N-terminus is stabilized upon binding of copper ions [Jones *et al.*, 2004; Leclerc *et al.*, 2006].

Table 3: Biochemical and structural properties of different PrP isoforms.

	PrP ^C	PrP ^{Sc}	PrP ²⁷⁻³⁰
Infectivity	not infectious	infectious	infectious
Protease-resistance	sensitive	partial resistance	resistant
Solubility	soluble	insoluble	insoluble
Half-life time	2-4h	> 24h	> 24h
Molecular weight	33-35 kDa	27-35 kDa	27-30 kDa
State of aggregation	monomer, dimers, oligomers	dimers, aggregates	amyloid fibrils
Secondary structure	42% α -helical, 3% β -sheet	30% α -helical, 43% β -sheet	21% α -helical, 54% β -sheet

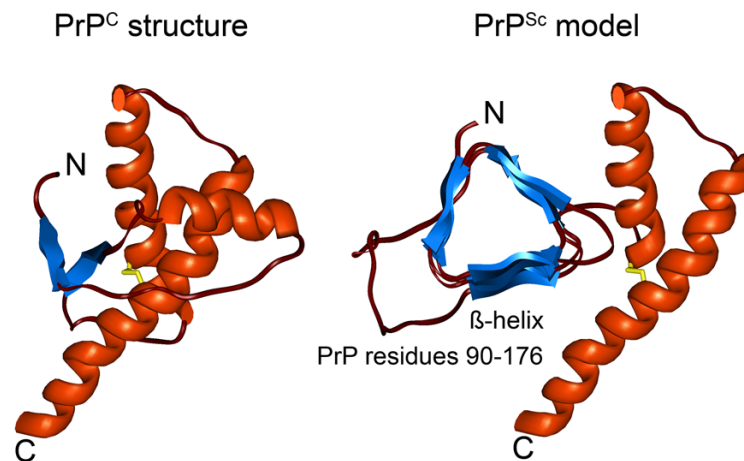


Figure 3: Nuclear magnetic resonance (NMR) structure of PrP^C (residues 121-231) and the corresponding model of PrP^{Sc}. The structure of PrP^C contains 3 α -helices (red) and 2 β -sheets (blue). The disulphide bond, connecting helix 2 and 3 is shown in yellow. PrP^{Sc} is rich in β -sheet structures. The model shows that helix 1 is replaced by several β -sheets, which are coiled up to form a β -helix, while helix 2 and 3 remain stable. Adapted from [Eghiaian, 2005].

Due to its extreme insolubility, an NMR-structure of PrP^{Sc} is still lacking. However, a theoretical model of the structure of PrP^{Sc} exists. In this model, helix 1 is replaced by 4 β -sheets, while helix 2 and 3 are preserved [Huang *et al.*, 1996]. Recent studies of 2D-crystals, which were obtained from PrP²⁷⁻³⁰ molecules, revealed that helix 1 and both related β -sheets (residues 98-175) are more likely changed into a left-handed β -helix. In this model helix 2 and 3, which are connected via the disulphide bond are preserved as well as the flexible N-terminus. Thus, three molecules are able to form a trimer with β -helical structures in the center. Finally, several of these trimers can build up a fibril or so-called "prion-rod" (Fig 4) [Wille *et al.*, 2002; Govaerts *et al.*, 2004].

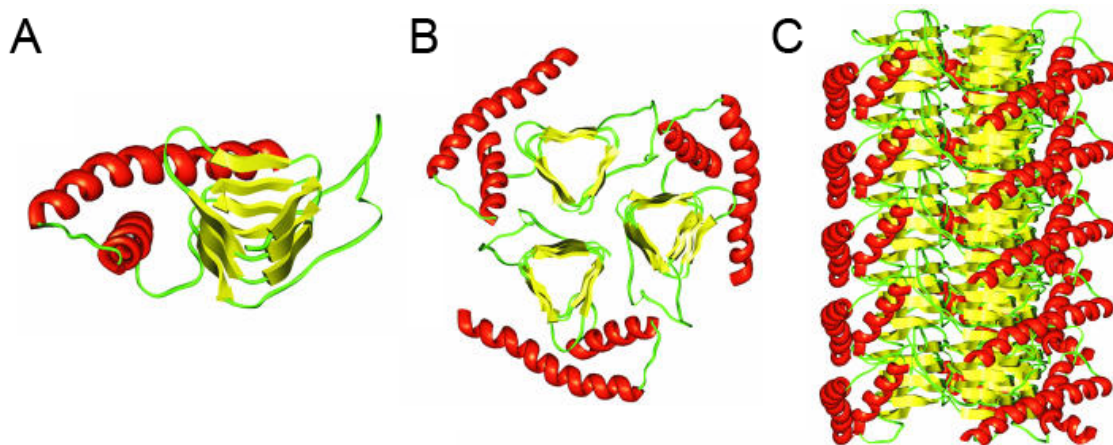


Figure 4: Model of PrP^{Sc} aggregation. (A) PrP^{Sc} monomer, displaying a β -helical structure and two α -helices. (B) Formation of a PrP^{Sc} trimer. (C) PrP^{Sc} trimers build up a fibril or so called "prion-rod". Adapted from [Govaerts *et al.*, 2004].

1.4.4 Models for prion replication

The replication of the pathological PrP isoform plays a central role in prion pathogenesis. Prions are believed to replicate by an autocatalytic, PrP^{Sc} dependent conversion of PrP^C to PrP^{Sc} [Prusiner, 1989]. To date the cellular localization of prion replication is still elusive. Several studies suggest endosomal or lysosomal compartments, while other findings propose lipid rafts inside the plasma membrane as site of prion replication [Mayer *et al.*, 1992; Arnold *et al.*, 1995; Baron and Caughey, 2003; Botto *et al.*, 2004; Marijanovic *et al.*, 2009].

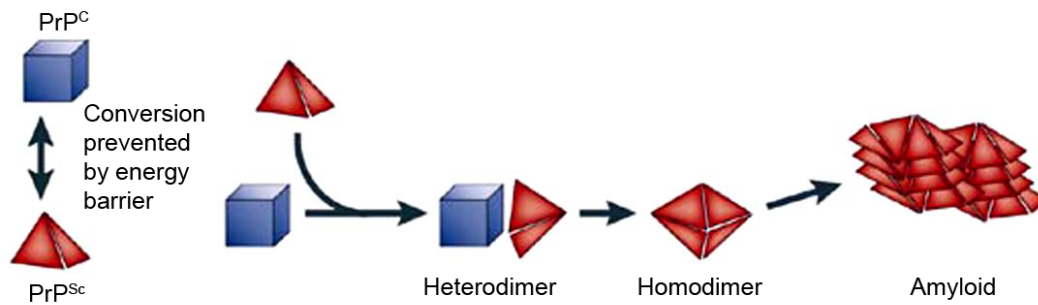
Currently, two different models are postulated for the conversion process. The refolding model or "heterodimer" model (Fig 5a) postulates an interaction of exogenously introduced PrP^{Sc} (e.g. upon prion infection) and endogenous PrP^C. After binding of PrP^{Sc} to a partially unfolded PrP^C molecule, a heterodimer is formed and PrP^C adapts the conformation of PrP^{Sc}. The reaction scheme represents a linear autocatalysis with an exponential formation rate of PrP^{Sc}. However, in normal conditions a spontaneous conversion of PrP^C into PrP^{Sc} is prevented by a high energy barrier [Prusiner, 1991]. This assumption would be in good agreement with the finding, that spontaneous prion diseases are extremely rare. Furthermore the heterodimer model could explain the existence of inherited prion diseases, as a point-mutation could lower the energy barrier and thus enhance the conversion frequency. Moreover a cellular factor X, displaying a chaperon-like function, was postulated to facilitate the conversion reaction, but to date no factor X could be identified [Telling *et al.*, 1995].

Another model for prion replication is the "seeding" or nucleation-polymerization model (Fig 5b). The seeding model assumes the existence of a thermodynamic equilibrium between PrP^C and PrP^{Sc} with PrP^C being the favored state. Once a seed or nucleus has been formed, the growth of the aggregates is faster than their dissociation rate. As a consequence, more and more PrP^{Sc} is formed and can aggregate to infectious seeds and further to amyloid-like deposits. Finally a fragmentation of PrP^{Sc} deposits increases the number of infectious seeds, leading to a chain reaction of replication [Come *et al.*, 1993; Caughey *et al.*, 1995].

The seeding model might explain the existence of different prion strains, each characterized by an individual lesion profile, distinct incubation periods and neuropathology [Aguzzi *et al.*, 2007]. The specific properties of the different strains could be encoded and transmitted by such polymerized aggregates. It was shown that the conversion of recombinant PrP is possible *in vitro*, while strain-specific characteristics are preserved [Bessen *et al.*, 1995; Kocisko *et al.*, 1994]. Moreover the protein misfolding cyclic amplification technique (PMCA) supports the seeding model. During PMCA, a brain homogenate of a healthy animal is once seeded with a small amount of PrP^{Sc}-containing material. The seed initiates the replication of PrP^{Sc}. Each round of PMCA is termi-

nated with a sonification step, leading to a fragmentation of formed PrP^{Sc}-aggregates and the generation of new seeds. Thus, after several rounds of PMCA an exponential multiplication is achieved without further addition of infectious material [Saborio *et al.*, 2001].

a) "Refolding" model



b) "Seeding" model

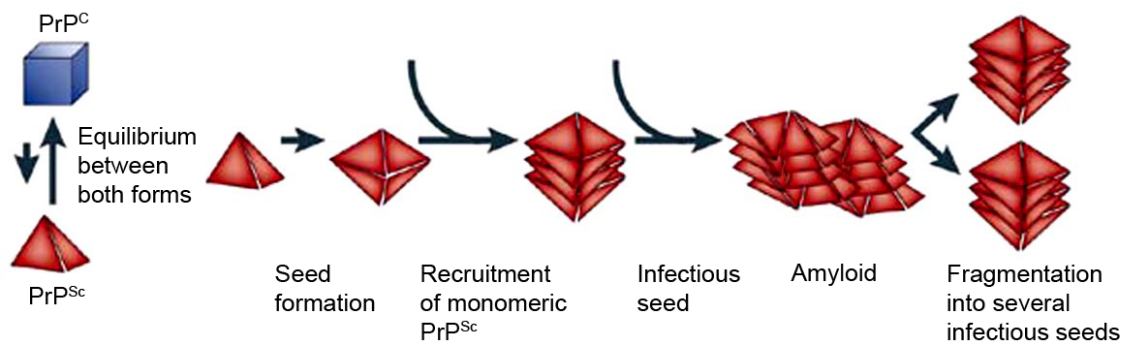


Figure 5: Models for the conversion of PrP^C into PrP^{Sc}. (a) Due to the refolding model, a spontaneous conversion of PrP^C to PrP^{Sc} is inhibited by a high energy barrier. Upon introduction of exogenous PrP^{Sc}, a heterodimer is formed and catalyzes the conversion process. (b) According to the seeding model, PrP^C and PrP^{Sc} are in an equilibrium with PrP^C as favored state. Once a seed has formed, the conformation of PrP^{Sc} is stabilized and monomeric PrP^{Sc} is recruited, leading to an equilibrium shift and PrP^{Sc} aggregation. Fragmentation of PrP^{Sc} deposits enhances the number of infectious seeds. Adapted from [Aguzzi and Polymenidou, 2004].

1.5 Prion Pathogenesis

1.5.1 Neuroinvasion of prions: the spread of prions from peripheral sites to the CNS

Although the distribution of the infectious agent in the tissue of the infected host is quite variable, the spread of prions through the body is characterized by several phases: after oral uptake prions spread from the intestine to lymphoid tissues and via the peripheral nervous system (PNS) the infectious agent ascends to the CNS. Prion replication and accumulation in the CNS finally leads to neurodegeneration and clinical signs become obvious. Furthermore a hematogenous spread of prions cannot be excluded since vCJD-cases have been described, in which transmission probably occurred after blood transfusion [Mabbott and MacPherson, 2006; Beekes and McBride, 2007].

After ingestion of contaminated material, prions have to cross the intestinal epithelium, which is protected by a single layer of epithelial cells bound by tight junctions. Within this epithelium microfold cells (M-cells) are located, which are specialized for transepithelial transport. M-cells are also supposed to translocate TSE agents across the gut epithelium [Heppner et al., 2001] but also dendritic cells (DC) have been proposed. Furthermore it was reported that partially digested fragments of PrP^{Sc} complexed with ferritin can be translocated independently of M-cells [Rescigno et al., 2001; Mishra et al., 2004].

Once crossed the gut epithelium, prions proceed to lymphoid tissues. Current data suggest that an uptake of prions by migratory DCs and macrophages within the intraepithelial pocket, which is a large invagination of the basolateral membrane of M-cells, is likely [Maignien et al., 2005; Huang et al., 2002].

The early accumulation of prions in lymphoid tissues occurs within the germinal centers of B-cell follicles, on follicular dendritic cells (FDC) and within macrophages and is essential for efficient neuroinvasion [Kitamoto et al., 1991; Sigurdson et al., 2002; Mabbott et al., 2000; Jeffrey et al., 2000]. The absence of Peyer's patches impairs neuroinvasion of orally infected scrapie prions [Prinz et al., 2003] as well as removal of the spleen before intraperitoneal inoculation [Fraser and Dickinson, 1970]. Moreover the accumulation of prions in FDCs is crucial, as their absence delays neuroinvasion and reduces disease susceptibility [Montrasio et al., 2000; Mabbott et al., 2003]. B-cells provide different cytokines for FDC maturation, and consequently depletion of B-cells also inhibits prion replication in lymphoid tissue [Mabbott et al., 2000; Klein et al., 1997; Prinz et al., 2002].

How FDCs take up prions after they have been delivered to B-cell follicles is uncertain. Many cell types, including DCs, lymphocytes, mast cells and platelets are able to secrete exosomes [Denzer et al., 2000a; Fevrier et al., 2004] and it was reported that FDCs are able to bind exosomes on their surface [Denzer et al., 2000b]. Therefore

prion transport via vesicles seems possible. It was also hypothesized that prions might become opsonised by FDCs via complement components [Klein *et al.*, 2001; Mabbott *et al.*, 2001; Blanquet-Grossard *et al.*, 2005].

Detailed analysis of PrP^{Sc} distribution in orally infected mice indicate that prions spread from lymphoid tissues to the CNS via the PNS. It is believed that prions reach their CNS target sites by spreading retrogradely along efferent fibers. Sympathetic nerve fibers (e.g. the splanchnic nerves) as well as parasympathetic (e.g. the vagus nerve) seem to be involved. In contrast to sympathetic fibers, parasympathetic nerves enter the CNS directly without passing the spinal cord. Thus prions can enter the CNS by several routes (Fig 6) [Beekes and McBride, 2000; McBride *et al.*, 2001; Beekes and McBride, 2007].

How exactly prions spread from FDCs to the PNS is not known. A direct transfer seems to be unlikely as FDCs and peripheral nerve fibers are anatomically separated (Fig 6) [Felten, 1993; Defaweux *et al.*, 2005]. Again DCs or exosomes have been proposed as transport vehicles from FDCs to nerve fibers [Février *et al.*, 2005]. Moreover the transmission of prions within the PNS is dependent on PrP^C expression [Blättler *et al.*, 1997; Glatzel and Aguzzi, 2000; Race *et al.*, 2000]. Finally prions arrive at the CNS, where their accumulation leads to neuronal damage accompanied by the typical neuropathological changes [Mabbott and MacPherson, 2006].

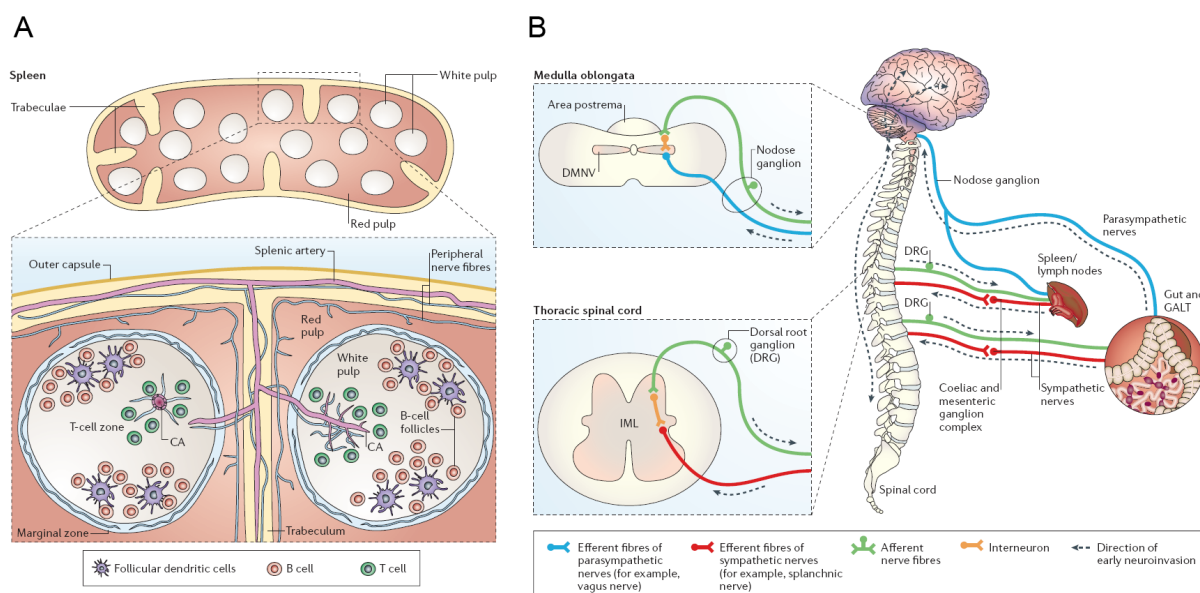


Figure 6: Neuroinvasion of prions. (A) Innervation of the spleen by peripheral nerve fibers. Nerve fibers are mainly associated with the capsule and the red pulp. Only few nerve fibers enter the white pulp, where FDCs, B- and T-cells are located. (B) Neuroinvasion of prions from lymphoid tissues and intestine to the CNS via sympathetic and parasympathetic nerve fibers. DMNV: motor nucleus of the vagus nerve, GALT: gut-associated lymphoid tissue. Adapted from [Mabbott and MacPherson, 2006].

1.5.2 Prion-induced neurodegeneration

Spongiform changes, loss of neurons, activation of microglia and astrocytes as well as the formation of amyloid plaques are classical neuropathological hallmarks of prion diseases, which do not always correlate with clinical disease symptoms [Flechsig and Weissmann, 2004]. Beside this, the molecular mechanisms of prion toxicity and the chain of events leading to the clinical disease are still poorly understood, although several hypothesis have been proposed.

In general two different mechanisms are proposed: 1. PrP^{Sc} may exhibit neurotoxic properties, e.g. by initiating apoptotic pathways, disrupting synaptic functions, mechanical damage or by impairing axonal transport mechanisms (\rightarrow *toxic gain-of-function*). 2. a toxic effect might also contribute to a loss of PrP^C function. Here a loss of neuroprotective properties of PrP^C, such as anti-apoptotic or anti-oxidative features, might be responsible for neuronal death (\rightarrow *loss-of-function situation*) [Collinge, 2001; Hetz et al., 2003]. However, neither the former nor the later theory could be confirmed to date and studies that intended to unravel the toxic mechanism of prions have often produced contradicting results. For instance changes in synaptic plasticity are a constant finding of clinical prion disease [Clinton et al., 1993]. In addition, neuronal loss initiated by apoptotic pathways was shown in different TSE animal models as well as in human TSE cases [Giese et al., 1995]. However, apoptosis was not directly associated with synaptic pathology and neither a loss of PrP^C function nor accumulation of PrP^{Sc} can sufficiently explain the observations [Park et al., 2000]. After intracerebral (i.c.) inoculation, wild-type mice (*Prnp*^{+/+}) exhibit clinical signs at 158 days post infection (dpi), while mice carrying only one allele of *Prnp* (*Prnp*^{+/-}) develop scrapie symptoms at 290 dpi. Surprisingly both lines demonstrate a similar pathology at 140 dpi, suggesting that large quantities of PrP^{Sc} can be tolerated for several months [Büeler et al., 1994]. On the contrary the amount of brain-derived PrP^{Sc} did not correlate to the extent of prion induced neuropathology, suggesting that a small amount of PrP^{Sc} might be sufficient to induce neuropathological changes [Lasmézas et al., 1997]. Beside this, immunodeficient mice show neuropathological changes in the CNS but do not develop clinical symptoms after prion infection [Frigg et al., 1999].

The fact that mice with PrP^C-depletion show no major phenotype, first excluded a simple loss-of-function concept [Büeler et al., 1992]. Later it was suggested that a functional homologue of PrP might substitute PrP^C function in early embryonic development and consequently mice with postnatal PrP depletion were generated. Again no phenotypic alterations were obvious but it turned out that depletion of PrP in prion infected mice could reverse spongiform changes [Mallucci et al., 2002, 2003].

Another constant finding in prion disease are severe motor impairments at the late stage of the disease. To date several studies point out a role for motor neurons (MN) in

the clinical manifestation of prion disease. Kimberlin and Walker first postulated clinical target areas (CTA), distinct neuronal populations in the brainstem and the spinal cord, in which prions have to access and replicate to cause clinical prion disease [Kimberlin and Walker, 1988]. More recently it was reported that transgenic mice expressing truncated PrP^{Δ32–93} demonstrate no detectable brain pathology upon prion challenge but 20% neuronal loss in the spinal cord [Flechsig et al., 2000]. Moreover application of prions into the sciatic nerve of hamster led to the infection of spinal cord projecting neurons. The infection of such neurons, which are connected to brain centers responsible for motor control (e.g. nucleus ruber, nucleus lateralis vestibule and cortex), appeared to be sufficient to cause clinical disease in hamster [Bartz et al., 2002]. From these studies it was concluded that neuronal loss in the spinal cord is sufficient to cause clinical disease. In addition impairments of axon functions such as synaptic degeneration, protein accumulation and changes of microtubule distribution were detected in CJD patients [Clinton et al., 1993; Kovács et al., 2005], animals and also in *in vitro* models of prion disease [Medrano et al., 2008; Novitskaya et al., 2007], suggesting axonal transport defects in prion disease. Indeed it has been reported that impaired axonal transport in MN of nucleus ruber and motor cortex correlate with the onset of clinical disease. This observation was a constant finding in different mouse-models and upon usage of different prion strains [Ermolayev et al., 2009a].

1.6 Dominant-negative effect of PrP polymorphisms

Numerous PrP^C polymorphisms are known affecting genetic predisposition, the clinical course of the disease as well as natural resistance and susceptibility to prion disorders [Mead, 2006]. Epidemiological studies of sheep populations revealed the efficiency of protective or dominant-negative *Prnp* alleles [Woolhouse et al., 2001]. Sheep homozygous for glutamine at codon 171 (171 Q/Q) develop scrapie, while at least one arginine at this position (171 R/Q or 171 R/R) provides resistance to the disease [Goldmann et al., 1994; Westaway et al., 1994]. These results were later confirmed in infection studies and as a consequence distinct breeding strategies were elaborated to generate scrapie-resistant sheep flocks [O'Rourke et al., 1997; Tuo et al., 2002]. Interestingly such sheep are not completely resistant to intracerebral BSE-infection [Houston and Gravenor, 2003]. Whether those sheep can be infected via the oral route remains elusive. So far no infection after oral exposure to BSE was observed, although transport of the infectious agent into lymph by crossing the intestinal barrier was described [Bellworthy et al., 2005; Sales, 2006]. In general it is assumed that sheep carrying protective polymorphisms are less susceptible to natural occurring TSEs [Díaz et al., 2005]. In deer, leucine at codon 132 provides resistance to CWD, while methionine at this position is associated with susceptibility [Browning et al., 2004].

Polymorphisms are also described in human prion diseases (Fig 7). As mentioned before, several *Prnp* mutations are associated with inherited prion disease, like GSS, fCJD and FFI. Moreover a genetic predisposition is described even for non hereditary human prion disease. Codon 129 strongly influences the susceptibility to sCJD, Kuru and vCJD. Thus 129 M/M homozygosity is found in most sCJD cases and in almost all tested vCJD patients [Collinge, 2001]. In contrast lysine at codon 219 (219 E/K or 219 K/K) seems to have protective properties in sCJD, as E/K heterozygosity was not found in 85 autopsied sCJD cases [Shibuya *et al.*, 1998].

The protective character of such polymorphisms is called dominant-negative effect [Caughey, 2001]. The dominant-negative effect of different *Prnp* polymorphisms was investigated in various *in vitro* and *in vivo* approaches and has been initially described in cell culture in 1994 [Priola *et al.*, 1994]. Especially the sheep polymorphism 171 Q/Q and the human polymorphism 219 E/K were investigated in prion-infected murine cell lines. Codon 171 in sheep corresponds to 167 in mouse and 219 in human to 218 in mouse. It was shown that both *Prnp* mutants, namely Q167R and E218K, inhibited prion propagation in cell culture and were not converted into PrP^{Sc} itself [Kaneko *et al.*, 1997b; Zulianello *et al.*, 2000].

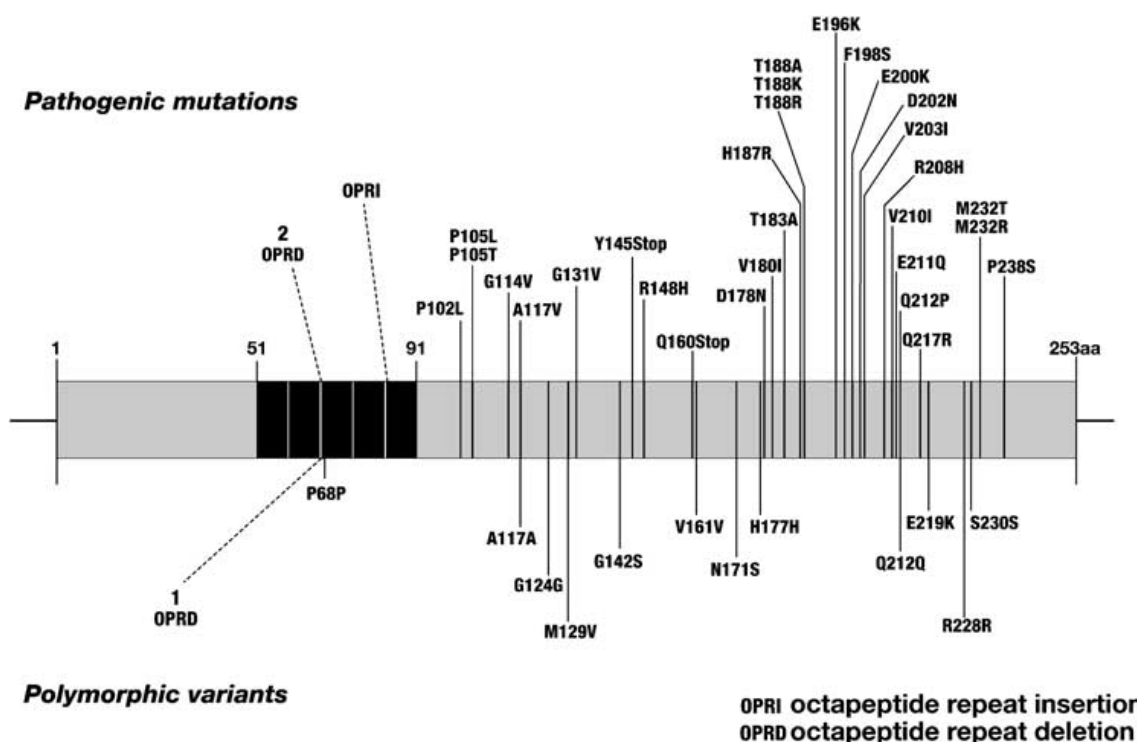


Figure 7: Human *Prnp* polymorphisms. Definite or suspected pathogenic mutations are shown above this representation of the prion protein gene. Neutral or prion disease susceptibility affecting polymorphisms are shown below. Adapted from [Mead, 2006].

The murine *Prnp*^{Q167R} mutant was further characterized in transgenic mice. Transgenic mice carrying *Prnp*^{Q167R} or *Prnp*^{Q218K} substitutions on a *Prnp*^{0/0} background, were unable to replicate and propagate prion disease. After reinsertion of the wild-type allele, the conversion of wild-type PrP^C into PrP^{Sc} was dramatically slowed down and correlated with an increase in incubation time [Perrier *et al.*, 2002]. Moreover lentiviral gene transfer of PrP^{Q167R} and PrP^{E218K} into prion infected cells efficiently inhibited prion replication [Crozet *et al.*, 2004]. Recently an effective gene therapy approach in transgenic mice, using PrP^{Q167R} virions, was described [Toupet *et al.*, 2008].

The mechanism how dominant-negative PrP mutants counteract prion replication is still under debate. For example it has been speculated that PrP^{Q167R} and PrP^C compete for the binding site at PrP^{Sc} molecules. Therefore they can inhibit the conversion without being transformed into an abnormal PrP isoform itself [Perrier *et al.*, 2002; Lee *et al.*, 2007]. Another hypothesis is that dominant-negative PrP mutants affect prion propagation by competing with PrP^C for a putative cofactor, necessary for prion replication [Kaneko *et al.*, 1997b]. The remarkable inefficient generation of prion infectivity *in vitro* suggests the existence of such additional factors [Legname *et al.*, 2004]. It was proposed that a cofactor might be associated with caveolae-like domains of the cell surface or endosomes [Kaneko *et al.*, 1997a; Nunziante *et al.*, 2003]. Other studies assumed polyanionic molecules such as nucleic acids. As the site of prion replication is not identified yet, the nature and location of an auxiliary cofactor remains speculative [Deleault *et al.*, 2007]. The seeding model for prion replication provides another theory for a dominant-negative mechanism. The hypothesis considers that dominant-negative PrP molecules can be regarded as "defective" monomers that can not be converted into PrP^{Sc} but are recruited to growing seeds. Attached to the seed, dominant-negative PrP provides no reactive interface for the recruitment and conversion of additional monomers. Therefore the seed is effectively "capped" and protected from further growing [Horiuchi *et al.*, 2000].

1.7 Cre/loxP system

The Cre-loxP technology was first introduced in the 1980s and is based on the enzymatic activity of Cre-recombinase (Cre). Cre is a 38 kDa family member of site-specific integrases derived from bacteriophage P1 [Sternberg *et al.*, 1981; Sauer and Henderson, 1988] and catalysis the recombination between two 34 bp palindromic loxP DNA sequences (Fig 8). *In vivo* the function of Cre is to circularize the P1 genome during infection and maintain the genome in a monomeric state for cell division. At least two loxP sites and Cre itself are required for recombination. Beside this, no further cofactors or sequences are needed, regardless of the cellular environment.

The number and orientation of loxP sites influences the recombination event. Thus

Cre-recombination can either result in excision, inversion or translocation of the loxP-flanked DNA (Fig 9) [Nagy, 2000]. However, too many loxP sites can lead to chromosomal instability [Lewandoski and Martin, 1997]. The mechanism of Cre-recombination starts with the binding of two Cre monomers to each loxP site. Then a tetramer ("holliday" intermediate) is formed, bringing the two loxP sites together. Finally, recombination occurs within the spacer area [Voziyanov *et al.*, 1999].

Today, Cre is widely used as a genetic tool to control site specific recombination events in genomic DNA and has been successfully applied in mammalian cell cultures, yeasts, plants, mice and other organisms [Araki *et al.*, 1997]. Various approaches are used to introduce Cre-recombinase into cells and organisms. For transient expression *in vitro*, usually electroporation or calcium precipitation is used. *In vivo* approaches include injection of Cre-RNA, the protein itself or viral delivery of Cre in a tissue- or cell-specific manner. Another possibility is the establishment of transgenic mouse strains. Typically Cre and loxP strains are developed separately and crossed to produce a double-transgenic Cre-lox strain [Nagy, 2000].

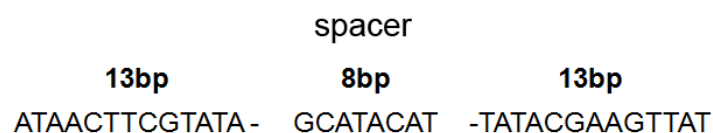


Figure 8: Sequence of a loxP site containing two 13 bp palindromic repeats and a 8 bp spacer.

Recently it has been reported that Cre-expression can be toxic to cells *in vitro* and *in vivo* and it was suggested that the mammalian genome contains so-called pseudo loxP sites, serving as functional recognition sites for Cre. Thus recombination of these pseudo loxP sites leads to DNA strand breaks and chromosome rearrangements [Pfeifer *et al.*, 2001; Silver and Livingston, 2001; Schmidt-Supprian and Rajewsky, 2007]. Therefore a spatial and temporal control of Cre-expression is not only important for the experimental setup but also to avoid Cre toxicity. Usually Cre-expression is controlled by the design of the transgenic construct, e.g by a tissue-specific promoter. Beside this a variety of strategies to overcome Cre-toxicity have been developed, including self-silencing or self-deleting Cre expression vectors and several inducible systems controlling Cre transcription or translation, e.g. by oral application of steroids (tamoxifen or RU486) or doxycycline [Pfeifer *et al.*, 2001; Silver and Livingston, 2001; Mähönen *et al.*, 2004].

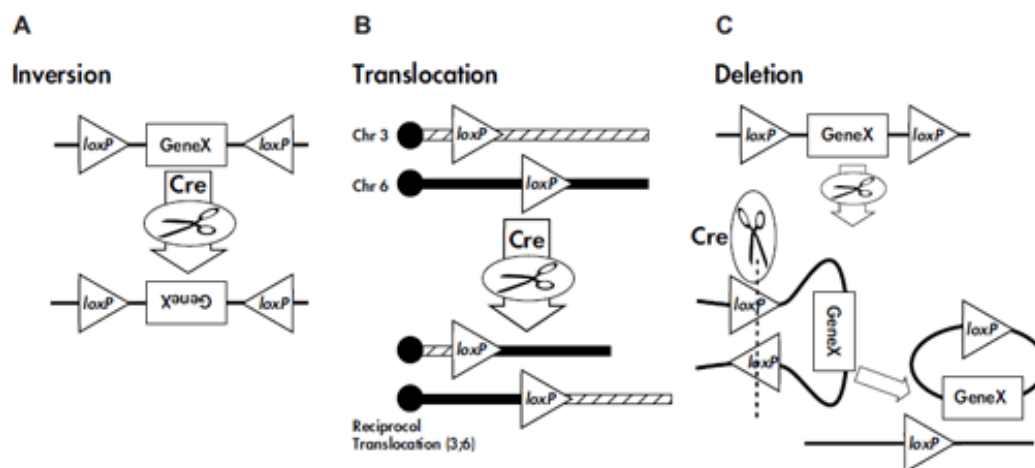


Figure 9: Cre-recombination is determined by the orientation and location of flanking loxP sites. (A) If the loxP sites are oriented in opposite directions, Cre recombinase mediates the inversion of the floxed segment. (B) If the loxP sites are located on different chromosomes (trans arrangement), Cre recombinase mediates a chromosomal translocation. (C) If the loxP sites are oriented in the same direction on a chromosome segment (cis arrangement), Cre recombinase mediates a deletion of the floxed segment. Adapted from (<http://jaxmice.jax.org>).

1.8 Adeno associated virus vectors

The human adeno associated virus (AAV) was discovered in 1965 as a contaminant of adenovirus preparations [Atchison *et al.*, 1965]. AAV is a small virus (22 nm capsid), which infects humans and other primate species. AAV belongs to the family of Parvoviridae, which is included into the genus of Dependovirus. Despite a high seroprevalence among humans (approximately 80% of the population are AAV2 positive), the virus has not been linked to any human disease and has only limited capacity to induce an immune response. AAV can infect a variety of dividing and non-dividing cells and is able to incorporate its DNA into the host genome. These features make AAV a highly attractive candidate for gene therapy [Grieger and Samulski, 2005; Gonçalves, 2005].

AAV has a single stranded DNA (ssDNA) of 4,7 kilobase pairs, that can be either of positive or negative sense. Moreover the genome has two inverted terminal repeats (ITR), which can form a T-shaped hairpin structure that is needed for DNA replication. Two open reading frames encode for rep and cap proteins. Rep proteins are essential for the AAV life cycle, while the later are needed for the formation of the capsid. AAV does not encode a polymerase, depending instead on cellular polymerase activities for DNA replication [Gonçalves, 2005; Carter, 2005].

To date 11 different serotypes have been described with serotype 2 (AAV2) being the best characterized and therefore the most popular serotype in AAV research [Mori

et al., 2004]. AAV2 shows natural tropism towards e.g. skeletal muscles, neurons, vascular smooth muscle cells and hepatocytes [Bartlett *et al.*, 1998; Manno *et al.*, 2003; Richter *et al.*, 2000; Koeberl *et al.*, 1997]. For host-cell infection, several cell surface receptors have been described. AAV2 attaches to heparan sulfate proteoglycan (HSPG), while internalization is aided by the co-receptors $\alpha_v\beta_5$ integrin, fibroblast growth factor receptor type 1 (FGFR-1) and hepatocyte growth factor receptor (c-Met). The use of HSPG receptors may explain the broad tropism of the virus that include human, non-human primate, canine, murine and avian cells [Summerford and Samulski, 1998; Qing *et al.*, 1999; Summerford *et al.*, 1999; Kashiwakura *et al.*, 2005].

After attachment to a receptor AAV is internalized most likely via clathrin-coated pits and submitted to endosomal trafficking. Intracellular transport of AAV involves microtubule and motor proteins. After escape from late endosomal or lysosomal compartments, AAV is translocated to the nucleus probably via the nuclear pore complex [Gonçalves, 2005]. After entry to the nucleus, AAV can follow two interchangeable pathways: the lytic or lysogenic. The lytic pathway only develops in presence of a helper-virus, such as adeno (Ad) or herpes simplex virus (HSV) [Handa and Carter, 1979]. In the absence of a helper-virus, AAV integrates into the host genome, targeting a distinct integration site on human chromosome 19 [Surosky *et al.*, 1997]. These features also make AAV an attractive candidate for gene therapy. Because only a minimal set of adenoviral genes is required for efficient generation of AAV particles, AAV can be produced in a helper-virus free system [Matsushita *et al.*, 1998]. Therefore plasmids carrying the transgenic DNA, which is flanked by two AAV ITRs, and some additional plasmids, encoding for helper functions, are co-transfected into the producer cell line (Fig 13).

AAV vectors have already been used in several first- and second phase clinical trials for treatment of cystic fibrosis, haemophilia and also in Parkinson's disease. As AAV showed good tolerance even in the central nervous system, other trials are in process, e.g. gene therapy approaches for Canavan disease and muscular dystrophy [Carter, 2005; Kaplitt *et al.*, 2007]. Although AAV vectors seem to be a promising tool, the vector system still needs further improved. More recently, double-stranded AAV (dsAAV) have been used, showing enhanced gene expression in comparison to single-stranded AAV vectors. dsAAV can be produced by mutating a distinct DNA motif inside the ITR, called terminal resolution site (trs). A modified trs prevents the two DNA strands from separation during the AAV replication cycle. As a consequence dsAAV does not require the conversion of ssDNA to dsDNA, a relatively slow process that is carried out by the cell machinery, providing faster and more effective gene expression in the target cells [Wang *et al.*, 2003].

2 Aim of the study

The primary objective of the study was to examine if motor neurons (MN) are vulnerable cell populations for triggering the onset of clinical prion disease and whether the protection of these cells against prion-induced dysfunctions can interfere with the development of the disease on a subclinical level.

Towards this, we developed a conditional mouse model with expression of dominant-negative PrP^{Q167R} in the cells of interest. The MN-specific expression of protective PrP^{Q167R} was achieved by mating the novel transgenic line Tg floxed LacZ-PrP^{Q167R} to various Cre-strains. Expression of Cre under control of the Hb9 promoter led to the deletion of the floxed *LacZ* marker gene and consequently to the expression of PrP^{Q167R} in MN of the spinal cord [Arber *et al.*, 1999]. The NF-L promoter directed Cre-expression to most neurons of the spinal cord as well as to various neurons of the brain [Schweizer *et al.*, 2002]. Transgenic mice and age-matched control littermates were inoculated with mouse-adapted prions to investigate the effect of dominant-negative PrP^{Q167R} on incubation periods, survival and prion pathogenesis.

In a second part, a double-stranded AAV-2-Cre vector (dsAAV2-Cre) was used to transfer Cre-recombinase into Tg floxed LacZ-PrP^{Q167R} mice. It has been reported that AAV2 is able to proceed retrogradly from muscle tissue to MN of the spinal cord [Kaspar *et al.*, 2003]. Therefore dsAAV2-Cre was injected into the hind limb muscles of Tg floxed LacZ-PrP^{Q167R} mice to target a broader cell population and thus enhance expression levels of protective PrP^{Q167R} in the spinal cord. Another goal of this strategy was to avoid time consuming intercrossing of Tg floxed LacZ-PrP^{Q167R} mice and Cre-strains as well as optimizing PrP^{Q167R} expression by variation of the virus titer or the site of application.

In a last part we investigated if neurons and in particular MN are involved in the early accumulation of PrP^{Sc} and prion infectivity in splenic tissue. Therefore a transgenic model with neuronal PrP depletion was established. *Lox2*^{+/-} mice, carrying one allele of floxed *Prnp* on a *Prnp*^{0/0} background [Rossi *et al.*, 2001], were mated to Hb9-Cre and NF-L-Cre strains to achieve a MN-specific or a pan-neuronal PrP knockout, respectively. The resulting double-transgenic offsprings were inoculated with mouse-adapted prions and the accumulation of PrP^{Sc} and prion infectivity in spleen and spinal cord was analyzed at 50 days post inoculation.

3 Material

3.1 Laboratory equipment and software

Material	Company
ABI PRISM 7500	Applied Biosystems
AIDA software	Raytest Isotopenmessgeräte
Autoclav	Müncher Medizin
Balance	Satorius
Centrifuge	Eppendorf, Hettich, Sorvall
Clean Bench	Nuaire
Cryostat (CM 1900)	Leica
Cuvettes (UV-ette)	Eppendorf
Dark Box LAS 3000	Fuji Photo Film
Digital camera	Diagnoistic instruments
Electrophorese chamber	Institute of Virology
ELISA-Reader	Molecular Devices
FACScalibur	Becton-Dickinson
Fluorescence microscope	Zeiss, Leica
Freezer	Bosch
Hamilton syringe (33gauge)	Hamilton
Humid chamber for IHC	self made
Ice machine	Scotsman
Image Reader software	Fuji Photo Film
Incubator	Heraeus
Isoflurane anesthesia chamber	Institute of Virology
Magnetic stirrer	Ika Werke
Metal plate (2x5x1mm)	Institute of Virology, Würzburg
Micro Centrifuge	Eppendorf
Micro pestle	Eppendorf

Microtome (SM 2000R)	Leica
Microwave	Severin
Mini Trans-Blot cell	Biorad
Millex-GV (0,22µm)	Millipore
Neubauer chamber	Marienfeld
Optical tubes for PCR	Applied Biosystems
Pap pen	Dako
Parafilm	Parafilm
pH meter	Denver Instruments
Photometer	Biorad
Pipetts	Gilson, Eppendorf
Pipet controler, accu-jet	Brand
Power supply	Consort, Biometra
Prism 4.0 software	GraphPad
PVDF membrane	Roth
Shaker	Heidolph
Super Frost Plus Slides for microscopy	Langenbrinck Medizintechnik
Surgical instruments	World Precision Instruments
SDS-Gels for PAGE (12% tris-glycine)	Lonza
Thermocycler	Eppendorf
Tissue Tek	Sakura
Thermomixer	Eppendorf
UV-system	Intas
USP 5.0 Vicryl sutures	Ethicon, Johnson & Johnson
Vortex Mixer	neoLab
Whatman blotting paper	Schleicher and Schüll
Water bath	GFL
X-ray films	Amersham

Materials like cell culture flasks, petri dishes, pipette tips, falcon tubes, micro-centrifuge tubes, cryo tubes, syringes and needles were ordered from Hartenstein Laborbedarf, Greiner, Eppendorf, Nunc GmbH, BD Bioscience and Carl Roth GmbH.

3.2 Buffers and chemicals

Buffer/Reagent	Composition	Company
0,1% Sarkosyl	0,1 % (w/v) L-Leuroyl-Sarcosine in PBS	Sigma
2xHeBs	50mM HEPES 280mM NaCl	AppliChem AppliChem
4% NaPTA	4% (w/v) phosphotungstic acid 170mM MgCl ₂ in ddH ₂ O	Sigma Sigma
4% Sarkosyl	4% (w/v) L-Leuroyl-Sarcosine in PBS	Sigma
500µl DNA-mix for transfection of cells	50µl sterile 2,5M CaCl ₂ 15µg of plasmid DNA in Ampuwa	Sigma Fresenius
50x TAE	2M Tris, pH 8.0 5,7% (v/v) Acetic acid 0,05M EDTA-Na ₂ , pH 8.0	AppliChem AppliChem AppliChem
5x SDS sample buffer	250mM Tris/HCl, pH 6.8 30% (v/v) Glycerol 10% Sodium dodecyl sulfate (SDS) 5% (v/v) β-mercaptoethanol 0,005% (w/v) bromophenol blue	AppliChem AppliChem Sigma Merck Serva
Aceton	100% (v/v)	AppliChem
AEC (3-Amino-9-Ethylcarbazol)	tablets	DCS
Agarose	1-2,5% (w/v) in 1xTAE	AppliChem
Agarose (SeaKem GTG)	0,8% (w/v) in 1x TAE	Cambrex
Aquatex	ready-to-use	Merck

ATV	0,05% Trypsin (1:250, Difco) 0,5mM EDTA 137mM NaCl 5,4mM KCl 0,058% NaHCO ₃	BD Sigma AppliChem AppliChem Sigma
Benzonase nuclease	321u/μl; diluted 1:10 in PBB	Sigma
Bradford staining solution	Biorad protein assay	Biorad
Bovine serum albumine (BSA)	1mg/ml in ddH ₂ O	Sigma
Cell lysis buffer	50mM Tris/HCl, pH 7.5 150mM NaCl 0,5% (v/v) Triton X-100 0,5% Desoxycholic acid in PBS	AppliChem AppliChem Sigma Sigma
Citrate-buffer	20mM Citric acid monohydrat 2g Sodium hydroxide pellets dissolved in 1l ddH ₂ O, pH 6.0	AppliChem AppliChem
dNTP Mix (10mM)	1,25mM in sterile ddH ₂ O	Fermentas
Dimethyl sulfoxide (DMSO)	100% (v/v)	Sigma
Ethylenediamine tetraacetic acid (EDTA)	in ddH ₂ O	Sigma
Entellan	100% (v/v)	Merck
Eosin	1% (w/v) in ddH ₂ O	Merck
Ethidium bromide (EtBr)	1μg/μl Ethidium bromid in 1xTEA	Roth
Ethanol	100% (v/v)	AppliChem
FACS buffer	10mM EDTA, pH 8.0 2% FCS 0,1% Sodium azid in PBS	Sigma Biochrom Sigma
Fix solution for cells	2% formaldehyde 0,2% glutaraldehyde in PBS	Roth Roth

Fluorescence mounting medium	ready-to-use	Dako
Formic acid	99-100% (v/v)	AppliChem
Goat serum	100% (v/v)	Zymed
Hydrogen peroxide	30% (v/v)	AppliChem
IHC blocking-buffer	10% (v/v) CAS-Block in TBS-T	Zymed
Isofluran	3-4% (v/v) in O ₂ for anesthesia	Abbot
Ketanest/Rompun	7,5mg/ml Rompun 7,5mg/ml Ketanest in sterile PBS	Bayer Leverkusen Parke-Davis GmbH
Mayers Hemalaun	ready-to-use	Roth
Methanol	100% (v/v)	AppliChem
OptiMEM growth medium	OptiMEM Glutamax 10% Fetal Calf serum (FCS) 1% Penicillin/Streptavidin	Gibco Biochrom AG Sigma
Phosphate buffered saline (PBS)	137mM NaCl 2,7mM KCl 4,3mM Na ₂ HPO ₄ 1,47mM KH ₂ PO ₄ in sterile ddH ₂ O, pH 7.4	AppliChem AppliChem Sigma Sigma
PFA (4%, RotiHistofix)	buffered, pH 7.5	Roth
Proteinase K	20mg/ml (50U/ml)	Roche Diagnostics
Protease inhibitor, Complete EDTA-free	tablets	Roche Diagnostics
Rinse-buffer	5mM EGTA 0,01% (w/v) Desoxycholate 0,02% (v/v) Igepal CA-630 2mM MgCl ₂ in PBS	Sigma Sigma Sigma Sigma
SDS-running buffer	25mM Tris 192mM Glycin 1% (w/v) Sodium dodecyl sulfate (SDS) in ddH ₂ O, pH 8.4	AppliChem AppliChem Sigma
Sodium Butyrate	500mM stock	Sigma

Stripping-buffer	0,2M Glycin 1mM EDTA-Na ₂ 0,5M NaCl in ddH ₂ O, pH 2.5	AppliChem Sigma AppliChem
TBS	10mM Tris 150mM NaCl in ddH ₂ O, pH 7.6	AppliChem AppliChem
TBST	10mM Tris 150mM NaCl 0,1% v/v Tween20, pH 7,6	AppliChem AppliChem AppliChem
TBS-T	0,4% (v/v) Triton-X 100 in TBS	Sigma
TBS-T2	1% (v/v) Triton-X 100 in TBS	Sigma
TBST/MP	TBST + 5% (w/v) non-fat dry milk	Biorad
Tissue lysis buffer	0,5% (w/v) Desoxycholic acid 0,5% (v/v) Igepal CA-630 protease inhibitor Complete EDTA-free in PBS	Sigma Sigma Roche
Transfer-buffer	25mM Tris 192mM Glycin 1% (w/v) Sodium dodecyl sulfate (SDS) 20% (v/v) Methanol in ddH ₂ O, pH 8.4	AppliChem AppliChem Sigma AppliChem
Trypan blue	0,4%	Sigma
X-Gal	1mg/ml in Dimethylformamide	Roth Sigma
X-Gal staining solution for cells	2mM MgCl ₂ 5mM K ₃ [Fe(CN)] ₆ 5mM K ₄ [Fe(CN)] ₆ 1mg/ml X-Gal in PBS	Sigma Sigma Sigma Roth
X-Gal staining solution for mice	5mM K ₃ [Fe(CN)] ₆ 5mM K ₄ [Fe(CN)] ₆ 1mg/ml X-Gal in Rinse-buffer	Sigma Sigma Roth
Xylol	100% (v/v)	Roth

3.3 Enzymes and synthetic oligonucleotides

Enzymes were purchased from New England Biolabs GmbH. Synthetic oligonucleotides were obtained from Sigma-Aldrich and Invitrogen.

Primer	Sequence 5' → 3'	Target gene
Actin_for	AGC CAT GTA CGT AGC CAT CC	mouse <i>Actb</i> (β -actin)
Actin_rev	GCT GTG GTG GTG AAG CTG TAG	mouse <i>Actb</i> (β -actin)
Cre_for	AAA TGC TTC TGT CCG TTT GC	<i>Cre</i> gene of Enterobacteria phage P1
Cre_rev	ATT GCT GTC ACT TGG TCG TG	<i>Cre</i> gene of Enterobacteria phage P1
LacZ_ROSA_for	ATC CTC TGC ATG GTC AGG TC	<i>LacZ</i> gene of Escherichia coli.
LacZ_ROSA_rev	CGT GGC CTG ATT CAT TCC	<i>LacZ</i> gene of Escherichia coli.
LoxP1_for	CAG AGC TGT TGT GGT CAG G	transgene floxed LacZ-PrP ^{Q167R}
LoxP2_PrP_rev	CCA CTA GGA AGG CAG AAT GC	transgene floxed LacZ-PrP ^{Q167R}
Nco	TAT TGC ATG GTT GTT ACG CC	<i>Prnp lox2</i> allele
P3	ATT CGC AGC GCA TCG CCT TCT GCC	mouse <i>Prnp</i> ^{-/-} (neo) allele
P3'NC	CCC TCC CCC AGC CTA GAC CAC GA	mouse <i>Prnp</i>
P5	GCT TTC TTC AAG TCC TTG CTC CTG CTG TAG	<i>Prnp lox2</i> allele
P10	GTA CCC ATA ATC AGT GGA ACA AGC CCA GC	mouse <i>Prnp</i>
3'loxP3	GGG CAG GAG AAA CAG TTT GG	<i>Prnp lox1</i> allele (Zürich II)
PrP_167_For	GAT CCA TTT TGG CAA CGA C	mouse <i>Prnp</i> , exon3
PrP_167_Rev	TCA TCT TCA CAT CGG TCT CG	mouse <i>Prnp</i> , exon3

3.4 Antibodies

Primary antibody	Company
monoclonal mouse anti- β -actin (clone AC-15)	Sigma
mouse anti- β -galactosidase	Sigma
monoclonal mouse anti-PrP (clone 3F4)	Chemicon
monoclonal mouse anti-PrP SAF32	Spibio
anti-PrP B2-43	AG Klein
monoclonal mouse anti-Cre	Sigma
biotin-conjugated mouse anti-NeuN	Chemicon
biotin conjugated anti-WFA	Sigma
rabbit anti-GFAP	Dako
Secondary antibody	Company
HRP-rabbit anti-mouse IgG1	Zymed
HRP-rabbit anti-mouse IgG2a	Zymed
Alexa Fluor 488 Fab2 rabbit anti-mouse IgG	Molecular Probes
Streptavidin-Texas Red	Dianova
Polylink secondary Ab (biotin-conj.)	DCS
Label streptavidin label (HRP-conj.)	DCS

3.5 Kits

Kit	Company
ABsolute TM QPCR Green Low ROX Mix	ABgene
AEC Kit	DCS
DNeasy Blood & Tissue Kit	Qiagen
GoTaq Flexi DNA polymerase PCR kit	Promega
Link and Label system	DCS

Qiaquick gel extraction Kit	Qiagen
Kits for plasmid preparation	Qiagen
SuperSignal West Pico Chemoluminescent substrate	Pierce

3.6 DNA and Protein molecular weight markers

Marker	Company
Gene ruler 1kb DNA ladder	Fermentas
Gene ruler 100bp DNA ladder	Fermentas
MagicMark TM XP Western Protein Standard (20-220kDa)	Invitrogen
PageRuler TM Prestained Protein ladder	Fermentas

3.7 Cells

Human embryonic kidney cells (HEK or 293T cells), immortalized with the Ad5 E1A protein expressing the large SV40 T-antigen [Graham *et al.*, 1977] were used to test the expression of plasmids.

3.8 Mouse strains

3.8.1 C57BL/6

C57BL/6 is the most widely used wild-type inbred strain. The C57BL/6 strain was created by Dr. CC Little in 1921 from Miss Abbie Lathrop's stock.

3.8.2 *Prnp*^{0/0}(Zürich I knockout)

Prnp^{0/0} or Zürich I knockout mice are devoid of PrP^C because the open reading frame (ORF) of exon 3 was disrupted by insertion of a neomycin (neo) cassette. The neo gene replaces codon 3 to 188, therefore PrP^C is not expressed and consequently *Prnp*^{0/0} mice are resistant to prion infection. *Prnp*^{0/0} mice were generated on a wild-type C57BL/6 129/Sv background (Fig 10). Although *Prnp*^{0/0} mice are devoid of PrP^C, they display normal development and behaviour [Büeler *et al.*, 1992, 1993].

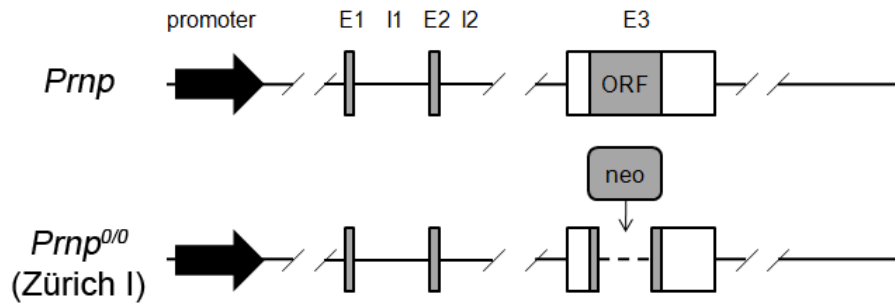


Figure 10: Structure of the wild-type murine *Prnp* gene and the disrupted open reading frame (ORF) in *Prnp*^{0/0} mice. The *Prnp* gene consists of three exons (E1-E3) and two introns (I1, I2) under control of the endogenous *Prnp* promoter. In *Prnp*^{0/0} mice the ORF of E3 is disrupted by a neomycin (neo) cassette, therefore these mice are devoid of PrP^C. Adapted from [Weissmann and Flechsig, 2003].

3.8.3 *Prnp* lox2

Prnp lox2 (Lox2) mice were obtained during the generation of a second *Prnp*-knockout strain called Zürich II. In Lox2 mice exon 3 of the *Prnp* gene was flanked by two loxP sites to enable a selective deletion of exon 3 by Cre-recombinase. Lox2 mice carry 2 alleles of floxed *Prnp* under control of the endogenous *Prnp* promoter. Further breeding of these mice to distinct Cre-strains leads to a selective PrP^C-knockout similar to the situation in Zürich II (Fig 11) [Rossi et al., 2001].

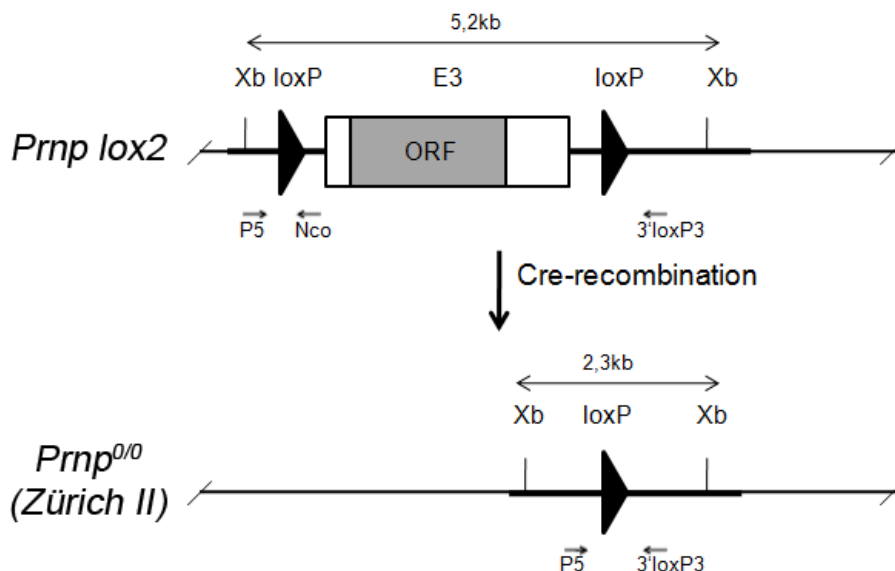


Figure 11: Structure of the *Prnp* lox2 allele. Exon 3 (E3) was flanked by two loxP sites leading to a deletion of E3 upon Cre-recombination. Adapted from [Rossi et al., 2001].

3.8.4 Tga20

Tga20 mice express approximately 5 to 8-fold of PrP^C as compared to wild-type under control of the endogenous *Prnp* promoter. Tga20 mice were generated on a *Prnp*^{0/0} background. Due to the overexpression of PrP^C these mice develop scrapie at 60-62 days post intracerebral infection with RML prions (dose: 3x10⁵LD₅₀) [Fischer *et al.*, 1996].

3.8.5 Tg(SHaPrP) (Tg(SHaPrP)3922-*Prnp*^{0/0})

Tg(SHaPrP) mice express approximately 20-fold of syrian hamster PrP^C under control of the syrian hamster *Prnp*-promoter on a *Prnp*^{0/0} background [Scott *et al.*, 1989].

3.8.6 NF-L-Cre

NF-L-Cre mice express Cre-recombinase of bacteriophage P1 under control of the human neurofilament light chain (NF-L) promoter. Therefore Cre is expressed in facial and spinal motor neurons and in various neuronal populations of the brain. NF-L-Cre mice were bred on a CD-1 background and backcrossed to C57BL/6 [Schweizer *et al.*, 2002].

3.8.7 Hb9-Cre (B6.129S1-Mnx1^{tm4(Cre)Tmj}/J)

In Hb9-Cre mice the expression of Cre-recombinase is directed to motor neurons of the spinal cord. While mice heterozygous for Hb9-Cre are viable and fertile, homozygous Hb9-Cre mice die at or soon after birth. Hb9-Cre mice were generated on a 129/Sv background and backcrossed to C57BL/6 [Arber *et al.*, 1999; Yang *et al.*, 2001].

3.9 Scrapie inoculum

As inoculum the mouse-adapted Rocky Mountain Laboratory (RML) scrapie strain [Chandler, 1961] passaged in Swiss-CD-1 mice (Charles River Laboratories) was used. RML was diluted in PBS containing 5% BSA. The titer of this standard inoculum was 8.6 log LD₅₀ units/ml of a 10% (w/v) brain homogenate.

4 Methods

4.1 Animal methods

4.1.1 Generation of Tg floxed LacZ-PrP^{Q167R} mice

Cloning. The plasmid pLL4 was based on the pLL3.7 vector [Rubinson *et al.*, 2003], in which the U6 and eGFP genes were replaced by a multiple cloning site between Apal and Pcil of pLL3.7. The transgenic DNA consisted of a floxed *LacZ* gene and the coding sequence of a murine dominant-negative *Prnp* gene, mutated at codon Q167R as well as at L108M and V111M (3F4-tag) [Kascsak *et al.*, 1987]. The transgene including the entire polyA site of murine *Prnp* was introduced into the NotI/SphI cloning site. The human ubiquitin C (UbiC) promoter and a murine β -globin intron were inserted upstream of the transgenic DNA via PacI/Ascl and EcoRI, respectively. The floxed *LacZ* gene was originally cloned from a transgene designated Fabpl 4 at-132/loxP β -gal/hGH [Saam and Gordon, 1999], while the UbiC promoter was derived from a plasmid designated FUW [Lois *et al.*, 2002].

Purification. The transgenic DNA was released from the backbone by PacI/SphI digestion. 18 μ g DNA per preparation were digested for 2h at 37 °C by 50units of PacI and SphI using appropriate buffer conditions and BSA concentrations as recommended by the manufacturer. After digestion the DNA was heated for 10min at 50 °C to stop the enzymatic reaction and afterwards purified twice by electrophoresis through a 0,8% SeaKem GTG agarose gel. The 9,3kb construct was isolated from the gel and extracted using the Qiaquick Gel Extraction kit. To increase the purity of the final DNA fragment, all buffers of the kit were filtered through a 0,22 μ m Millex-GV prior to use.

Microinjection. The purified construct was injected into the male pronucleus of fertilized oocytes obtained from C57BL/6 mice. The microinjection was performed by Prof. Dr. T. Rüllicke at the Institute of Laboratory Animal Science, Vienna. Transgene positive founders were identified by PCR, mated to C57BL/6 and analyzed for transgene expression. The transgenic line was called Tg floxed LacZ-PrP^{Q167R}.

4.1.2 Mating of Tg floxed LacZ-PrP^{Q167R} mice to Hb9-Cre and NF-L-Cre strains

Further breeding to Hb9-Cre mice or to NF-L-Cre mice revealed double transgenic Tg floxed LacZ-PrP^{Q167R}/Hb9-Cre or Tg floxed LacZ-PrP^{Q167R}/NF-L-Cre mice on a *Prnp*^{+/+} mixed C57BL/6 x 129/Sv background.

4.1.3 Mating of *Lox2* mice to *Hb9-Cre* and *NF-L-Cre* strains

Lox2 mice carry two alleles of loxP flanked murine *Prnp* under control of the endogenous *Prnp* promoter. *Lox2* mice were mated to *Prnp*^{0/0} mice (Zürich I) in order to obtain heterozygous *lox2*^{+/-} mice. *Hb9-Cre* mice and *NF-L-Cre* mice were also established on a *Prnp*^{0/0} background and further breeding of these Cre-strains to *lox2*^{+/-} mice resulted in double transgenic *lox2*^{+/-}/*Hb9-Cre* and *lox2*^{+/-}/*NF-L-Cre* mice with *Prnp*^{0/0} background. Thus a selective knock-out of PrP^C was achieved in cells with Cre-expression.

4.1.4 Tail biopsy and earmarks

Generally mice were weaned at the age of 18-21 days. At the same time earmarks were placed and tail biopsies were taken for genotyping. Tails were immediately frozen on dry ice and stored at -20 °C until use.

4.1.5 Intramuscular application of AAV-Cre vectors

For intramuscular (i.m.) application of AAV-Cre vectors, Tg floxed LacZ-PrP^{Q167R} mice were anaesthetized with 40mg/kg Ketanest/Rompun and both hind limb muscles were exposed by a short skin cut. A volume of 30µl per side was injected slowly into the muscle tissue using a 0,3ml insulin syringe. After injection the skin was closed with resorbable USP 5.0 vicryl sutures. At various time points mice were sacrificed and organs were recovered to check Cre-recombination by PCR and western blot analysis.

4.1.6 Scrapie inoculation of mice

All animal experiments were performed according to the German governmental and institutional guidelines. As inoculum the mouse-adapted RML scrapie strain [Chandler, 1961] passaged in Swiss-CD-1 mice (Charles River Laboratories) and diluted in PBS containing 5% BSA was used. The titer of this standard inoculum was 8.6 log LD₅₀ units/ml of a 10% (w/v) brain homogenate. For intracerebral (i.c.) inoculations a 30µl volume was injected using a high-dose (3*10⁵LD₅₀) of RML inoculum. For intraperitoneal (i.p.) inoculations a 100µl volume was injected containing either a high-dose (10⁶LD₅₀) or a low-dose (10³LD₅₀) of RML. Intranerval (i.n.) inoculations were performed as described in [Ermolayev *et al.*, 2009b]. Briefly, animals were anaesthetized with 40mg/kg Ketanest/Rompun. The right sciatic nerve was surgically exposed by dislodging *M. gluteus superficialis* and *M. biceps femoris*, placed on a metal plate (2x5x1mm) and 1µl of high-dose (10⁴LD₅₀) RML was injected using a 33-gauge Hamilton syringe over a period of 5min. Great care was taken to visually control and assure accurate uptake of the inoculum into the nerve. After inoculation, the sciatic nerve was

repositioned and the lesion was closed with resorbable USP 5.0 vicryl sutures. Following inoculation, the neurological status of the mice was assessed three times a week according to typical scrapie criteria as previously described [Carlson *et al.*, 1986] and animals were sacrificed on the day of onset of clinical signs of terminal prion disease.

4.1.7 Bioassay to determine prion infectivity

Scrapie infected lox2^{+/-}, lox2^{+/-}/NF-L-Cre and lox2^{+/-}/Hb9-Cre mice were sacrificed 50 days post inoculation (dpi) and 1% (w/v) spleen homogenates were prepared. 30µl of each 1% (w/v) spleen homogenate was intracerebrally injected into 4 to 5 Tga20 indicator mice. The incubation time until development of terminal scrapie sickness was determined and infectivity titers were calculated according to the relationship [Prusiner *et al.*, 1982]:

$$y = -0,0657 * x + 10,308$$

$$y = \log LD_{50}$$

$$x = \text{incubation time (days) to terminal disease}$$

4.1.8 Statistics

Results were analysed using Graph Pad Prism software. Kaplan-Meier curves were utilized to display survival data. One-way ANOVA followed by Bonferroni's post-hoc multiple comparison test and Kruskal-Wallis test followed by Dunn's post-hoc multiple comparison test were applied when appropriate. The null hypothesis was rejected on the basis of $P < 0,05$. Results are given as mean incubation time in days \pm SD. Asymptomatic animals/survivors were excluded from statistic.

4.2 Molecular biology techniques

4.2.1 Isolation of genomic DNA from tissue samples

Genomic DNA from mouse tail biopsies, brain, spinal cord and pancreatic tissue was isolated using the DNeasy Blood & Tissue kit. Genomic DNA from tail biopsies was extracted according to the manufacturers protocol and dissolved in 100µl elution buffer provided by the kit. To facilitate lysis of brain, spinal cord and pancreas samples, 300µl of lysis buffer/Proteinase K mixture was added and the tissue was homogenized through 19-23gauge needles prior to overnight digestion. After tissue lysis the DNA was isolated according to the provided protocol. DNA from brain, spinal cord and pancreas samples was eluted in 50µl to increase the final DNA concentration.

4.2.2 Determination of the nucleic acid concentration

The concentration and quality of double-stranded DNA (dsDNA), in particular contamination with salts and proteins, was estimated by measuring the absorption (optical density, OD) of the samples at 260nm and 280nm using a photometer. The concentration and quality was determined according to the equations given below. A pure dsDNA sample without protein contamination will give a ration of 1,7 to 2.

$$c(dsDNA) \left[\frac{\mu g}{\mu l} \right] = \frac{[OD_{260nm} * 50 * f]}{1000}$$

$$p(dsDNA) = \frac{[OD_{260nm}]}{[OD_{280nm}]}$$

c = concentration of dsDNA in $\mu g/\mu l$

OD = optical density in nm

f = dilution factor

p = purity of dsDNA in $\mu g/\mu l$

4.2.3 Polymerase chain reaction (PCR)

The polymerase chain reaction allows rapid amplification of specific nucleic acid sequences in a complex pool of DNA. The specificity of the amplified sequence is achieved by two synthetic oligonucleotides (primers) that are complementary to the 5'- or 3'-end of the template sequence. Depending on the primer-design the heatstable Taq-polymerase catalyses the sythesis of a new DNA strand in sense or antisense direction. This process leads to the production of the specific DNA region flanked by the two primers. Each round of amplification multiplies the amount of the target DNA [Saiki *et al.*, 1988].

4.2.3.1 Genotyping of transgenic mice by PCR. The genotypes of all transgenic mice were analysed by PCR. For amplification of the specific allele, genomic DNA was isolated from tail biopsies and PCR reactions were performed in a total volume of 25 μ l using an automatic thermocycler. After amplification 15 μ l of all PCR products were analysed by agarose gel electrophoresis.

Table 10: Composition of a 25µl standard PCR mix

Reagent	Stock conc.	1x Vol.
5x GoTaq Flexi Buffer	5x	5µl
dNTPs	1,25mM	5µl
MgCl ₂	25mM	1,5µl
DMSO	100%	1,3µl
Primer 1 (forward)	50pmol/µl	0,3µl
Primer 2 (reverse)	50pmol/µl	0,3µl
GoTaq DNA polymerase	5U/µl	0,2µl
ddH ₂ O		9,4µl
Genomic DNA	ca. 200-500ng	2µl

Table 11: PCR amplification conditions

Genotype	Primer	Product size	Amplification conditions		
Tg floxed LacZ-PrP^{Q167R}	LacZ_ROSA_for LacZ_ROSA_rev	314bp	95°C	5min	
			95°C	30s	
			60°C	30s	33cycles
			72°C	40s	
			72°C	5min	
Tg floxed LacZ-PrP^{Q167R}	PrP_167_for PrP_167_rev	203bp	95°C	5min	
			95°C	30s	
			60°C	30s	33cycles
			72°C	30s	
			72°C	5min	
NF-L-Cre Hb9-Cre	Cre_for Cre_rev	206bp	95°C	5min	
			95°C	30s	
			56°C	30s	33cycles
			72°C	30s	
			72°C	5min	
Lox2 (floxed <i>Prnp</i>)	P5 Nco	370bp	95°C	5min	
			95°C	40s	
			61°C	40s	33cycles
			72°C	40s	
			72°C	5min	
<i>Prnp</i>^{-/-} <i>Prnp</i>^{+/-}	P3 P10 P3' NC	<i>Prnp</i> ^{0/0} : 362bp	95°C	5min	
			95°C	30s	
		<i>Prnp</i> ^{0/+} : 568bp	60°C	30s	33cycles
			72°C	40s	
					72°C

4.2.3.2 PCR analysis of Cre-recombination. Cre mediated recombination of the DNA in different tissues of double transgenic mice was checked by PCR. Genomic DNA from brain and spinal cord tissue was isolated and PCR reactions were performed in a total volume of 25µl using the same mastermix composition as listed in table 10. Primers, PCR conditions and product sizes for the analysis of Cre-recombination in the different transgenic mice are given in table 12. After amplification 15µl of all PCR products were analysed by agarose gel electrophoresis.

Table 12: PCR conditions to analyse Cre-recombination

Genotype	Primer	Product size	Amplification conditions		
Tg floxed LacZ-PrP^{Q167R}/NF-L-Cre or Hb9-Cre	LoxP1_for LoxP2_PrP_rev	226bp	95 °C	5min	
			95 °C	30s	
			58 °C	30s	35cycles
			72 °C	30s	
			72 °C	5min	
lox2^{0/+}/NF-L-Cre or Hb9-Cre	P5 3'loxP3	360bp	95 °C	5min	
			95 °C	40s	
			61 °C	40s	33cycles
			72 °C	40s	
			72 °C	5min	

4.2.4 Copy number studies in Tg floxed LacZ-PrP^{Q167R} mice

Quantitative real time PCR (qPCR) is a technique based on the polymerase chain reaction that allows amplification and simultaneous quantification of a target nucleic acid. A common method of dsDNA quantification is the use of fluorescent dyes such as SYBR Green I. Binding of SYBR Green I to dsDNA causes fluorescence of the dye. Each round of amplification leads to an increase in PCR-product and therefore to an increase in fluorescence intensity. A certain threshold is set at the beginning of the log-linear phase. The first clear increase in fluorescence intensity can be measured, when the amplification passes into the exponential phase. At this timepoint the fluorescence signal reaches the threshold value and the cycle number is given as the Ct-value. The Ct-values of the sample and a reference are compared, allowing DNA concentrations to be quantified [Higuchi *et al.*, 1993]. Target nucleic acids can be quantified using either absolute or relative quantification. Absolute quantification determines the absolute amount of a target nucleic acid by relating the PCR signal to a standard curve, whereas relative quantification estimates the ratio between the amount of target nucleic acid to a reference.

In this work transgene copy numbers of different Tg floxed LacZ-PrP^{Q167R} mice were measured by relative quantification. The $2^{-\Delta\Delta Ct}$ method [Livak and Schmittgen, 2001; Ferreira et al., 2006] was used to estimate copy numbers of the *Prnp* gene in each sample of genomic DNA. This method requires two main pre-requisites. The first is the existence of at least one calibrator sample consisting of template DNA with known copies of the studied gene. The second is the need to have a house-keeping gene of constant copy numbers in each sample permitting normalization of the quantitative data.

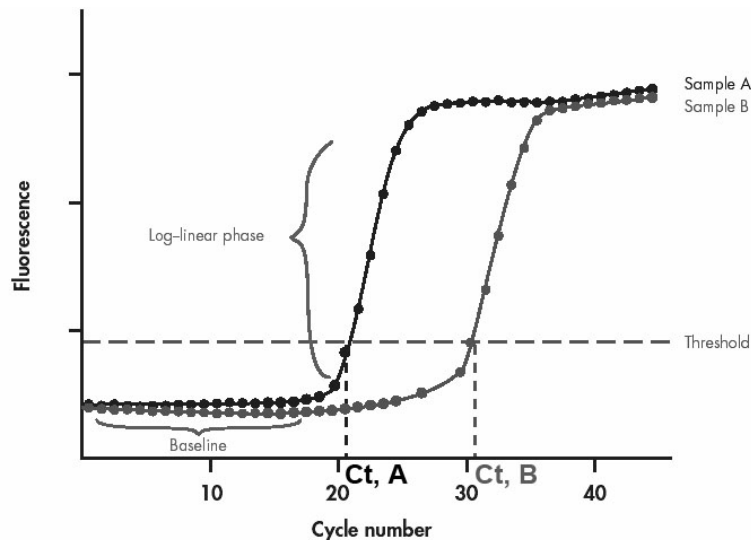


Figure 12: Typical amplification plot of a real time PCR. Adapted from Qiagen handbook.

In this study genomic DNA from *Prnp*^{+/+}-mice or *Prnp*^{+/-}-mice and were taken as calibrators, mouse *Actb* served as house-keeping gene. Samples from *Prnp*^{0/0}-mice and samples without DNA were used as negative controls.

Absolute copies were calculated as follows:

$$\Delta\Delta Ct = (Ct_{Prnp} - Ct_{Actb})_{unknown\ sample} - (Ct_{Prnp} - Ct_{Actb})_{calibrator}$$

$$n\ fold = 2^{-\Delta\Delta Ct}$$

$$absolute\ copies = n\ fold * copies\ calibrator$$

Genomic DNA was isolated from tail biopsies and the DNA concentration was adjusted to 10ng/ μ l. Individual real-time PCR reactions were carried out in 20 μ l volumes in Optical Tubes containing 10 μ l AbsoluteTM QPCR SYBR Green Low ROX Mix, 8,2 μ l ddH₂O, 0,8 μ l Primer Mix (stock: 10pmol/ μ l) and 10ng genomic DNA. For the amplification of *Prnp* the primers PrP_167_for and PrP_167_rev and for the amplification of *Actb* the primers Actin_for and Actin_rev (3.3) were utilized. Real-time PCR was performed in the ABI PRISM 7500 with 15min of pre-incubation at 95°C (activation of the

polymerase) followed by 35 cycles at 95 °C for 30s (denaturation), 60 °C for 30s (annealing of the primers) and 72 °C for 40s (elongation and fluorescence read-out) followed by 10min at 72 °C (termination). In addition melting-curve analysis were performed at the end of each PCR assay to control the specificity of the reaction. Specific reactions should result in a single melting peak corresponding to the PCR product being amplified. Each individual sample was run in doublets and the Ct-value of each tube was recorded. The average and standard deviation (SD) was determined and the average value was accepted if the failure rate was $\leq 5\%$ [Ferreira *et al.*, 2006]. Absolute gene copy numbers were calculated according to the equations given above and rounded to a whole number.

4.2.5 Restriction enzyme digestion of DNA

Restriction enzymes are a class of bacterial endonucleases that protect bacteria from viral infections by cleaving foreign DNA molecules. Restriction endonucleases are classified into three different types depending on their subunit composition, cofactor requirement etc. Type II restriction enzymes are the only class used in the laboratory for DNA analysis and gene cloning. They cut DNA at defined positions close to or within their recognition sequence, usually a short (4-8bp) palindromic DNA sequence [Roberts, 1976].

Restriction enzyme digestion of DNA fragments was performed by incubating ds-DNA with an appropriate amount of restriction enzyme in its respective buffer conditions as recommended by the supplier. Standard digestions include 2-10U of restriction enzyme per 1 µg of DNA or 22 µl of PCR product. The reaction was incubated for 1-3h at 37 °C.

4.2.6 Agarose gel electrophoresis of DNA

Agarose gel electrophoresis is used to separate nucleic acid fragments according to their size. Larger fragments move more slowly through the gel matrix than smaller ones when an electric field is applied. Depending on the size of the DNA fragments 0,8-3% agarose gels in 1xTAE were prepared. Depending on the agarose concentration, a constant electric field of 80-180V was applied to separate the DNA fragments. After electrophoresis the gel was stained in EtBr-solution and analysed in ultraviolet light.

4.2.7 Production of adeno-associated virus vectors (dsAAV2-Cre) expressing Cre-recombinase

The double-stranded recombinant adeno-associated virus vector expressing Cre-recombinase (dsAAV2-Cre) was cloned and produced in the lab of Prof. T. Cathomen. The structure and a schematic overview of the virus production in cell culture are given in Fig. 13. The recombinant dsAAV2-Cre vector consisted of 2 inverted terminal repeats (ITR), a cytomegalo virus (CMV) promoter and the *Cre* gene of Enterobacteria phage P1. For better detection of Cre expression and to direct Cre-recombinase into the cell nucleus of the target cells, a haemagglutinin tag (HA) and a nuclear localization signal (NLS) were introduced upstream of the *Cre* open reading frame. Because of a special modification in the terminal resolution site (*trs*) of the ITR, the viral DNA remains double-stranded, leading to enhanced gene expression in eukaryotic cells. Moreover a bovine growth hormone polyadenylation signal (bGH PolyA) was placed downstream of *Cre* in order to increase gene expression and protein production in transgenic mice.

dsAAV2-Cre was produced in a helper virus free system. Briefly 293T-cells were co-transfected with the recombinant dsAAV2 DNA encoding for Cre-recombinase, a plasmid carrying *rep/cap* packaging signals and a helper plasmid providing distinct adenovirus gene products necessary for dsAAV2-production. Two days after 293T cell transfection, supernatants containing dsAAV2-Cre virions were harvested. Furthermore dsAAV2-Cre was purified and concentrated via dialysis and the virus titer (genomic particles/ml) of each batch was determined by real time PCR.

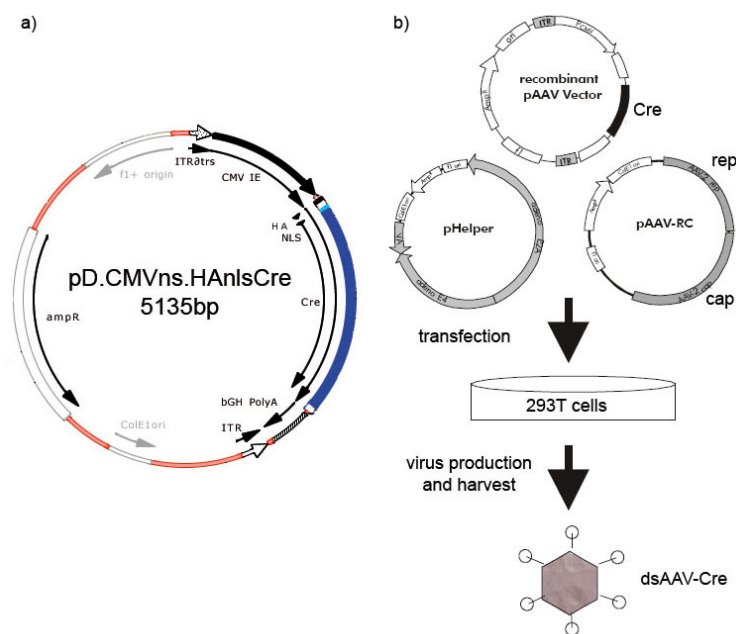


Figure 13: Structure and production of recombinant ds-AAV-Cre particles. a) structure of the recombinant pD-dsAAV2-Cre vector, b) dsAAV-Cre production in a helper-free system. Adapted from Invitrogen handbook.

4.3 Cell culture techniques

4.3.1 Culture conditions, passaging and seeding of cells

Human embryonic kidney cells (293T) were kept in T75 culture flasks containing Op-tiMEM growth medium. Cells were cultured at 37°C in a humidified incubator in 5% CO₂. Cells were passaged at 70-80% confluency. Therefore cells were washed twice with sterile PBS and covered with 2ml ATV. After 1min ATV was removed and cells were incubated at 37°C for 3min before 10ml of growth media was added and cells were resuspended in the medium. A 1:10 dilution of cells in growth medium was made and cells were replaced in a fresh culture flask. For counting of cells, 15µl of cell suspension was mixed with 15µl of trypan blue and cell counting was performed using a Neubauer chamber. For transient transfection, 10⁶ cells were seeded in a 10cm culture dish.

$$\text{cells/ml} = \text{mean}_{(\text{cell count of 4 squares})} * \text{dilution factor} * 10^4$$

4.3.2 Transient calcium-phosphate transfection of 293T cells

10⁶ 293T cells were seeded in a 10cm culture dish. A culture flask containing OptiMEM growth medium was kept o/n at 37°C in the incubator to allow equilibration. The next day the medium was replaced by 4ml of equilibrated medium. For each transfection a 500µl DNA-mix, containing 15µg of plasmid DNA and 50µl 2,5M CaCl₂ in Ampuwa water, was prepared and 2ml of 2xHeBs buffer was placed in a FACS tube. The 500µl DNA-mix was added dropwise to the 2xHeBs buffer, while air was bubbled through the solution in order to enhance the formation of CaCl₂ crystals [Wigler *et al.*, 1979]. The DNA/2xHeBs mix was incubated for 30min at room temperature and then added dropwise to the plated cells. The next day 200µl sodium butyrate was added and cells were incubated at 37°C for 4-12h. After butyrate treatment the medium was replaced and cells were harvested for FACS analysis or western blot.

4.3.3 Fluorescence-activated cell sorting (FACS)

Fluorescence-activated cell sorting (FACS) is a method for sorting and characterization of individual cells by a fast quantitative recording of fluorescent signals. Proteins on the cell surface, which are labeled by antibodies coupled to fluorescent dyes can be analyzed. In this study FACS analysis was performed to study the expression of PrP^{Q167R} on the cell surface of 293T-cells after transfection with PrP^{Q167R} expressing plasmids.

Therefore transfected 293T cells were washed 2x with 10ml PBS (4°C) and incubated in 5ml PBS/20mM EDTA at 37°C for 2min to detach the cells from the surface.

Cells were collected, counted and 10^5 cells were transferred into a FACS tube. 2ml of FACS buffer was added and cells were centrifuged at 1300rpm for 5min. The supernatant was discarded and the 1st antibody, diluted in 250 μ l was added to the cell pellet. Cells were incubated on ice for 1h. 3ml FACS buffer was added and cells centrifuged at 1300rpm for 5min. The 2nd antibody in 250 μ l was added to the pellet and cells were again incubated on ice for 1h. After washing 3x with 3ml of FACS buffer, cells were resuspended in 250 μ l FACS buffer and the fluorescence was measured in a FACScalibur system.

Table 13: Antibodies for immunodetection in FACS analysis

Primary antibody	Stock	Dilution
monoclonal mouse anti-PrP (clone 3F4)	2mg/ml	1:500 in FACS buffer
anti-PrP B2-43	1mg/ml	1:500 in FACS buffer
Secondary antibody		
goat anti-mouse IgG/FITC	1mg/ml	1:100 in FACS buffer

4.3.4 X-Gal assay to detect β -galactosidase in 293T cells

X-Gal ($C_{14}H_{15}BrClNO_6$) is an organic compound consisting of galactoside linked to indole that is cleaved by the bacterial enzyme β -galactosidase (β -gal). The cleavage results in a dark blue precipitate. X-Gal can be used to indicate whether β -gal, which is encoded by the *LacZ* gene, is expressed in cells or a certain tissue. 2 to 3 days after transfection, 293T cells were washed with PBS and 5ml of fix solution was added. Cells were incubated at 4 °C for 5min, washed 3x with PBS, covered with 5ml of staining solution and incubated at 37 °C for 2h. Cells were rinsed with PBS and analysed by light microscopy or stored at 4 °C.

4.3.5 293T cell lysis for western blot analysis

Transfected cells were washed with icecold PBS, collected and centrifuged at 1300rpm for 5min. The pellet was resuspended in 1ml PBS and centrifuged again at 2000rpm for 5min. 200 μ l of lysis buffer was added and the pellet was incubated on ice for 5min. After centrifugation at 1000rpm for 1min, the supernatant was collected and stored at -20 °C for western blotting.

4.4 Biochemical methods

4.4.1 Preparation of tissue homogenates

To prepare 10% (w/v) brain and spinal cord homogenates, 9 volumes of lysis buffer were added to the tissue. 10% (w/v) spleen homogenates were prepared in 9 volumes of sterile PBS + protease inhibitor. Brains were passed through 18-25gauge needles, spinal cords and spleens were homogenized using a micro-pestle prior to passing the tissue through 18-25gauge needles. Finally homogenates were centrifuged at 2000rpm for 5min and the supernatants stored at -20°C until use.

4.4.2 Bradford assay to determine of protein concentrations

Protein concentrations of 10% (w/v) tissue homogenates were quantified using the photometric Bradford protein assay. This assay is based on the observation that the absorbance maximum of Coomassie blue G-250 shifts from 494nm to 595nm when the dye binds to a protein [Bradford, 1976].

Three dilutions of each sample (200x, 400x and 500x) were mixed with Bradford staining solution and the absorption at 595nm was compared to a straight calibration line obtained from a standard BSA dilution series (125-12,5µg/ml). After determination of protein concentrations, 10% homogenates were adjusted to 8mg/ml.

4.4.3 Proteinase-K digestion

For the differentiation between the cellular and the pathogenic form of PrP, a protein digestion with Proteinase K (PK) was performed prior to SDS polyacrylamid gel electrophoresis. Therefore usually 80µg of total protein from 10% (w/v) tissue homogenates were digested with 1,6µg PK for 30min at 37°C. An appropriate amount of 5x SDS sample buffer was added and the samples were boiled at 95°C for 10min in order to stop the enzymatic digestion, denature the proteins and disrupt the disulfide bonds.

4.4.4 Peptide-N-glycosidase F (PNGase F) digestion

Peptide-N-glycosidase F (PNGase F) is an enzyme used for deglycosylation of glycoproteins, such as PrP^C. The glycosidase digestion of brain and spinal cord homogenates with PNGase F was performed as indicated by the manufacturer. After digestion an appropriate amount of 5x SDS sample buffer was added and samples were boiled at 95°C for 10min.

4.4.5 Sodium phosphotungstic acid (NaPTA) precipitation of PrP^{Sc}

The precipitation of PrP^{Sc} from spleen and spinal cord homogenates was done according to the protocol published in [Safar *et al.*, 1998]. 10% (w/v) tissue homogenates were prepared, protein concentrations were determined and samples were adjusted to 8mg/ml. To 1000µg/200µg of total protein 125µl/25µl 4% sarkosyl was added and samples were incubated at 37°C for 15min. For the removal of nucleic acids, samples were digested with 5µl/1µl benzonase and 5µl/1µl 50mM MgCl₂ was added. Samples were incubated at 37°C for 30min. In order to specifically precipitate PrP^{Sc}, samples were treated with PK. To 1000µg total protein 27,5µl PK (0,215mg/ml) was added and digestions were carried out at 37°C for 30min. 200µg samples remained untreated. Afterwards samples were treated with 25µl/5µl 4% NaPTA and 47,5µl/9,5µl protease inhibitor was added. Samples were incubated again at 37°C for 30min and then centrifuged for 30min at 14000rpm (18°C) before the pellets were resuspended in 15µl 0,1% sarkosyl and boiled in 5x SDS sample buffer at 95°C for 10min.

4.4.6 SDS polyacrylamid gel electrophoresis

Sodium dodecyl sulfate polyacrylamid gel electrophoresis (SDS-PAGE) is a technique used to separate proteins according to their electrophoretic mobility [Laemmli, 1970]. The proteins are denatured and rendered monomeric by boiling in the presence of disulfide bond reducing agents (e. g. β -mercaptoethanol) and anionic detergents like SDS. SDS unfolds the structure of a protein and applies a uniform negative charge along the length of the polypeptide. The distance a SDS-denatured protein migrates through the gel during electrophoresis can be directly related to its molecular mass.

Protein samples were denatured at 95°C for 10min in 5x SDS sample buffer and separated through a 12% Tris-Glycine gel in SDS running buffer, applying a constant current of 150V for ca. 1h. The SDS-PAGE was performed in a Mini Trans-Blot cell.

4.4.7 Western blotting and immunodetection of proteins

Western blot is an analytical technique used to analyse specific proteins in a given sample by antibody detection. It uses gel electrophoresis for protein separation before the proteins are transferred to a membrane where they are immobilized and can be probed with antibodies specific to the target protein [Towbin *et al.*, 1979].

After SDS-PAGE, proteins were transferred to a polyvinylidene difluoride membrane (PVDF). Prior to blotting the PVDF membrane was activated in 100% methanol and immersed in transfer buffer. Proteins were blotted according to the wet blot method for 1,5h applying a constant current of 350mA (Mini Trans-Blot cell). The blotted membrane was blocked over night at 4°C in TBST/MP. After blocking the membrane was

incubated for 1h at room temperature in TBST/MP containing the primary antibody in an appropriate dilution (table 14), then washed 2x 10min in TBST and afterwards incubated 1h at room temperature in TBST/MP containing the respective secondary antibody conjugated to horseradish peroxidase. Excess antibodies were removed by washing the membrane 4x 10min in TBST. Membranes were developed on X-ray films using the SuperSignal West Pico Chemoluminescent substrate according to the suppliers protocol.

Table 14: Antibodies for immunodetection in western blot

Primary antibody	Stock	Dilution
monoclonal mouse anti- β -actin (clone AC-15)	1mg/ml	1:20 000 in TBST/MP
mouse anti- β -galactosidase	1mg/ml	1:5000 in TBST/MP
monoclonal mouse anti-PrP (clone 3F4)	2mg/ml	1:5000 in TBST/MP
monoclonal mouse anti-PrP SAF32	1mg/ml	1:5000 in TBST/MP
anti-PrP B2-43	1mg/ml	1:10 000 in TBST
monoclonal mouse anti-Cre	2mg/ml	1:10 000 in TBST/MP
Secondary antibody		
HRP-rabbit anti-mouse IgG1	1mg/ml	1:10 000 in TBST/MP
HRP-rabbit anti-mouse IgG2a	1mg/ml	1:10 000 in TBST/MP

4.4.8 Stripping and re-exposure of western blot membranes

If necessary membranes were stripped to allow exposure of a different set of antibodies. Therefore membranes were washed 3x 10min in stripping buffer and 2x 10min in TBST to readjust the pH value. Afterwards membranes were probed again with primary and secondary antibody.

4.4.9 Densitometric analysis of protein signals

For quantification of PrP signals in brain and spinal cord homogenates of transgenic mice, PVDF membranes were analysed in a LAS-3000 Darkbox. Digital images of chemoluminescent signals were obtained using the Image Reader LAS-3000 software. Signal intensities ratios were quantified using the AIDA software. As an internal control PrP signals were normalized to β -actin prior to quantification.

4.5 Histological techniques

4.5.1 Tissue preparation for histological analysis

4.5.1.1 Tissue preparation for X-Gal assay. One-day old transgenic offsprings were sacrificed, the tail was removed for genotyping and the body immediately transferred into 50mL 4% buffered PFA and stored for 48-72h at 4°C. After fixation the tissue was embedded in Tissue TeK and frozen on dry ice. The embedded tissue was kept for 24h in -20°C before 30µm head and body section were prepared on SuperFrost Plus microscope slides using a CM 1900 cryostat. Sections were stored at -20°C until use.

4.5.1.2 Tissue freezing and preparation of frozen sections. Mice were sacrificed and native tail, brain, spinal cord, spleen and pancreas tissue for western blot or PCR analysis was immediately frozen on dry ice and stored at -20°C or -80°C until use. Native brain and spinal cord tissue for immunohistochemical analysis was placed in a cryo tube, embedded in Tissue TeK and frozen on dry ice. The frozen tissue was stored at -20°C until use. 10µm thick sections were prepared on SuperFrost Plus slides using a CM 1900 cryostat. Sections were stored at -20°C until use.

4.5.1.3 Paraffin embedding and preparation of paraffin sections. Mice were sacrificed and brain, spinal cord and spleen tissue was recovered and immediately transferred into a 15ml falcon tube containing 15ml 4% buffered PFA. The tube was sealed and stored for at least 24h. Prion-infected material was inactivated for 1h in 98-100% formic acid, again rinsed in 4% PFA before the dehydration process was accomplished by passing the tissue through a series of increasing EtOH concentrations (70-100%). The dehydrated tissue was embedded in paraffin wax and 5µm sections were prepared using a microtome. Sections were floated in a 40°C water bath to allow spreading and subsequently transferred onto SuperFrost Plus slides. Dried sections were stored at room temperature until further use.

4.5.2 X-Gal assay to detect β -galactosidase (β -gal)

After thawing 30µm head and body sections were shortly air dried and washed 3x for 15min at room temperature in rinse buffer. For X-Gal staining slides were incubated over night in the dark at 37°C in staining solution. X-Gal was diluted from a 40mg/ml stock in dimethylformamide. The staining solution was poured off and slides were washed in PBS. To intensify the blue staining slides were stored for several hours in PBS at 4°C. Finally sections were mounted with Aquatex and analysed by light microscopy.

4.5.3 Immunohistochemistry (IHC)

4.5.3.1 IHC of β -gal and neuron-specific nuclear protein (NeuN). To show the expression of the marker gene *LacZ* in neurons of the brain and spinal cord of Tg floxed *LacZ-PrP^{Q167R}* mice, a co-staining of β -gal and the NeuN was accomplished. Frozen sections were marked with PAP-pen and fixed for 2min in ice-cold acetone. After fixation and 3x 5min of washing in TBS-T, sections were blocked in IHC blocking-buffer for 1h at room temperature in a humid chamber. Blocking was followed by an over-night incubation at 4°C (humid chamber) with primary antibodies, mouse anti- β -gal and biotin-conjugated mouse anti-NeuN. After washing 3x 5min in TBS, sections were incubated for 1h at room temperature with secondary antibodies, Alexa Fluor 488 Fab2 rabbit anti-mouse IgG and Streptavidin-Texas Red (table 14). Sections were washed again 3x 5min in TBS-T before they were covered with fluorescent mounting medium.

4.5.3.2 IHC of β -gal and wisteria floribunda agglutinin (WFA). To detect the expression of *LacZ* in the red nucleus (*Nucleus ruber*) of Tg floxed *LacZ-PrP^{Q167R}* mice, an IHC co-staining of β -gal and WFA was performed on 10 μ m native cryo brain sections. WFA is a lectin that labels selectively N-acetylgalactosamines beta 1 residues of glycoproteins within the extracellular matrix of distinct neuron populations, e. g. neurons of the red nucleus. Frozen brain sections were marked with PAP-pen and fixed for 2min in ice-cold acetone. After fixation and 3x 5min of washing in TBS, sections were blocked for 1h at room temperature in a humid chamber using IHC blocking-buffer. Blocking was followed by an over-night incubation at 4°C (humid chamber) with primary antibodies mouse anti- β -gal and biotin-conjugated anti-WFA. After washing 3x 5min in TBS, sections were incubated for 1h at room temperature with secondary antibodies Alexa Fluor 488 Fab2 rabbit anti-mouse IgG and Streptavidin-Texas Red (table 15). Sections were washed 3x for 5min in TBS and covered with fluorescent mounting medium.

4.5.3.3 IHC of 3F4 tagged PrP^{Q167R}. For IHC detection of PrP^{Q167R} frozen brain and spinal cord sections were marked with PAP-pen and fixed for 10min in ice-cold acetone. After fixation and washing (3x 5min TBS-T2), sections were blocked for 1h at room temperature in a humid chamber using IHC blocking-buffer. Blocking was followed by an over-night incubation at 4°C (humid chamber) with the primary antibody mouse anti-PrP-3F4. After washing 1x 5min in TBS-T2 and 2x 5min in TBS, sections were probed at room temperature for 1h with the secondary antibody Alexa Fluor 488 Fab2 rabbit anti-mouse IgG (table 15). Sections were washed 1x 5min in TBS-T2 and 2x 5min in TBS and covered with fluorescent mounting medium.

4.5.3.4 Hematoxylin-eosin (HE) staining. To remove the paraffin wax, paraffin sections were washed 2x 10min in xylol and then passed through an EtOH serial with decreasing concentrations (100%, 96% and 70%, 2x 5min each). Afterwards sections were shortly rinsed in ddH₂O and stained for 15min in Mayers hemalaum solution. The stained sections were rinsed for 10min in running tap water, washed 1min in ddH₂O and were co-stained for 1-5min in 1% (w/v) eosin. After eosin staining, sections were dehydrated by washing 1x 1min in 96% EtOH, 2x 2min in 100% EtOH and 2x 10min in xylol before they were mounted with Entellan.

4.5.3.5 Glial fibrillary acidic protein (GFAP) immunohistochemistry. A GFAP staining was performed on paraffin brain sections to visualize activated astrocytes in brains of scrapie affected mice. Sections were washed 2x 10min in xylol and then passed through an EtOH serial with decreasing concentrations (100%, 96% and 70%, 2x 5min each). To reexpose the antibody epitopes in the fixed tissue, sections were boiled for 5min in citrate-buffer and then cooled down in TBS for 10min. After a short rinse in ddH₂O, the endogenous peroxidase was inactivated by a 15min treatment in 0,7% (v/v) hydrogen peroxide. The sections were washed in TBS, blocked for 30min in 10% (v/v) goat serum and incubated over night at 4°C (humid chamber) with the primary antibody rabbit anti-GFAP (table 15). For the detection of rabbit anti-GFAP, the Link and Label system was used according to the suppliers instructions. Sections were washed in TBS and developed with 3-Amino-9-Ethylcarbazol (AEC) and co-stained with hemalaum.

Table 15: Antibodies for IHC detection

Primary antibody	Stock	Dilution
mouse anti- β -galactosidase	1 mg/ml	1:250 in IHC-blocking buffer
biotin-conjugated mouse anti-NeuN	1 mg/ml	1:250 in IHC-blocking buffer
biotin conjugated anti-WFA	1 mg/ml	1:750 in IHC-blocking buffer
mouse anti-PrP 3F4	2mg/ml	1:2000 in IHC-blocking buffer
rabbit anti-GFAP	1 mg/ml	1:300 in 10% goat serum
Secondary antibody		
Alexa Fluor 488 Fab2 rabbit anti-mouse IgG	1 mg/ml	1:1000 in IHC-blocking buffer
Streptavidin-Texas Red	1 mg/ml	1:1000 in IHC-blocking buffer
Polylink secondary Ab (biotin-conj.)		ready-to-use
Label streptavidin label (HRP-conj.)		ready-to-use

5 Results

5.1 Transgenic mice with inducible expression of dominant-negative PrP^{Q167R} in motor neurons

5.1.1 Generation and characterization of Tg floxed LacZ-PrP^{Q167R} mice

Structure and recombination of transgenic DNA for nuclear injection. The transgenic DNA for nuclear injection consists of the human ubiquitin C (UbiC) promoter followed by a floxed *lacZ* marker gene and the dominant-negative *Prnp* mutant *Prnp*^{Q167R}. For optimal expression in transgenic mice, a murine β -globin intron was introduced downstream of the promoter and a polyadenylation signal (poly-A) was inserted. To distinguish between *Prnp*^{Q167R} and endogenous wild-type *Prnp*, a PvuI restriction site was generated simultaneously to the Q→R mutation at codon 167. Moreover, the hamster-specific 3F4-tag [Kascsak *et al.*, 1987] was introduced into *Prnp*^{Q167R} by a L→M and V→M mutation at codon 108 and 111, respectively. Therefore the PrP^{Q167R} protein can be detected by the monoclonal anti-PrP-3F4 antibody, which does not react with wild-type mouse PrP (Fig 14).

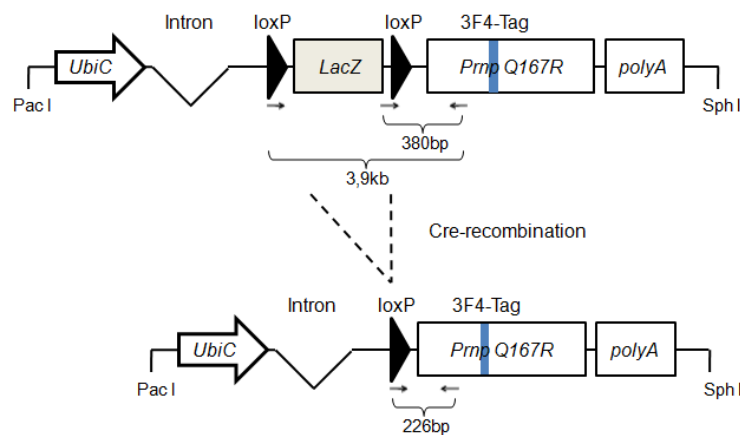


Figure 14: Structure and recombination of the transgenic DNA used for pronuclear microinjection. Cre-recombination can be detected on DNA level. The recombinant DNA yields a 226bp PCR product.

In Tg floxed LacZ-PrP^{Q167R} mice *LacZ* is expressed ubiquitously, the dominant-negative *Prnp*^{Q167R} mutant remains silent. Expression of PrP^{Q167R} is achieved by mating Tg floxed LacZ-PrP^{Q167R} mice to a Cre-strain, with Cre-recombinase under control of a tissue specific promoter. Cre belongs to an integrase family of site-specific recombinases and catalysis the recombination between two palindromic loxP recognition sites [Nagy, 2000]. Depending on the expression pattern of Cre, the loxP-flanked *LacZ* marker gene is deleted, leading to the expression of PrP^{Q167R} in the cells of interest.

Functionality of the transgenic construct in cell culture. Expression and recombination of the transgenic construct pLL4-UbiC-floxed-LacZ-PrP^{Q167R}-3F4 (pLL4-Tg) was verified in cell culture. Human embryonic kidney cells (293T cells), which are per se devoid of PrP, were co-transfected with pLL4-Tg and a Cre-expressing vector designated pMC-Cre [Gu *et al.*, 1993]. X-gal staining of pLL4-Tg transfected cells revealed strong expression of enzymatically active β -galactosidase (β -gal) as indicated by a blue precipitate (Fig 15A).

FACS analysis of transfected 293T cells exhibited PrP^{Q167R} expression only in the presence of Cre. As PrP^{Q167R} was detectable by several anti-PrP antibodies, targeting different epitopes of PrP (anti-PrP-3F4: aa 108-111; anti-PrP B2-43: aa 146-151), we assumed that transgenic PrP^{Q167R} had normal conformation and was functionally exposed on the cell surface of 293T cells. The expression level of PrP^{Q167R} after Cre-recombination was comparable to a control plasmid (pCG-CMV-PrP^{Q167R}-3F4), providing PrP^{Q167R} under control of a strong viral promoter derived from cytomegalovirus (CMV). 293T cells transfected with pLL4-Tg alone, were PrP-negative as compared to cells expressing β -gal from pAD-MD-CMV-LacZ (Fig 15B).

In order to investigate Cre-recombination on DNA-level, genomic DNA was isolated from transfected cells and checked for recombinant DNA by PCR. The recombinant allele yielded a PCR product of 226bp, while the transgenic DNA including the *LacZ* gene yielded a 380bp product (Fig 14). Recombinant DNA was found exclusively in cells, which were co-transfected with pLL4-Tg and pMC-Cre (Fig. 15C).

Expression of PrP^{Q167R} was restricted to 293T cells co-transfected with pLL4-Tg and pMC-Cre, as shown by western blot. No leaky expression of PrP^{Q167R} from pLL4-Tg was found. Moreover, western blot analysis confirmed the specificity of the anti-PrP-3F4 antibody to the 3F4-epitope and thus to PrP^{Q167R} as anti-PrP-3F4 was unable to detect wild-type PrP^C in a brain homogenate of C57BL/6 mice (Fig. 15D).

In summary, the results obtained from cell culture experiments proved the functionality of the transgenic construct pLL4-UbiC-floxed-LacZ-PrP^{Q167R}-3F4. Consequently, the transgenic DNA for pronuclear injection UbiC-floxed-LacZ-PrP^{Q167R}-3F4 was released from the vector backbone by PacI/SphI digestion and purified for nuclear injection.

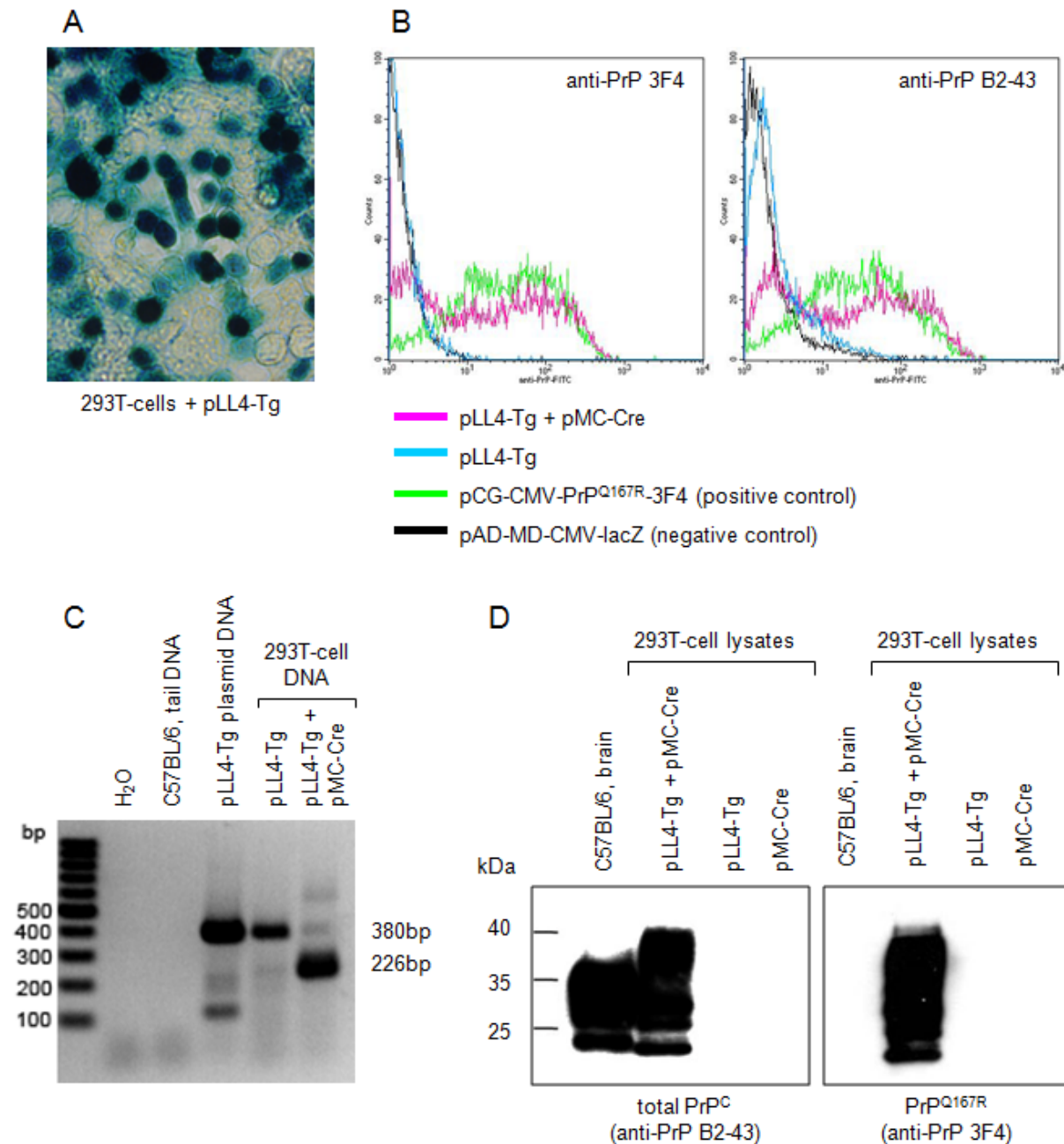


Figure 15: Co-expression of pLL4-UbiC-floxed-LacZ-PrP^{Q167R}-3F4 (pLL4-Tg) and Cre-recombinase in 293T cells. (A) X-gal staining of 293T cells, transfected with pLL4-Tg, revealed strong expression of the *LacZ* marker gene (blue precipitate). (B) FACS analysis of 293T cells, transfected with pLL4-Tg and pMC-Cre. PrP^{Q167R} was detected at the cell surface only in the presence of Cre-recombinase and was recognized by different anti-PrP antibodies. (C) Genomic DNA of 293T cells, co-transfected with pLL4-Tg and pMC-Cre, was analyzed by PCR. Recombinant DNA was only found in the presence of Cre and yielded a PCR product of 226bp. (D) Western blot analysis of 293T cell lysates. PrP^{Q167R} was expressed after Cre-recombination and could be detected by different anti-PrP antibodies.

Generation and characterization of Tg floxed LacZ-PrP^{Q167R} mice. The transgenic DNA was injected into the male pronucleus of fertilized oocytes obtained from C57BL/6 mice. The resulting offsprings were screened for the presence of transgenic DNA by a PCR directed at *LacZ* and *Prnp*^{Q167R}. The *LacZ* PCR resulted in a 314 bp product, while the 203 bp product, amplified from both *Prnp*^{Q167R} and wild-type *Prnp*, needed further PvuI digestion. The unique restriction site introduced into transgenic *Prnp*^{Q167R} resulted in a two-band pattern of the digested PCR product, confirming the presence of the transgenic DNA (Fig 16).

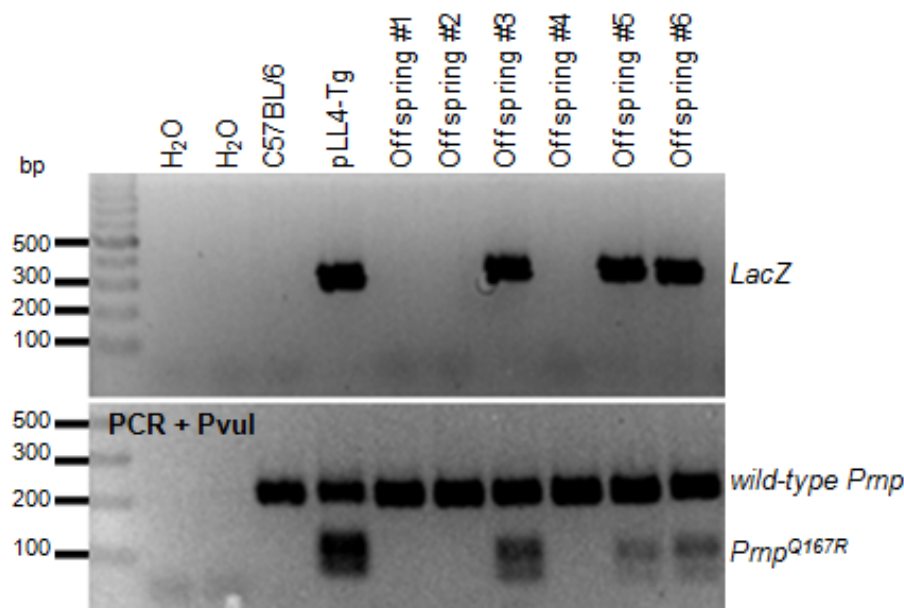


Figure 16: Identification of founder mice obtained from nuclear injection of UbiC-floxed-LacZ-PrP^{Q167R}-3F4. Offsprings were screened by PCR for the presence of the marker gene *LacZ* and *Prnp*^{Q167R}. Transgenic *Prnp*^{Q167R} was distinguished from wild-type *Prnp* by PvuI digestion.

In total 22 founders, carrying the transgenic DNA were identified and further mated to C57BL/6 on a wild-type *Prnp*^{+/+} background. Due to random integration, the expression of pronuclear injected transgenes is often highly variable between different lines containing an identical construct. These position effects are caused by integration of the transgene into transcription control elements of a host gene, a region of imprinting, a non-transcribed heterochromatin region or X and Y chromosomes [Rülicke and Hübscher, 2000]. Therefore each founder line is unique, even if harboring an identical transgene and has to be characterized separately.

F1 progenitors obtained from 22 transgenic lines (Tg115-136) were screened for expression of the marker gene *LacZ* by an enzymatic X-gal assay. Expression of functional β -gal was visualized by a blue precipitate on head and body sections derived from one-day-old offsprings. β -gal expression was evaluated by X-gal staining intensities and related to a relative scale ranging from + to +++++. Six out of 22 transgenic lines expressed the marker gene *LacZ*. The highest expression levels of β -gal in brain and spinal cord were observed in Tg117 and Tg127. These lines exhibited ubiquitous β -gal expression and the strongest X-gal staining intensities in the nervous tissue (Fig 17).

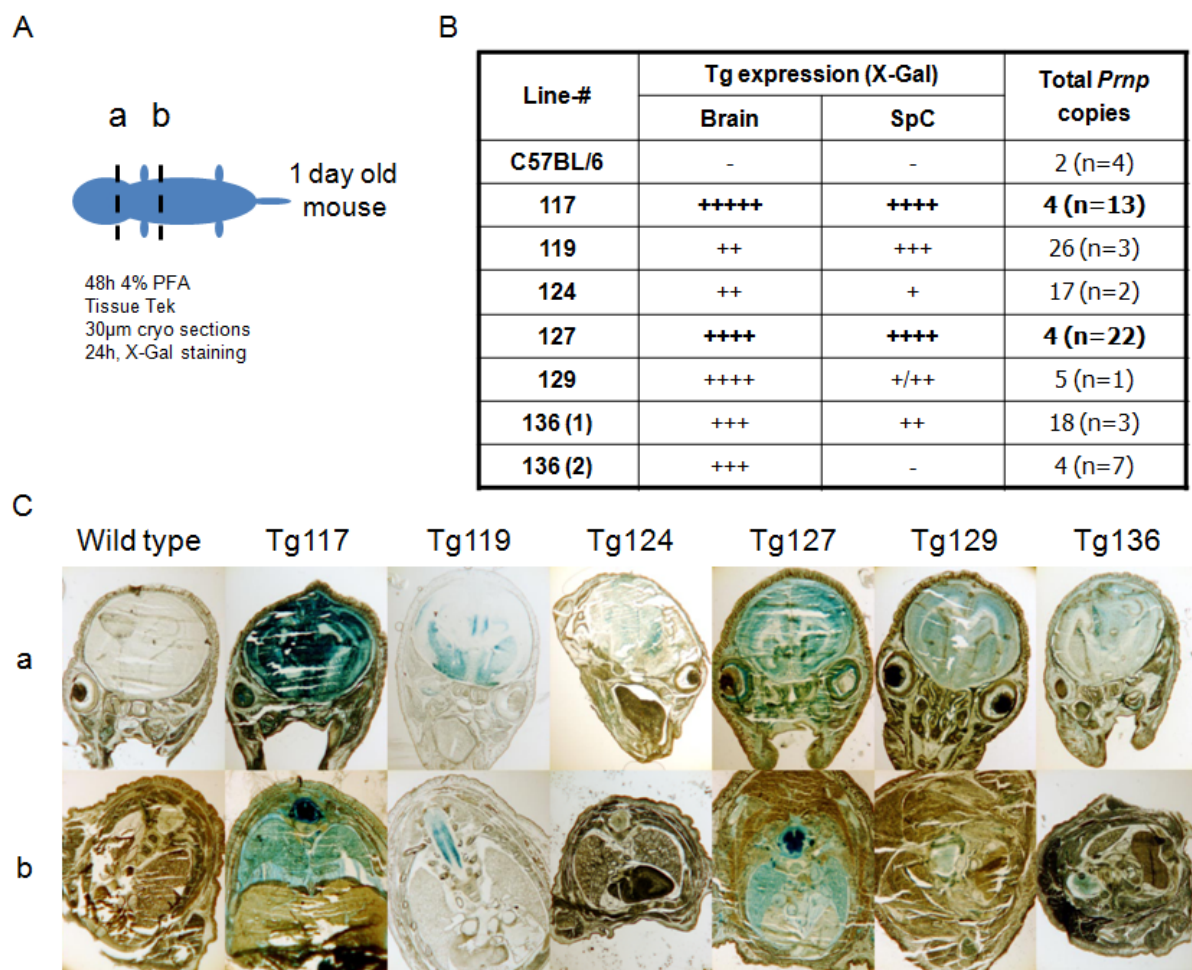


Figure 17: Expression pattern of β -gal and transgene copy numbers in F1 progenitors of different Tg floxed *LacZ*-PrP^{Q167R} lines. (A) Schematic representation indicating the sectional plane for X-gal analysis. a: head sections, b: body sections (B) Overview of transgenic lines: relative marker gene expression in brain and spinal cord was measured by X-gal assay; total *Prnp* copy numbers were calculated by quantitative real time PCR. (C) Comparison of marker gene expression in the different transgenic lines.

In detail, X-gal staining on serial, coronal brain sections of Tg117 and Tg127 displayed strong β -gal expression in cerebellum, various regions of the mid-brain, hippocampus and cortex (Fig 18).

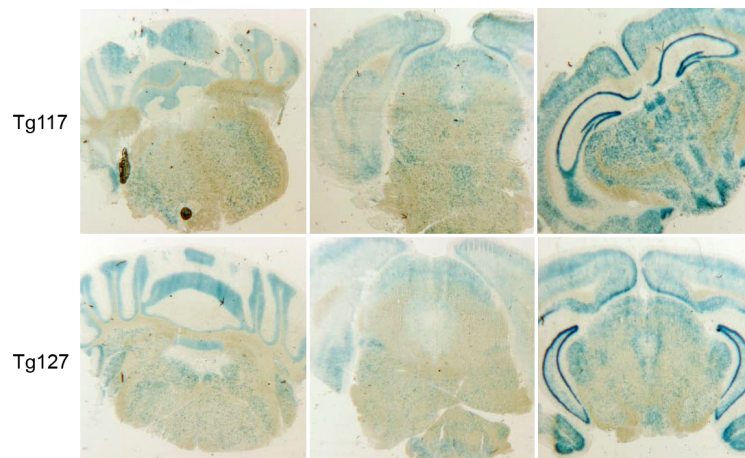


Figure 18: X-gal staining on serial, coronal brain sections of Tg117 and Tg127.

Moreover, total transgene copy numbers were measured by quantitative real time PCR (qPCR) using relative quantification and the $2^{-\Delta\Delta Ct}$ method [Ferreira *et al.*, 2006; Livak and Schmittgen, 2001]. Genomic DNA of *Prnp*^{+/+} and *Prnp*^{+/-} mice were taken as calibrators, mouse *Actb* served as house-keeping gene for normalization. DNA of *Prnp*^{0/0} mice was used as negative control (Fig 19). An average value of 4 *Prnp* copies was measured for Tg117 and also for Tg127. Considering that transgenic mice were bred on a *Prnp*^{+/+} background, both lines carried two copies of *Prnp*^{Q167R} (Fig 17).

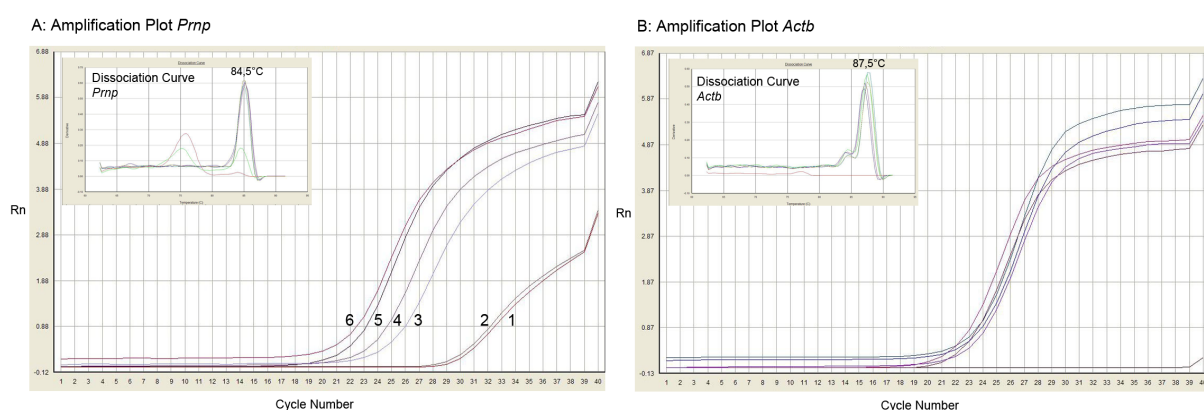


Figure 19: Example of a copy number study in Tg127. (A) Amplification plot and dissociation curve of *Prnp* in different DNA samples. (1) no template control, (2) *Prnp*^{0/0}, (3) *Prnp*^{+/-}, (4) *Prnp*^{+/+}, (5) Tg127 #1, (6) Tg127 #2. (B) Amplification plot and dissociation curve of *Actb*. The Ct value of the different aliquots is in the same range, indicating equal DNA concentration of the analyzed samples. Rn, normalized reporter signal.

Stable inheritance of the transgene is important with regard to consistent experimental conditions. While most transgenic lines showed stable inheritance, transgene segregation into two different gene cluster was observed in line Tg136, suggesting multiple transgene integration sites (Fig 17B). Although all transgenic mice displayed normal behavior, differences in fertility and lifespan were obvious and led to an exclusion of several lines for further analysis and experiments. For example mice of Tg119 tended to develop tumors at the age of about 40 weeks, suggesting that the transgene integrated into a tumor suppressor or oncogene. Mice of Tg129 bred inefficiently with average litter sizes of only 2-3 offsprings, while β -gal expression in Tg124 mice was too weak. Finally, lines Tg117 and Tg127 were chosen for further experiments, because they displayed normal phenotype and behavior, reproduced at high rate heterozygotically and the transgene segregation followed the expected Mendelian inheritance (Tab 16).

Table 16: Breeding efficiencies and transgene inheritance of Tg117 and Tg127 mice.

Breeding	litters (n)	pups/litter mean \pm SD	Tg pups/litter mean \pm SD	TgxCre pups/litter mean \pm SD
Tg117 x C57BL/6	7	6,9 \pm 2,7	3,7 \pm 1,8	
Tg117 x Hb9-Cre	18	10,2 \pm 5,1	4,7 \pm 3,8	2,0 \pm 1,8
Tg117 x NF-L-Cre	22	9,5 \pm 4,4	5,1 \pm 3,5	2,2 \pm 2,0
Tg127 x C57BL/6	9	9,4 \pm 4,7	4,8 \pm 2,5	
Tg127 x Hb9-Cre	21	10,4 \pm 4,9	4,7 \pm 3,3	2,1 \pm 2,3
Tg127 x NF-L-Cre	21	10,7 \pm 2,8	5,5 \pm 2,2	2,8 \pm 1,3

Immunofluorescence analysis revealed co-localization of β -gal and the neuronal marker NeuN in different brain areas responsible for motor control, e.g. in nucleus ruber (Fig 20) and motor cortex (Fig 21) as well as in the hippocampus (Fig 22). Nucleus ruber was labeled by wisteria floribunda agglutinin (WFA). The lectin WFA selectively labels distinct residues of glycoproteins inside the extracellular matrix of neurons and can therefore be used to identify functionally different neuronal populations, e.g. in nucleus ruber or cortex [Brückner *et al.*, 1996]. While nucleus ruber controls tonicity and posture, the motor cortex is involved in the control and execution of voluntary motor functions. Both are connected to each other and to the spinal cord.

In addition expression of the marker gene *LacZ* was observed in neurons of the dorsal and ventral horn of the spinal cord (Fig 23), as indicated by colocalization of β -gal and NeuN (Fig 23).

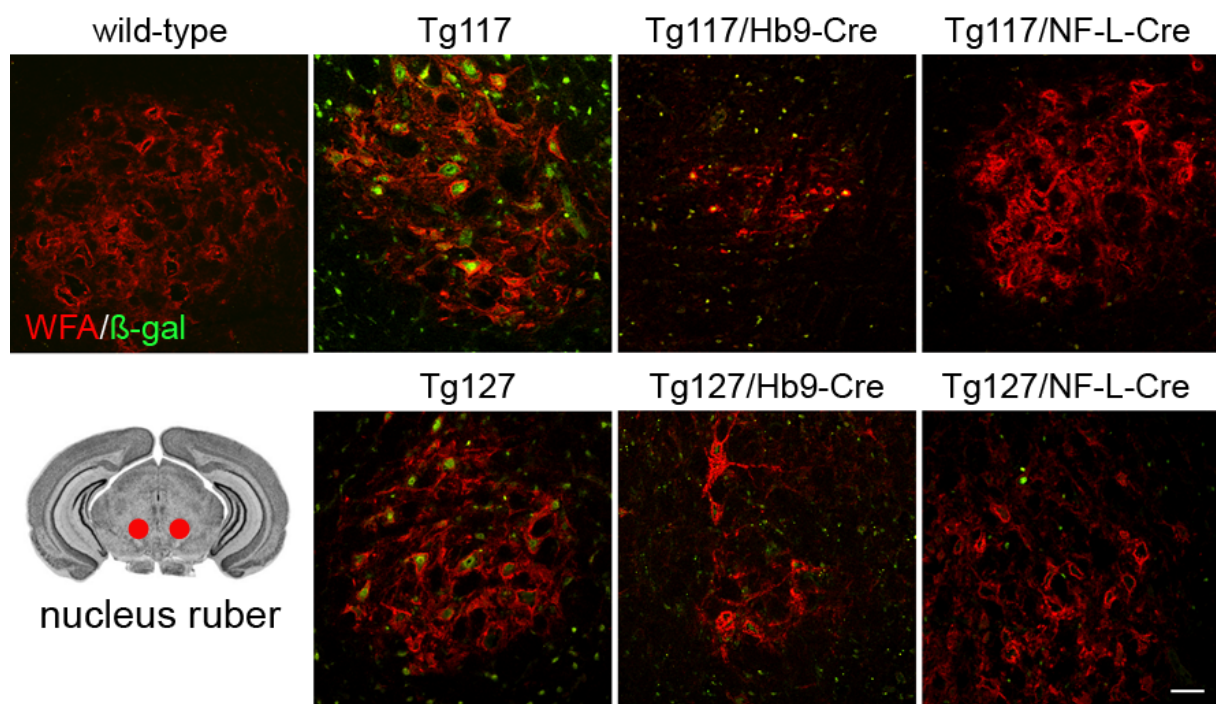


Figure 20: Expression of β -gal in nucleus ruber of transgenic mice. Immunofluorescence showed β -gal (green) in neurons of nucleus ruber in Tg117 and Tg127 mice. Due to the expression pattern of Cre, β -gal expression was diminished in Tg/NF-L-Cre mice but not in Tg/Hb9-Cre. Nucleus ruber was visualized by wisteria floribunda agglutinin (WFA, red), a marker for perineuronal nets. Scale bar: 50 μ m.

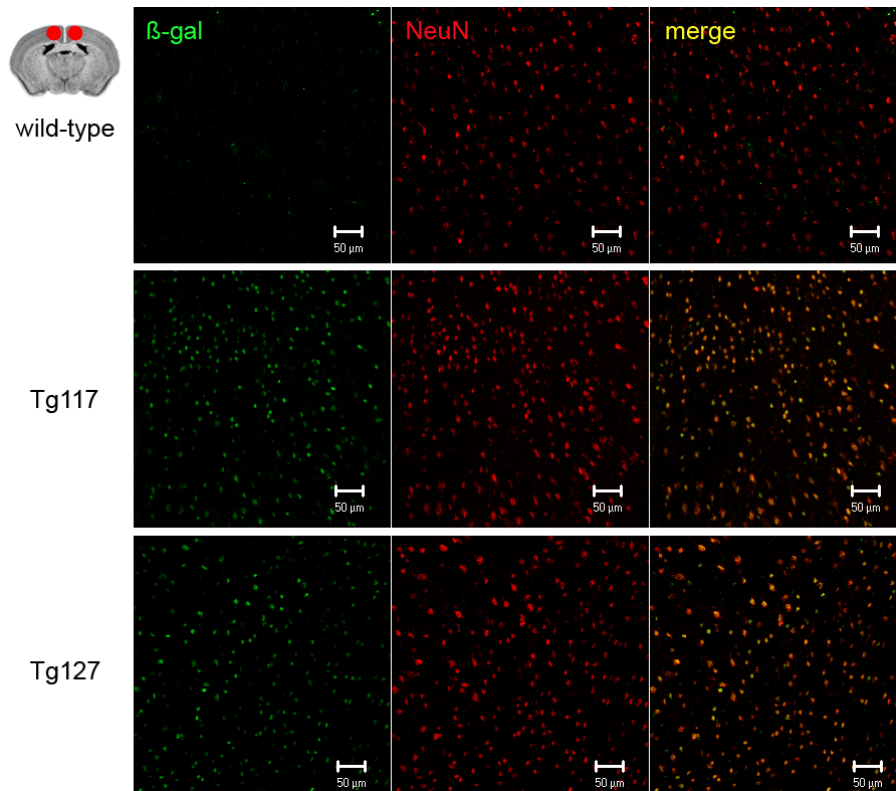


Figure 21: Immunofluorescent labeling exposed co-localization of β -gal (green) and the neuronal marker NeuN (red) in neurons of the motor cortex in Tg117 and Tg127 mice.

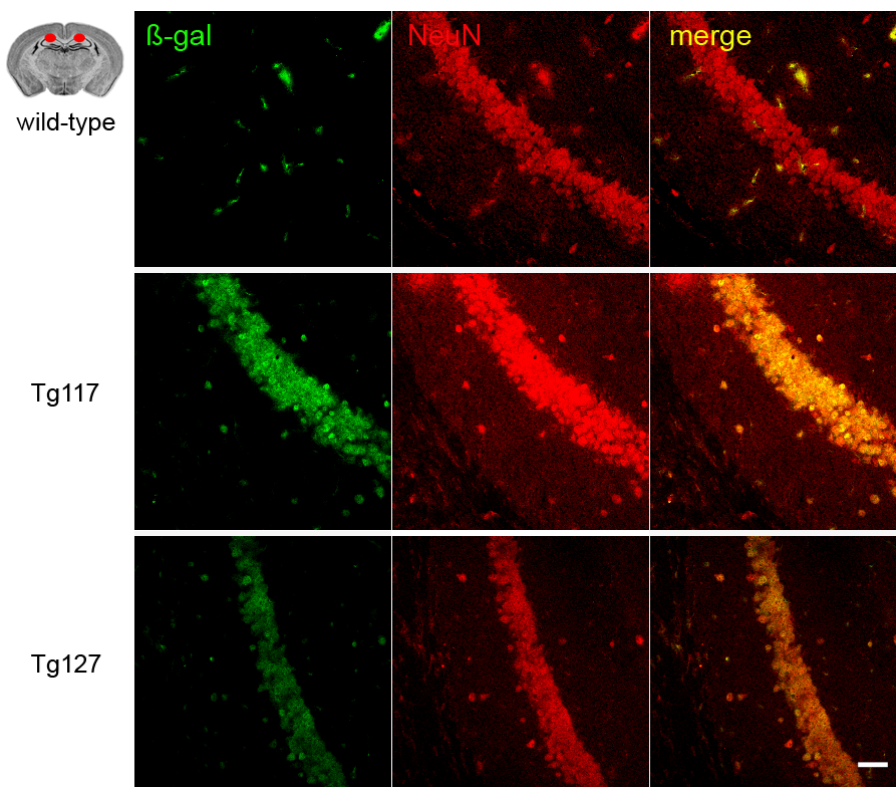


Figure 22: Expression of β -gal (green) in neurons (NeuN, red) of the hippocampus of Tg117 and Tg127 mice, visualized by immunofluorescent staining. Scale bar: 50 μ m.

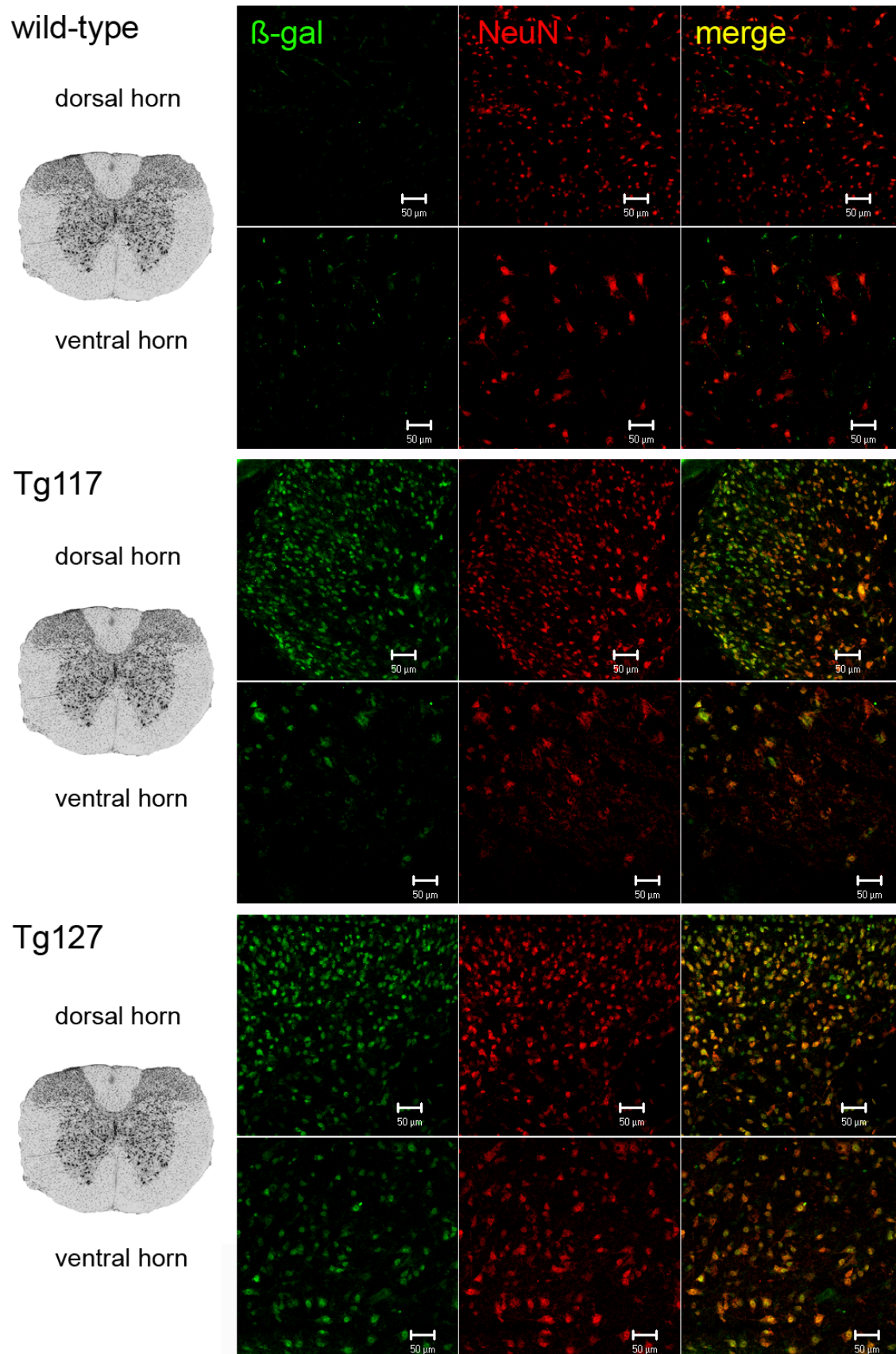


Figure 23: Neuronal expression of β -gal in the spinal cord of Tg117, Tg127 and wild-type mice. Immunofluorescence revealed co-localization of β -gal (green) and NeuN (red) in the dorsal and ventral horn of the spinal cord.

Expression of dominant-negative PrP^{Q167R} after inter-crossing of Tg floxed LacZ-PrP^{Q167R} mice to Cre-strains. Expression of dominant-negative PrP^{Q167R} in motor neurons (MN) was achieved by mating Tg floxed LacZ-PrP^{Q167R} mice to Hb9-Cre or NF-L-Cre strains. Cre expression in the cells of interest led to a deletion of the marker gene *LacZ* in MN of the spinal cord (Hb9-Cre) or in various neurons in brain and spinal cord (NF-L-Cre), inducing expression of protective PrP^{Q167R} on a *Prnp*^{+/+} background (Fig 14).

Cre-mediated recombination of genomic, transgenic DNA was detected by PCR in brain and spinal cord of Tg/NF-L-Cre and to a lesser extent restricted to the spinal cord in Tg/Hb9-Cre, suggesting that Cre-recombination was successful on DNA level in both transgenic lines (Fig 24).

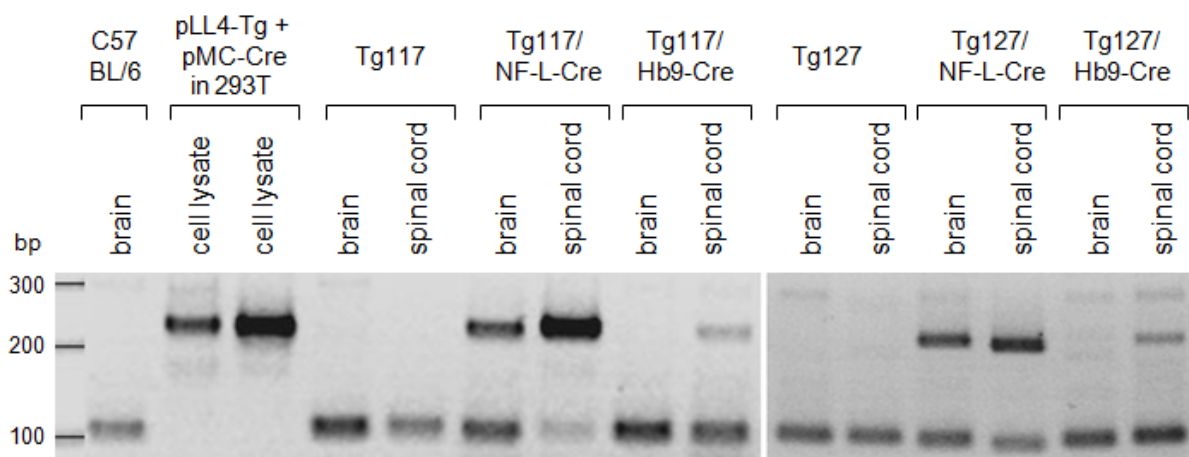


Figure 24: Cre-recombination on DNA level was analyzed by PCR of genomic DNA, isolated from brain and spinal cord tissue of transgenic mice. Recombinant DNA yielded a product of 226bp. Positive controls: DNA of 293T cells, co-transfected with pLL4-Tg and pMC-Cre.

In order to distinguish dominant-negative PrP^{Q167R} from endogenous, wild-type PrP^C on the protein level, a specific 3F4-epitope (aa 109-112) [Kascsak *et al.*, 1987] was introduced into the coding sequence of *Prnp*^{Q167R}. Western blot analysis using the monoclonal anti-PrP-3F4 antibody revealed PrP^{Q167R} expression in brain and spinal cord of Tg/NF-L-Cre mice, while Tg/Hb9-Cre mice showed PrP^{Q167R} expression exclusively in the spinal cord. As brain and spinal cord tissue homogenates also contained non-neuronal Cre-negative cells, the expression of β -gal was found throughout all genotypes, although to a lesser extent in Tg/NF-L-Cre.

Due to different glycosylation states, PrP^{Q167R} in brain and spinal cord of Tg117/NF-L-Cre and Tg127/NF-L-Cre mice exhibited the typical three band pattern. However only little amounts of mainly mono-glycosylated and predominately unglycosylated PrP^{Q167R} were found in the spinal cord of Tg117/Hb9-Cre and Tg127/Hb9-Cre mice, respectively. The results suggest that the Hb9 promoter targeted only a distinct subset of MN during embryonic development (Fig 25).

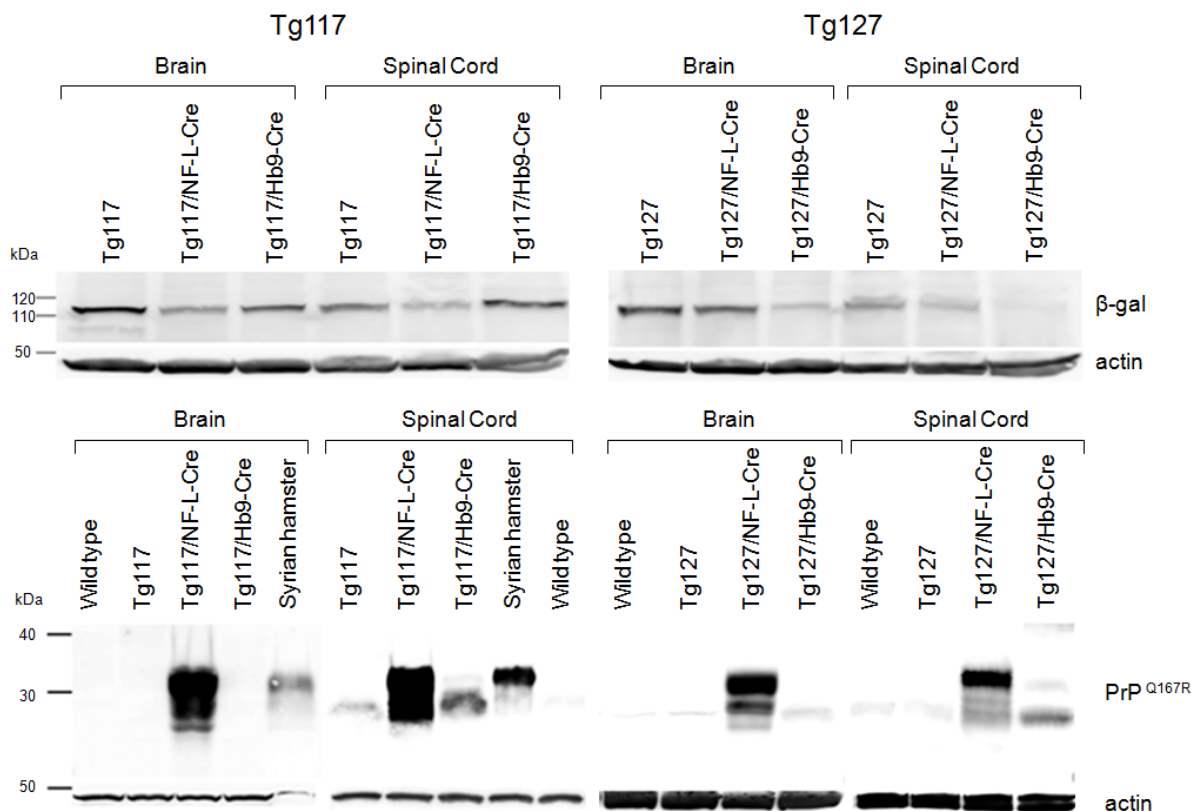


Figure 25: Expression of β -gal and PrP^{Q167R} in uninfected transgenic mice. Western blot exhibited expression of β -gal in brain and spinal cord of transgenic mice. Due to Cre-recombination, β -gal signals were weaker in Tg/Cre samples. The expression of PrP^{Q167R} was detected in brain and spinal cord of Tg/NF-L-Cre and restricted to the spinal cord in Tg/Hb9-Cre. Controls: wild-type and Syrian hamster brain homogenates; normalization with β -actin; 100 μ g total protein/lane.

In addition, glycosylation of PrP^C and PrP^{Q167R} in brain and spinal cord of transgenic mice was analyzed by a N-glycosidase F (PNGase F) treatment. PNGase F is an amidase that hydrolyzes nearly all types of N-glycan chains from glycopeptides. Digestion of homogenates with PNGase F resulted in a single band pattern in western blot analysis, confirming the removal of two sugar residues from wild-type PrP^C and transgenic PrP^{Q167R} (Fig 26).

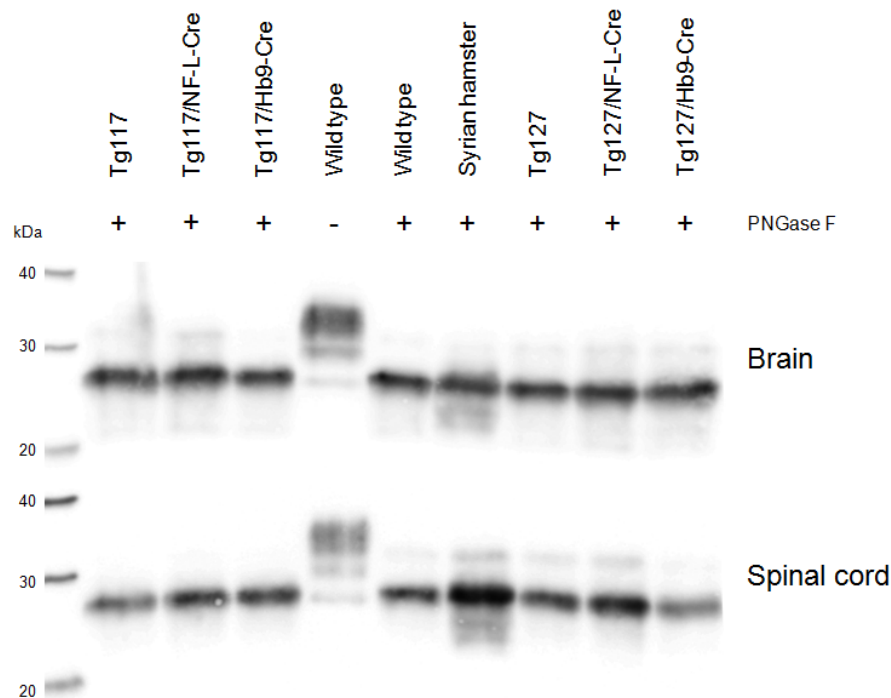


Figure 26: N-glycosidase F (PNGase F) treatment of brain and spinal cord samples of transgenic mice. Upon PNGase F digestion sugar residues of the di- and monoglycosylated forms of PrP^C and PrP^{Q167R} were cleaved off, reducing the typical three band pattern of PrP to a single protein signal.

In order to quantify PrP^{Q167R} in Tg/NF-L-Cre and Tg/Hb9-Cre mice, densitometric analysis of western blots were performed and analyzed using the AIDA software. The concentration of brain and spinal cord homogenates was carefully adjusted and equal amounts of total protein were blotted on a PVDF membrane. Endogenous wild-type PrP^C as well as transgenic PrP^{Q167R} was visualized by an antibody recognizing the N-terminal region of PrP (anti-PrP SAF32), which is identical in both forms of the protein. Total PrP levels were quantified by comparing PrP signal intensities of transgenic mice to PrP signals of wild-type littermates. As internal control PrP signals were normalized to β -actin. Because Tg/NF-L-Cre and Tg/Hb9-Cre mice express PrP^{Q167R} on a *Prnp*^{+/+} background, the difference in total PrP signal intensities (as compared to wild-type) was considered to reflect the amount of PrP^{Q167R} in brain and spinal cord. Total PrP levels were elevated about 20% in brain and 20-30% in spinal cord of Tg117/NF-L-Cre. In Tg127/NF-L-Cre an increase of total PrP of 5% in brain and 30-40% in spinal cord was measured in comparison to wild-type. No differences in total PrP were observed in brains of Tg117/Hb9-Cre and Tg127/Hb9-Cre. Spinal cord of Tg117/Hb9-Cre and Tg127/Hb9-Cre exhibited an increase of PrP of 10% and 20%, respectively (Fig 27).

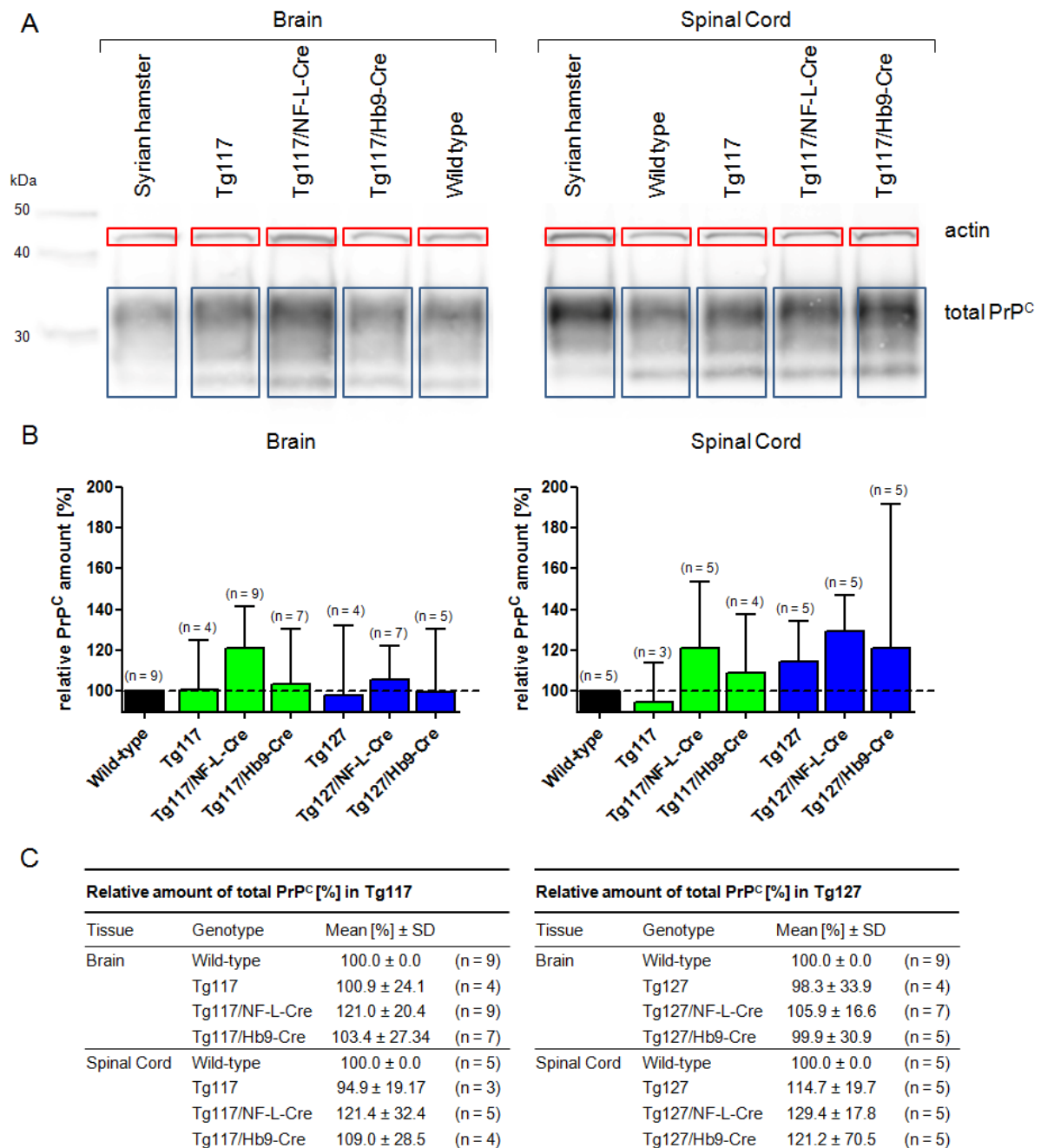


Figure 27: Quantification of PrP^{Q167R} in transgenic mice. (A) Example of densitometric analysis of western blots. Brain and spinal cord homogenates of transgenic mice were blotted and endogenous wild-type PrP^C as well as transgenic PrP^{Q167R} was visualized by anti-PrP-SAF32. PrP signal intensities were measured in a defined area (blue rectangle) and normalized to β -actin (red rectangle), which served as internal control. 30 μ g total protein/lane. (B) Comparison of relative PrP amounts in brain and spinal cord of Tg117 and Tg127 mice. PrP signals of wild-type *Prnp*^{+/+} mice were set as 100%. Columns display mean \pm standard deviation (SD); n = number of measurements. (C) Summary of relative PrP amounts in Tg117 and Tg127 mice in comparison to wild-type mice.

The expression of PrP^{Q167R} in brain and spinal cord of Tg117 and Tg127 after mating to Cre-strains was also analyzed by immunohistochemistry (IHC). IHC analysis of PrP^{Q167R} expression was performed on native brain sections. In the brain PrP^{Q167R} expression was observed in the hippocampus and motor cortex of Tg117/NF-L-Cre as well as in Tg127/NF-L-Cre mice. A weaker expression of PrP^{Q167R} was detected in the brain of Tg117/Hb9-Cre and Tg127/Hb9-Cre (Fig 28).

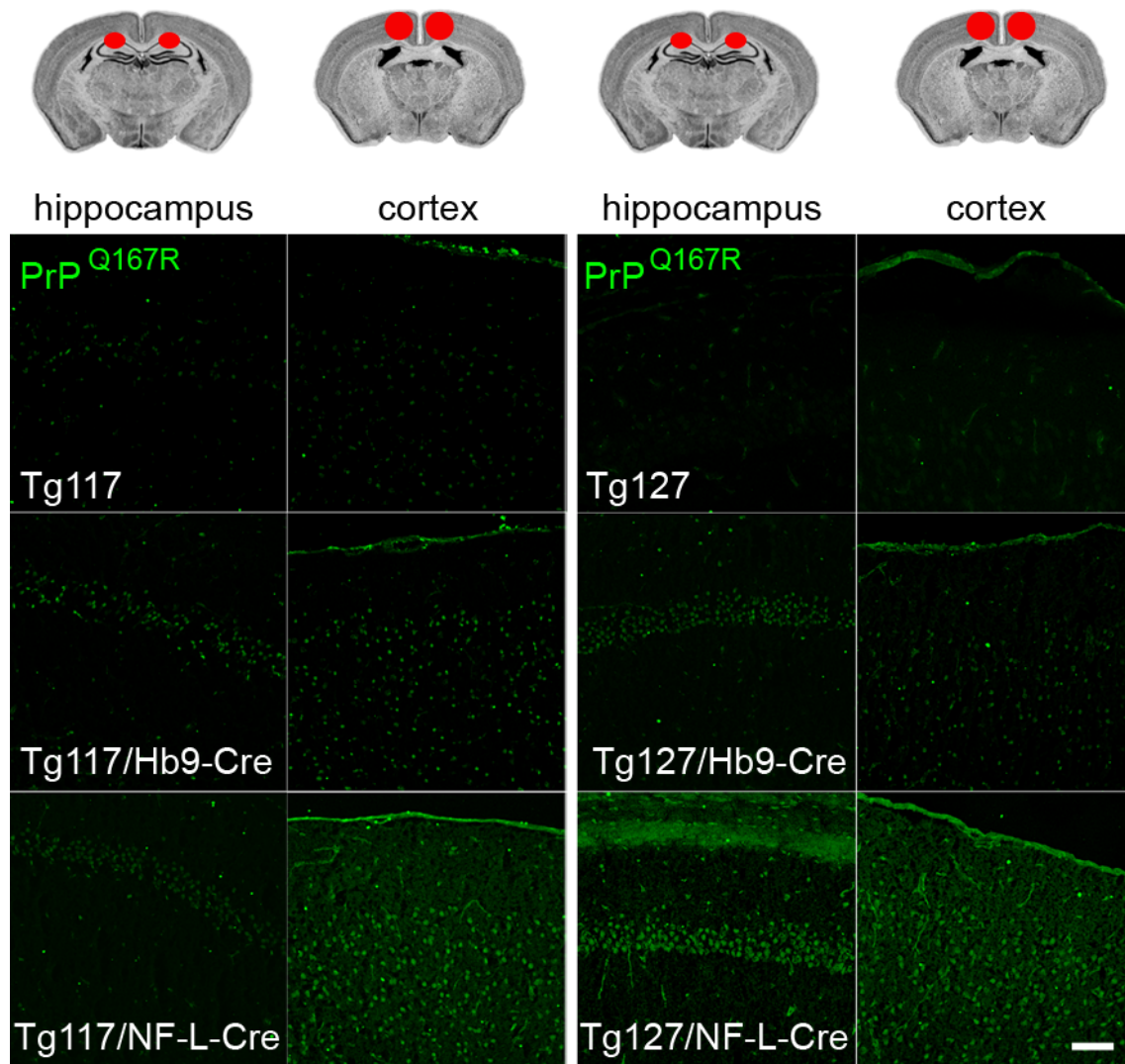


Figure 28: Immunofluorescent labeling of PrP^{Q167R} in the hippocampus and motor cortex of Tg/Cre mice. The strongest expression of PrP^{Q167R} was detected in Tg117/NF-L-Cre and Tg127/NF-L-Cre. Weaker signals were observed in Tg117/Hb9-Cre and Tg127/Hb9-Cre. Scale bar: 100µm.

In addition, IHC analysis of native spinal cord sections exposed PrP^{Q167R} expression in the ventral and dorsal horn of double-transgenic Tg117/NF-L-Cre and Tg117/Hb9-Cre mice (Fig 30). Comparable expression of PrP^{Q167R} in the spinal cord was observed for Tg127/NF-L-Cre and Tg127/Hb9-Cre, while transgenic mice without Cre-allele, did not exhibit any PrP^{Q167R} expression (Fig 29).

In comparison to the expression of β -gal and NeuN, which was located in the cytosol and in neuronal nuclei, the expression pattern of PrP^{Q167R} showed a diffuse distribution. Therefore we assumed that PrP^{Q167R} was mainly located on the neuronal surface as previously seen in cell culture.

In summary IHC analysis of brain and spinal cord sections of transgenic mice were in good agreement with previous western blot results and confirmed that the expression of PrP^{Q167R} was switched on as expected after Cre-recombination.

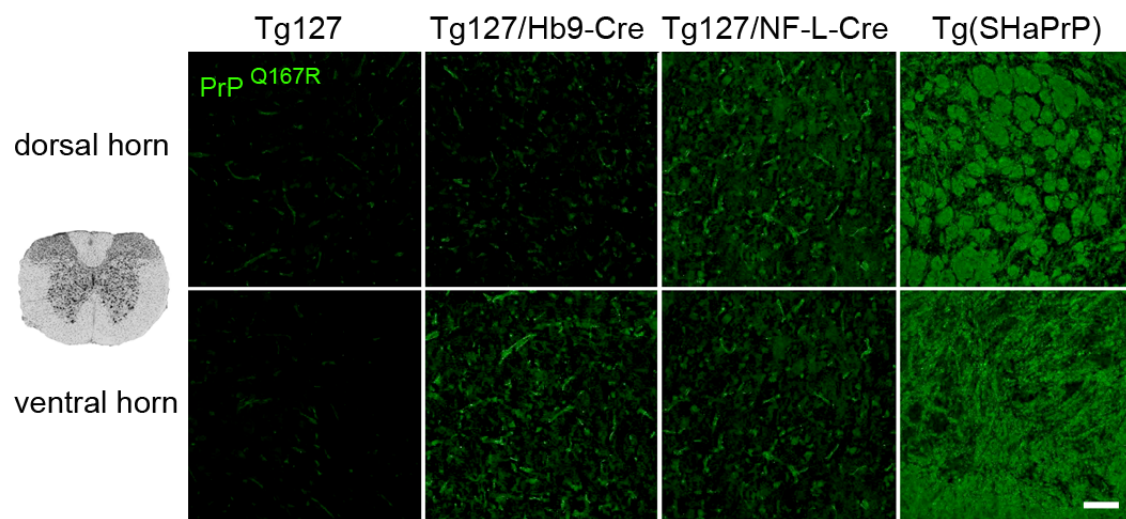


Figure 29: Expression of PrP^{Q167R} in the spinal cord of Tg127/Cre transgenic mice. The strongest PrP^{Q167R} signals were detected in the dorsal and ventral horn of Tg127/NF-L-Cre and in the ventral horn of Tg127/Hb9-Cre in comparison to Tg127 mice. Positive control: spinal cord sections of Tg(SHaPrP) mice, expressing 20-fold hamster PrP on a *Prnp*^{0/0} background. Scale bar: 100 μ m.

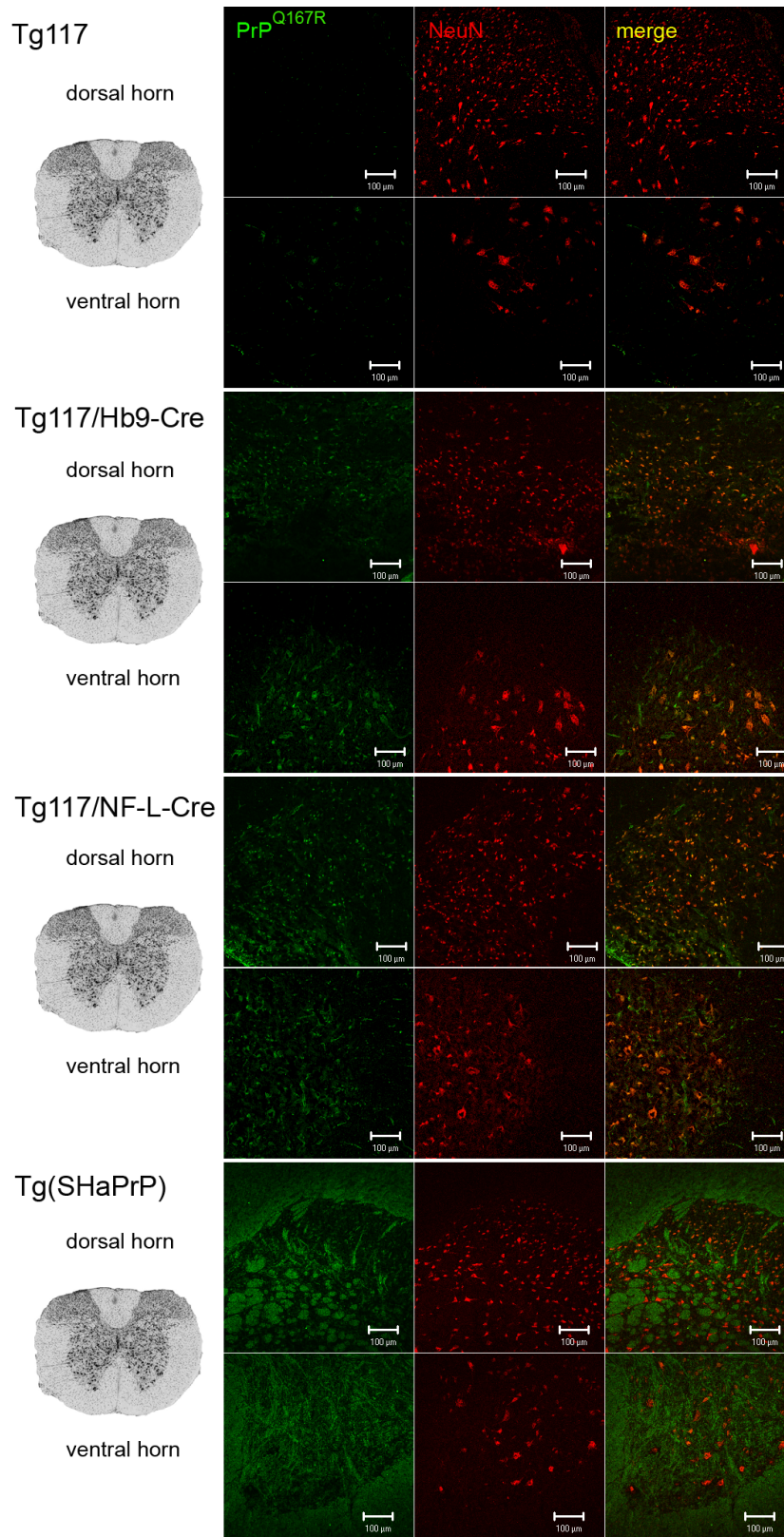


Figure 30: Expression of PrP^{Q167R} and NeuN in the spinal cord of Tg117/Cre transgenic mice. Consistent with the expression of Cre, the strongest PrP^{Q167R} signals were detected in the dorsal and ventral horn of Tg117/NF-L-Cre and in the ventral horn of Tg117/Hb9-Cre as compared to Tg117. In contrast to the allocation of NeuN, the distribution of PrP^{Q167R} was diffuse due to the expression of PrP^{Q167R} on the cell surface. Spinal cord sections of Tg(SHaPrP) mice served as positive control for anti-PrP-3F4 staining.

5.1.2 Survival and pathology of transgenic mice upon prion infection

Prion challenge of Tg floxed LacZ-PrP^{Q167R}/Cre mice via different inoculation routes. To investigate whether the expression of PrP^{Q167R} had an effect on survival and pathogenesis, transgenic mice and age-matched control littermates were inoculated with mouse-adapted prions of the Rocky Mountain Laboratory strain (RML) [Chandler, 1961].

In general, the shortest incubation periods in prion disease are observed upon intracerebral prion infection. On the contrary, naturally occurring prion diseases are typically initiated by peripheral infection, e.g. by consumption of infected material or by iatrogenic transmission. Therefore transgenic mice were challenged with RML prions via different inoculation routes, including intracerebral (i.c.), intraperitoneal (i.p.) or intranervous (i.n.) inoculation into the right sciatic nerve. After prion infection, all transgenic mice presented scrapie-like symptoms similar to those of wild-type mice, including ataxia, hind limb paresis and kyphosis at the late stage of the disease and independent of the inoculation route.

Susceptibility of Tg floxed LacZ-PrP^{Q167R}/Cre mice after prion infection. All mice of both transgenic lines, infected either i.c., i.n. or i.p. with a high dose of RML (i.c. 3×10^5 ; i.n. 10^4 ; i.p. 10^6 LD₅₀), developed terminal scrapie. No significant differences in survival were observed when compared to control groups. I.c. inoculated mice reached the terminal stage of the disease at 150-165 days post infection (dpi), i.n. infection led to an incubation time of 170-180 dpi and mice i.p. inoculated with a high dose of infectivity displayed terminal scrapie symptoms at about 200 dpi (Fig 31, Fig 32).

In contrast, low dose i.p. infection (10^3 LD₅₀) resulted in prolonged survival of Tg117/NF-L-Cre mice, expressing protective PrP^{Q167R} in the spinal cord and in various neurons of the brain. Tg117/NF-L-Cre exhibited clinical symptoms at 265 dpi, showing a statistically significant delay of 33 dpi (15%) in incubation time when compared to Tg117 littermates ($P < 0.0001$). Moreover, two mice of this inoculation group remained free of clinical symptoms and did not develop scrapie until 304 dpi, when the experimental observation was terminated and mice were excluded from the statistics.

Tg117/Hb9-Cre mice displayed a slightly enhanced incubation time (3,5%) and succumbed to clinical prion disease at 238 dpi, which was not significantly different from control groups, suggesting that PrP^{Q167R} expression exclusively in Hb9-positive MN was not sufficient to inhibit prion replication and spread to the central nervous system (CNS) (Fig 31).

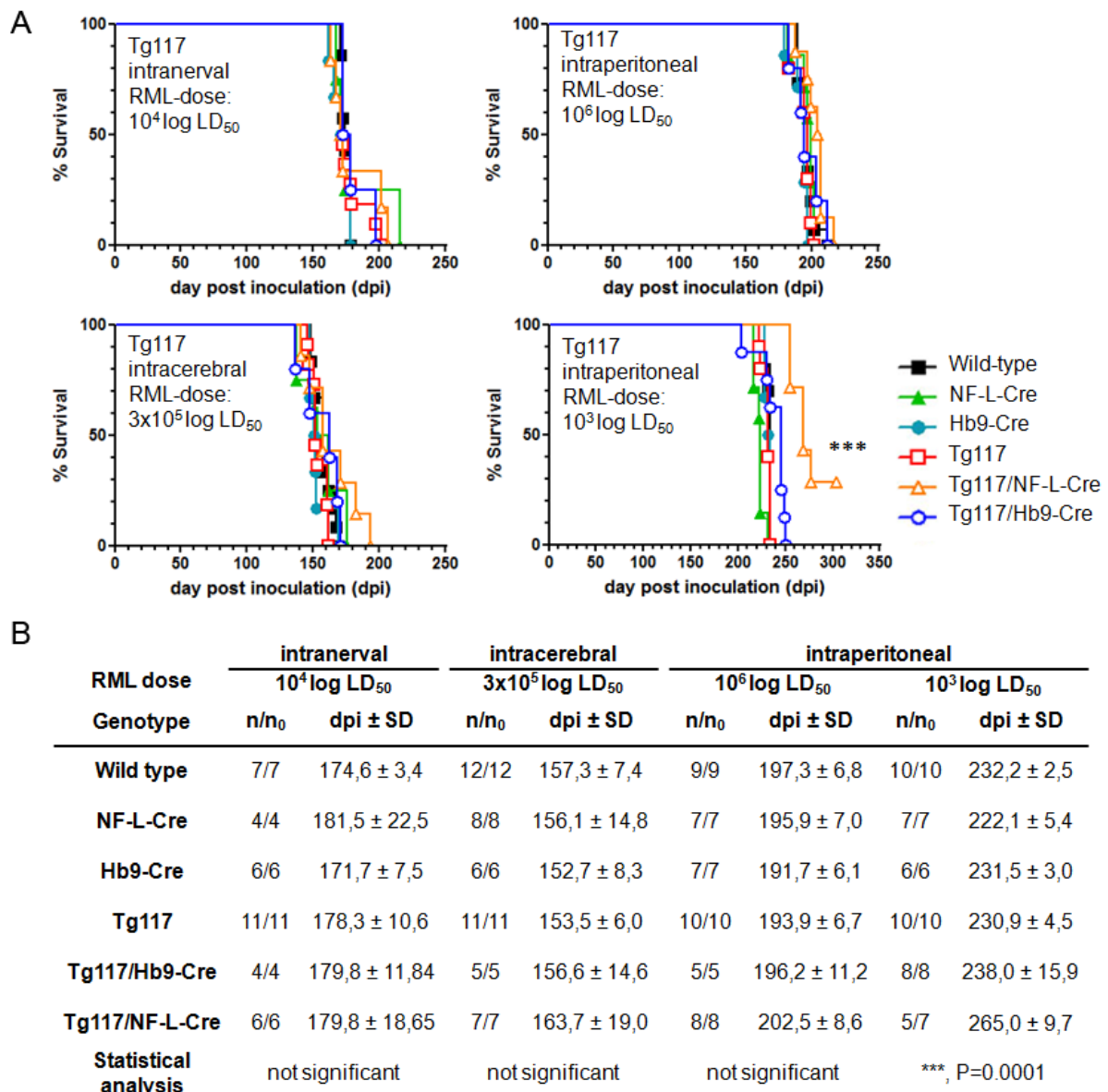


Figure 31: Survival analysis of Tg117 mice upon prion infection. (A) Kaplan-Meier survival plots of transgenic mice inoculated with RML prions via different routes using different doses of infectivity. ***, $P < 0.0001$. (B) Tabular overview of the different experimental groups. The mean survival time after prion infection is displayed as mean days post inoculation (dpi) \pm standard deviation (SD). RML doses are given in units/ml. n/n₀, number of scrapie affected mice / number of inoculated mice.

Surprisingly, the survival of Tg127/NF-L-Cre was not prolonged upon low dose i.p. infection. Tg127/NF-L-Cre mice succumbed to terminal scrapie at 227 dpi, which was comparable to control groups. However, several mice in this inoculation group did not develop clinical scrapie symptoms until the experiment was terminated at 315 dpi. In contrast to line Tg117, survivors were observed in several inoculations groups, suggesting an unexpected position effect of the transgenic DNA (Fig 32).

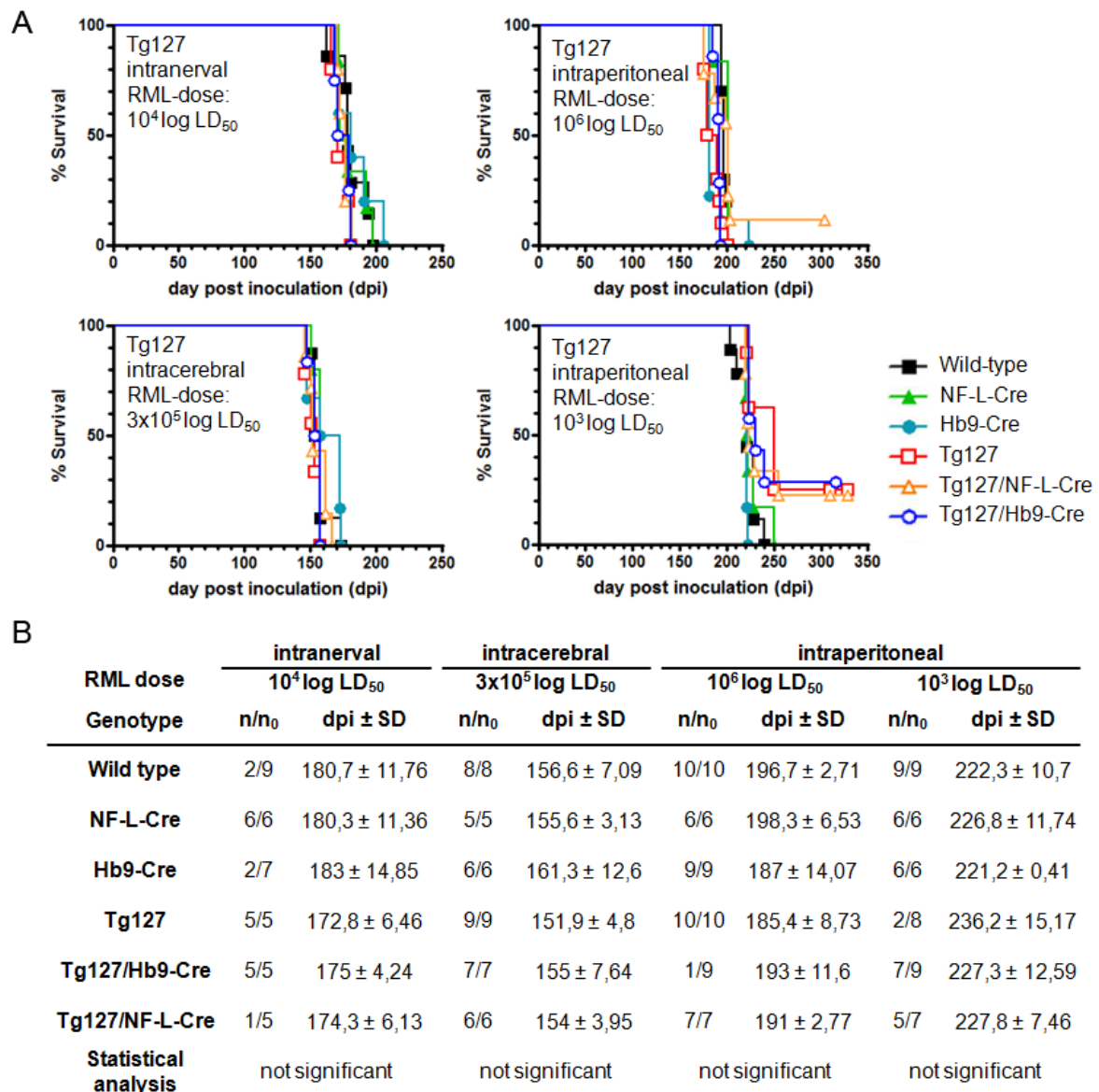


Figure 32: Survival analysis of Tg127 mice upon prion infection. (A) Kaplan-Meier survival plots of transgenic mice inoculated with RML prions via different routes using different doses of infectivity. (B) Tabular overview of the different experimental groups. The mean survival time after prion infection is displayed as mean days post inoculation (dpi) ± standard deviation (SD). RML doses are given in units/ml. n/n₀, number of scrapie affected mice / number of inoculated mice.

To investigate PrP^{Sc} accumulation in brain and spinal cord of transgenic mice, tissue homogenates were prepared, treated with PK and analyzed in western blot. Transgenic mice, i.c., i.n. or i.p. inoculated with a high dose of RML, displayed comparable amounts of PK-resistant PrP^{Sc} at the terminal stage of the disease in the brain as well as the in spinal cord. Total PrP^{Sc} was labeled using the anti-PrP B2-43 antibody. In addition, no PK-resistant PrP^{Q167R} was detected using the monoclonal anti-PrP-3F4 antibody, pointing out that PrP^{Q167R} was not converted into its pathological isoform and did not contribute to total PrP^{Sc} amounts. However, weak signals were detected by anti-PrP-3F4 in samples of i.n. inoculated transgenic mice. These signals were likely due to an unspecific antibody-reaction as they were also present in wild-type controls (Fig 33, Fig 34).

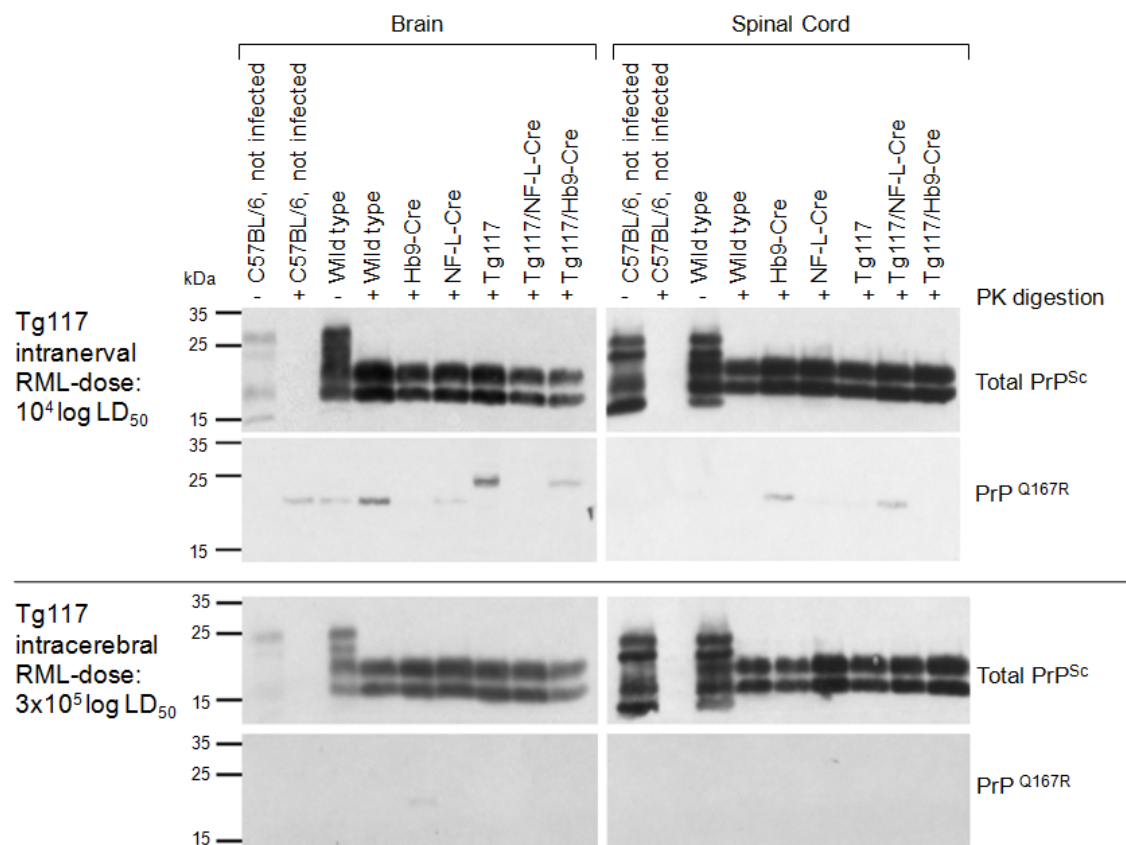


Figure 33: Western blot analysis of proteinase-K (PK)-resistant PrP^{Sc} in terminally scrapie affected mice after high dose intranerval (i.n.) and intracerebral (i.c.) infection with RML prions. Tg117/Cre mice and corresponding control littermates were analyzed. No differences in total PrP^{Sc} (anti-PrP B2-43) and no transgenic, PK-resistant PrP^{Q167R} (anti-PrP-3F4) was detected in the brain or spinal cord. Controls: i.c. and non-infected C57BL/6 mice.

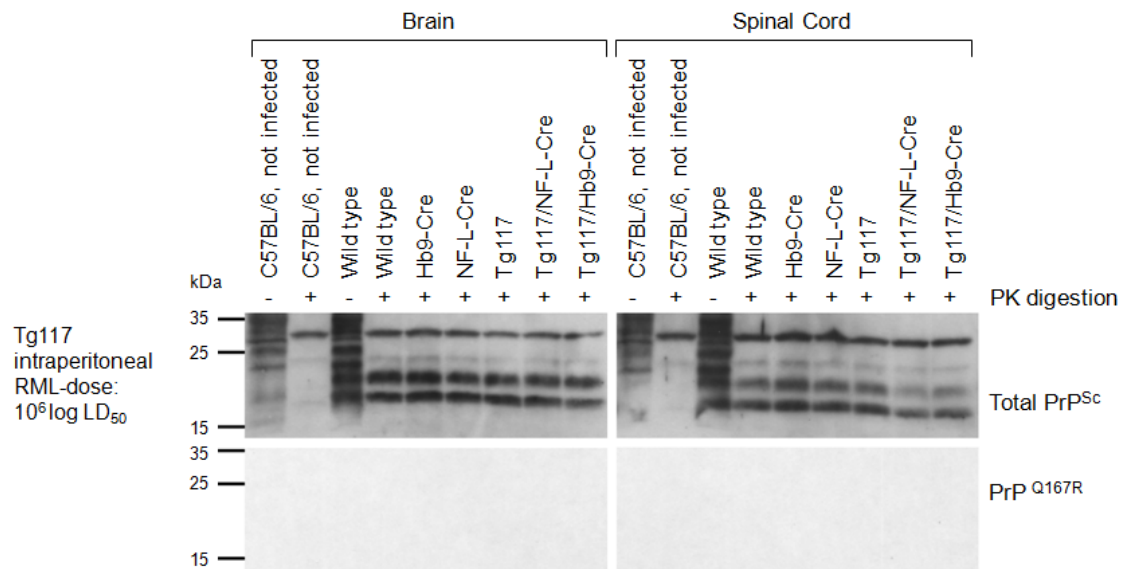


Figure 34: Western blot analysis of PK-resistant PrP^{Sc} in terminally scrapie affected mice after high dose intraperitoneal (i.p.) infection with RML prions. Tg117/Cre mice and corresponding control littermates were analyzed. No differences in total PrP^{Sc} (anti-PrP B2-43) and no transgenic, PK-resistant PrP^{Q167R} (anti-PrP-3F4) was detected in the brain or spinal cord. Controls: i.c. and non-infected C57BL/6 mice.

Similar results were observed for terminal scrapie-sick mice after low dose i.p. prion infection. Even terminal Tg117/NF-L-Cre mice, displaying an extended survival of 15%, accumulated PrP^{Sc} in brain and spinal cord to the same extent as their wild-type littermates. Again no transgenic, PK-resistant PrP^{Q167R} was detected.

In contrast, Tg117/NF-L-Cre mice that did not develop the disease and remained completely free of clinical signs failed to replicate PrP^{Sc} until 304 dpi after low dose i.p. infection. In these mice we did not find any evidence for PrP^{Sc} accumulation in the brain or spinal cord. It seemed that in these mice PrP^{Sc} replication was inhibited by the expression of PrP^{Q167R}, blocking the disease at a sub-clinical level (Fig 35). Similar results were obtained by western blot analysis of terminal scrapie-affected Tg127/Cre mice (data not shown).

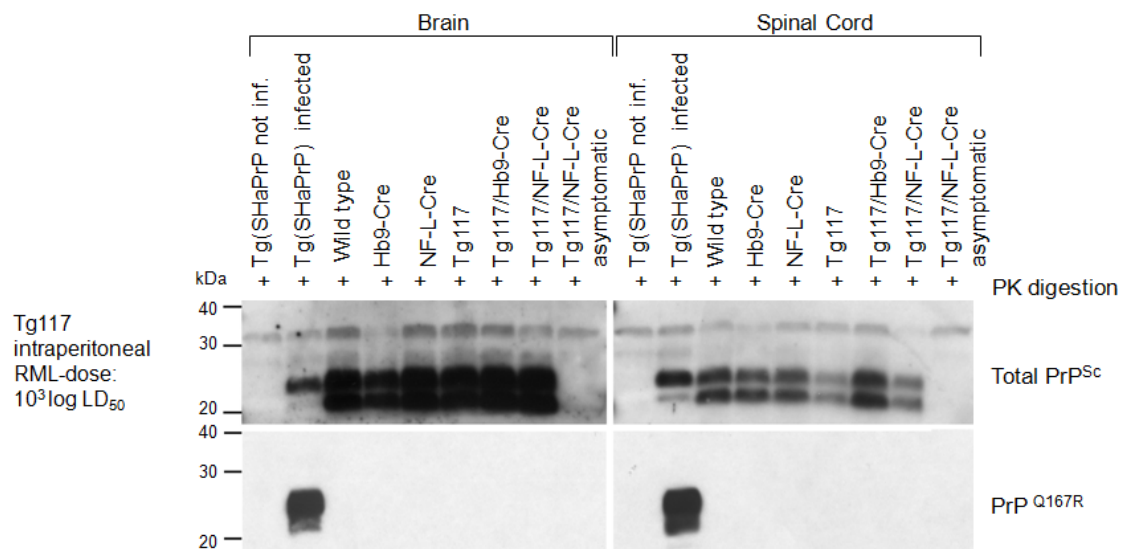


Figure 35: Western blot analysis of PK-resistant PrP^{Sc} in terminally scrapie affected mice after low dose i.p. infection with RML prions. No differences in total PrP^{Sc} (anti-PrP B2-43) and no transgenic, PK-resistant PrP^{Q167R} (anti-PrP-3F4) was detected in the brain or spinal cord. Asymptomatic Tg117/NF-L-Cre mice did not accumulate PrP^{Sc}. Controls: i.c. and non-infected Tg(SHaPrP) mice.

Immunohistochemistry (IHC) of the glial fibrillary acidic protein (GFAP) and hematoxylin-eosin (HE) staining of brain and spinal cord sections of terminally scrapie affected mice revealed no differences in pathology, despite different genotypes and incubation times. Upon the terminal stage of the disease, all transgenic animals developed pronounced astrogliosis in the hippocampus and in the spinal cord. No alterations of astrogliosis were found in Tg117/NF-L-Cre and Tg117/Hb9-Cre in comparison to their wild-type littermates (Fig 36). Similar results were obtained for Tg127/Cre (data not shown).

HE staining displayed the typical spongiform changes with vacuolization most prominently in the white matter of the spinal cord, in the hippocampus and in the thalamus. No differences in vacuolization pattern or intensities were observed for Tg117/NF-L-Cre or Tg117/Hb9-Cre. In agreement with western blot results, we did not find any evidence for neuropathological changes in Tg117/NF-L-Cre mice that did not develop scrapie after low dose i.p. infection. These mice did not show any signs of astrogliosis or vacuolization in brain and spinal cord (Fig 37). Again, comparable results were observed for Tg127/Cre (data not shown).

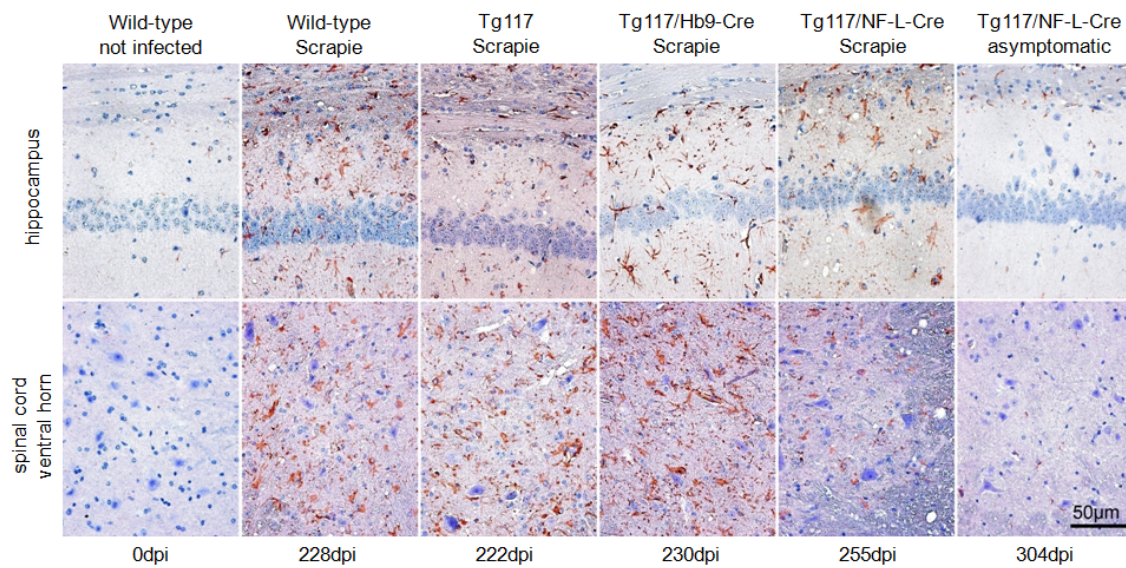


Figure 36: Immunohistochemistry (IHC) of the glial fibrillary acidic protein (GFAP). Low dose i.p. infected Tg117/Cre mice displayed comparable astrogliosis in hippocampus and in the ventral horn of the cervical spinal cord. Asymptomatic Tg117/NF-L-Cre mice remained free of astrogliosis until 304 dpi.

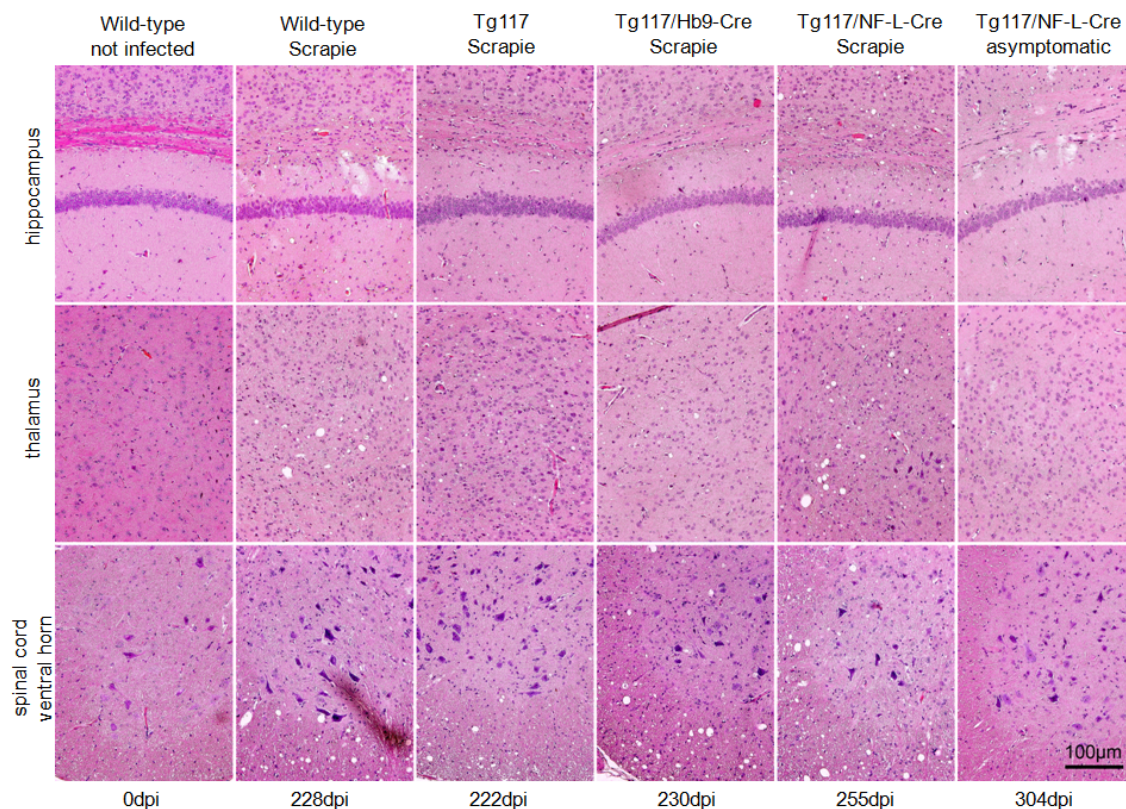


Figure 37: Hematoxylin-eosin (HE) staining of coronal sections of the hippocampus, thalamus and the cervical spinal cord obtained from low dose i.p. infected Tg117/Cre mice. Comparable vacuolization was observed in all scrapie affected mice, despite of the different genotypes and prolonged survival of Tg117/NF-L-Cre. Asymptomatic Tg117/NF-L-Cre mice remained free of vacuolization until 304 dpi (right column).

5.2 Transfer of Cre-recombinase into Tg floxed LacZ-PrP^{Q167R} mice by adeno-associated viral vectors (AAV-Cre)

After intramuscular (i.m.) application adeno-associated virus vectors (AAV) can enter the peripheral nervous system (PNS) and are transported into distinct brain areas (e. g. to nucleus ruber and motor cortex) where the encoded gene is efficiently expressed (Fig 38A) [Kaspar *et al.*, 2003]. A successful transfer of Cre into the CNS of transgenic mice using AAV or lentiviral vector systems has already been described [Kaspar *et al.*, 2002; Ahmed *et al.*, 2004].

For the transfer of Cre into Tg floxed LacZ-PrP^{Q167R} mice, double stranded AAV type 2 vectors, expressing Cre under control of a CMV promoter were used (dsAAV2-Cre). Because of a special modification of the terminal resolution site (trs), the viral DNA remains double stranded, providing a faster delivery and expression of the transgene in comparison to single stranded AAV vectors [Wang *et al.*, 2003].

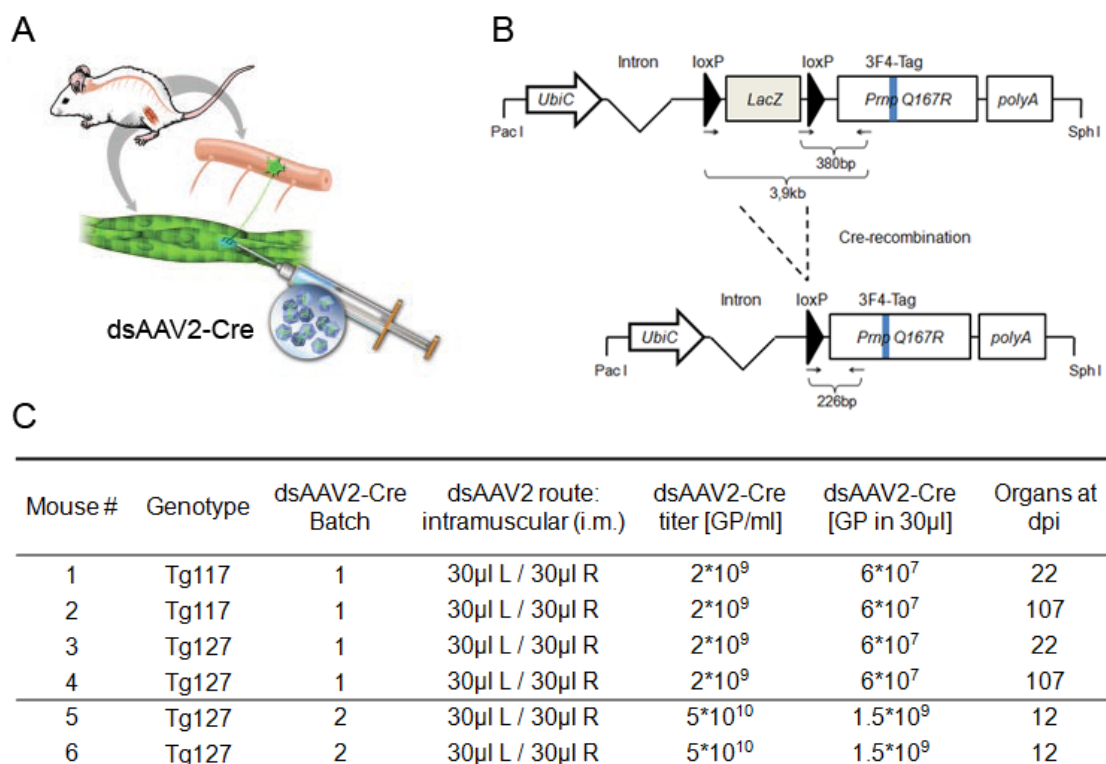


Figure 38: Intramuscular (i.m.) application of dsAAV2-Cre into Tg floxed LacZ-PrP^{Q167R} mice. (A) Application scheme: viral vectors were injected into the hind limb muscles of transgenic mice, from where they were retrogradely transported to the spinal cord. Adapted from [Kaspar *et al.*, 2003]. (B) Structure and recombination of the transgenic DNA in Tg floxed LacZ-PrP^{Q167R} mice upon expression of Cre-recombinase. (C) Tabular overview of dsAAV2-Cre inoculated mice. L, left side. R, right side.

Two independent dsAAV2-Cre batches with different viral titers were used. A volume of 30 μ l dsAAV2-Cre, was injected bilaterally into the hind limb muscles of Tg floxed LacZ-PrP^{Q167R} mice. Mice were sacrificed at different time points and brain, spinal cord and muscle tissue was analyzed by PCR and western blot in order to detect recombinant DNA and expression of PrP^{Q167R} or Cre in Tg floxed LacZ-PrP^{Q167R} mice (Fig 38B).

All mice inoculated with dsAAV2-Cre vectors displayed normal behavior and remained healthy up to 107 days post AAV infection. Tg floxed LacZ-PrP^{Q167R} mice, treated with batch 1, were sacrificed at 22 dpi and 107 dpi, respectively. Because no recombinant DNA was detected by PCR in the brain or spinal cord at the different time points, all mice were checked for the presence of viral DNA by a PCR directed at Cre. No Cre DNA was detected in the brain and spinal cord, suggesting that either the applied viral titer was too low for a PCR detection of Cre or that the foreign, viral DNA was already degraded before functional Cre was expressed and recombination could take place. The genotype of transgenic mice was confirmed by a *LacZ* PCR. The transgene was present in all tested samples (Fig 39).

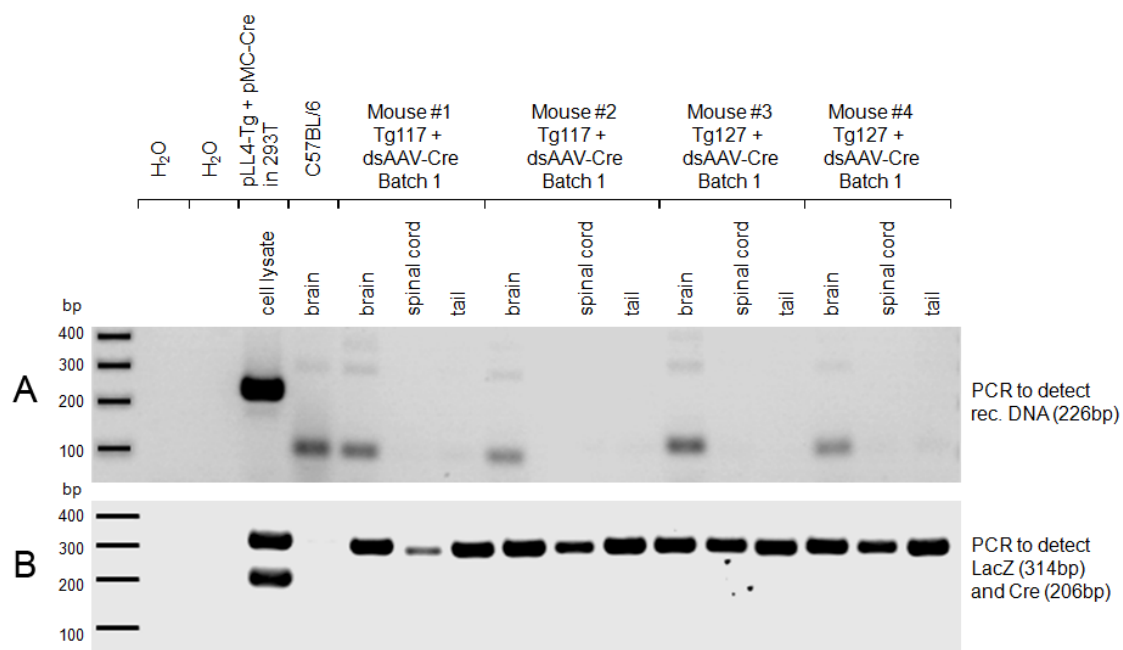


Figure 39: PCR analysis of Tg floxed LacZ-PrP^{Q167R} mice treated with dsAAV2-Cre of batch 1. (A) No recombinant DNA (226bp) was detected in brain or spinal cord of dsAAV2-Cre treated mice at 22 or 107 dpi. (B) A *LacZ* PCR confirmed the genotype of Tg floxed LacZ-PrP^{Q167R} mice. No viral *Cre* DNA was detected in the analyzed samples. DNA derived from 293T cells co-transfected with pLL4-Tg and pMC-Cre served as positive, C57BL/6 brain tissue as negative control.

Consequently, a second dsAAV2-Cre batch (batch 2) providing a higher virus titer was used and treated mice were sacrificed at 12 dpi. PCR analysis revealed recombinant, transgenic DNA as well as *Cre* DNA in hind limb muscle tissue but not in the brain or spinal cord of dsAAV2-Cre inoculated mice. The presence of recombinant DNA in the muscle tissue confirmed the expression of functional Cre at least at the site of virus application (Fig 40).

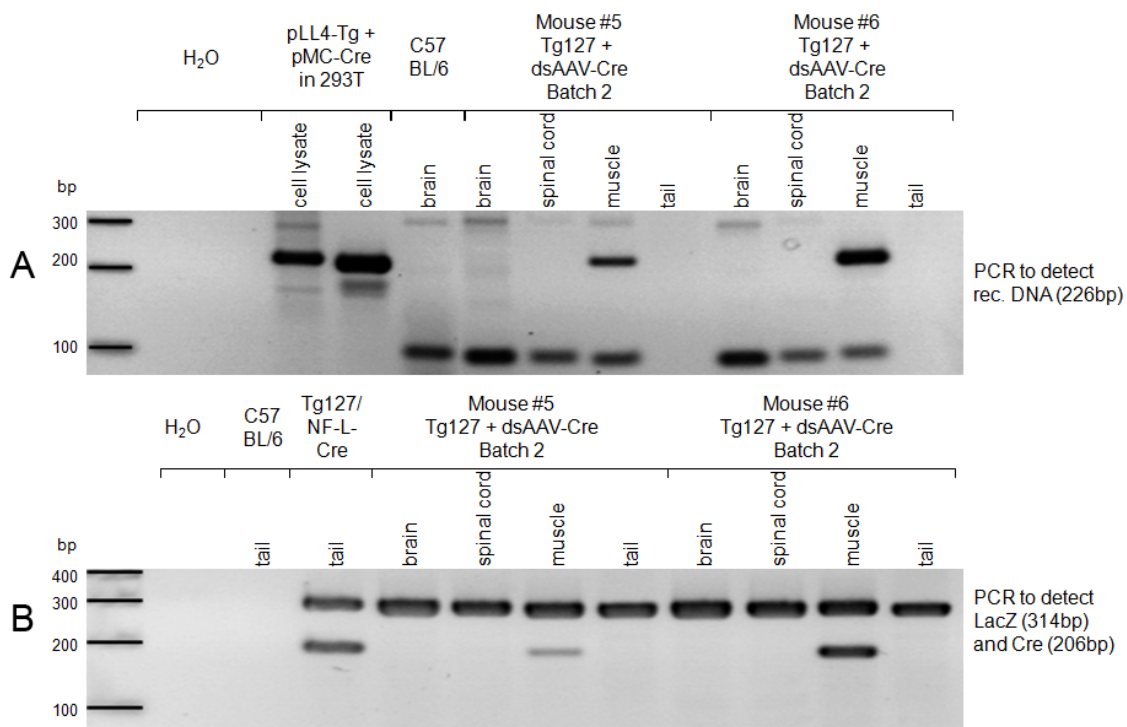


Figure 40: PCR analysis of Tg floxed LacZ-PrP^{Q167R} mice treated with dsAAV2-Cre of batch 2. (A) Recombinant DNA (226 bp) was detected exclusively in the muscle tissue of dsAAV2-Cre treated mice at 12 dpi. (B) A *LacZ* PCR confirmed the genotype of Tg floxed LacZ-PrP^{Q167R} mice. Viral *Cre* DNA was detected only in muscle tissue. DNA derived from 293T cells co-transfected with pLL4-Tg and pMC-Cre as well as DNA of Tg117/NF-L-Cre mice served as positive, C57BL/6 as negative control.

On the protein level, no transgenic PrP^{Q167R} was detected by the monoclonal anti-PrP-3F4 antibody in any of the analyzed tissues, regardless of Tg floxed LacZ-PrP^{Q167R} mice were treated with dsAAV2-Cre of batch 1 or 2. A second anti-PrP antibody, recognizing PrP^{Q167R} as well as wild-type PrP^C, confirmed that enough protein was loaded onto the gel as strong PrP signals appeared in the brain and spinal cord.

In addition, western blots were probed with a monoclonal anti-Cre antibody. In agreement with PCR results, Cre was detected in small amounts in muscle tissue of Tg floxed LacZ-PrP^{Q167R}, infected with dsAAV2-Cre of batch 2. As the molecular weight of Cre is 38 kDa and no evidence exist that Cre undergoes further processing, additional bands around 50-60 kDa were considered as an unspecific reaction of the anti-Cre antibody (Fig 41).

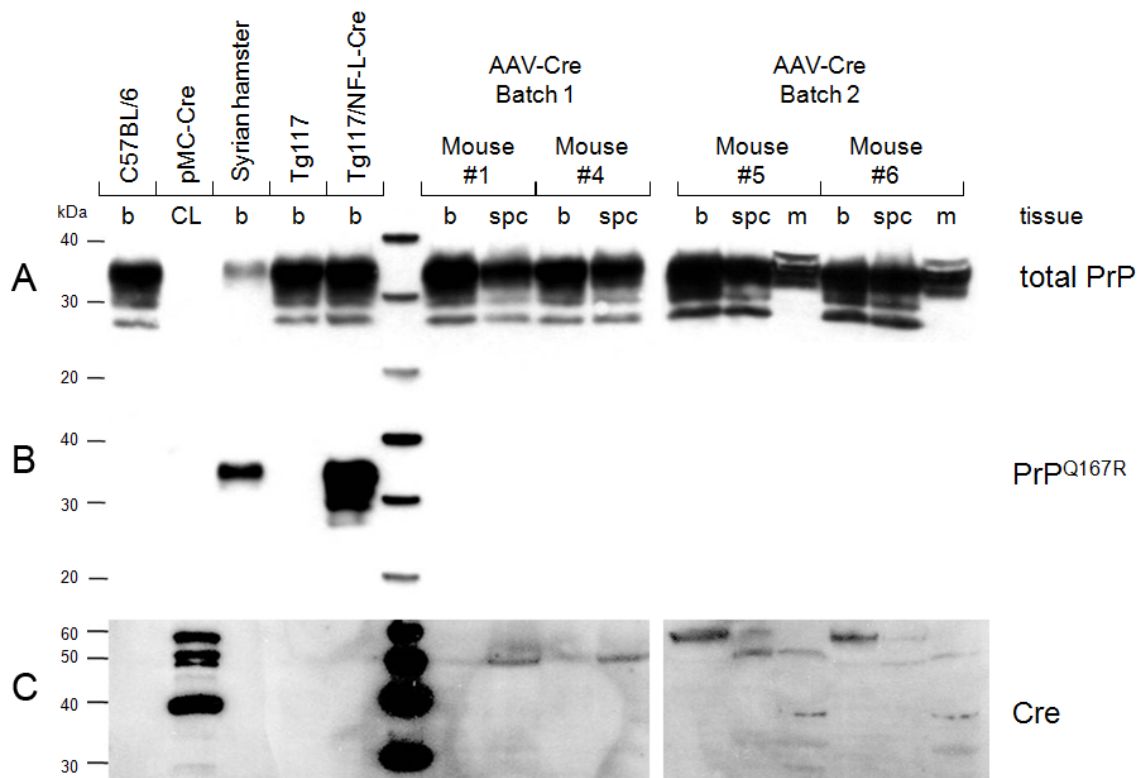


Figure 41: Western blot analysis of Tg floxed LacZ-PrP^{Q167R} mice, inoculated with different dsAAV2-Cre batches. (A) Strong signals of total PrP in the different samples showed that enough protein was loaded onto the gel. Positive control: C57BL/6 and Tg117. (B) No expression of PrP^{Q167R} in the brain, spinal cord or muscle tissue was observed after intramuscular application of dsAAV2-Cre vectors. Positive control: Syrian hamster and Tg117/NF-L-Cre mice. (C) The 38 kDa Cre protein was detected in small amounts selectively in muscle homogenates of Tg floxed LacZ-PrP^{Q167R} mice inoculated with dsAAV2-Cre of batch 2. Positive control: cell lysate transfected with pMC-Cre. 100µg total protein/lane; b: brain, CL: cell lysate; spc: spinal cord; m: muscle.

In summary the results suggest that dsAAV2-Cre vectors express functional Cre-recombinase, when applied at high titers ($\geq 5 \cdot 10^{10}$ GP/ml), but further improvement of the vector system is needed to achieve efficient transport from the site of application to the CNS and induce expression of PrP^{Q167R} in Tg floxed LacZ-PrP^{Q167R} mice.

5.3 Accumulation of PrP^{Sc} and prion infectivity in splenic tissue of neuronal PrP deficient mice

Although prion infectivity in splenic tissue is associated with follicular dendritic cells (FDC) and B- and T-lymphocytes [Raeber *et al.*, 1999; Kitamoto *et al.*, 1991], it is still unknown if those cell types are able to replicate the infectious agent or if other PrP expressing cell types, such as neurons innervating the LRS are involved. To investigate if neurons and in particular MN participate in the replication of prion infectivity in splenic tissue, we generated neuronal PrP deficient mice and studied the accumulation of PrP^{Sc} and prion infectivity in spleens at an early time point after prion infection.

Towards this, we established double-transgenic mice carrying one allele of floxed *Prnp* (*lox2*^{+/-}) [Rossi *et al.*, 2001] and either one allele of Hb9-Cre or NF-L-Cre on a *Prnp*^{0/0} background. Because of the expression pattern of Cre in these mice, a conditional PrP knockout was achieved in MN of the spinal cord (Hb9-Cre) [Arber *et al.*, 1999; Yang *et al.*, 2001] and in various neuronal populations of the spinal cord and brain (NF-L-Cre) [Schweizer *et al.*, 2002]. Heterozygous PrP-levels in *lox2*^{+/-} mice ensured high Cre-recombination efficiencies in the target cells.

5.3.1 Characterization of neuronal PrP deficient mice

Cre-mediated recombination of the floxed *Prnp* allele was detected by PCR in brain, spinal cord and tail of *lox2*^{+/-}/NF-L-Cre and to a lesser extent in brain, spinal cord and tail of *lox2*^{+/-}/Hb9-Cre suggesting that Cre-recombination was successful on DNA level in both transgenic lines, while the DNA remained unaltered in *lox2*^{+/-} without Cre allele (Fig 42). In contrast to Tg floxed LacZ-PrP^{Q167R}/Hb9-Cre, recombinant DNA was also found in brain lysates of *lox2*^{+/-}/Hb9-Cre mice. This may be due to a higher Cre-recombination efficiency in heterozygous mice or to a more sensitive PCR reaction.

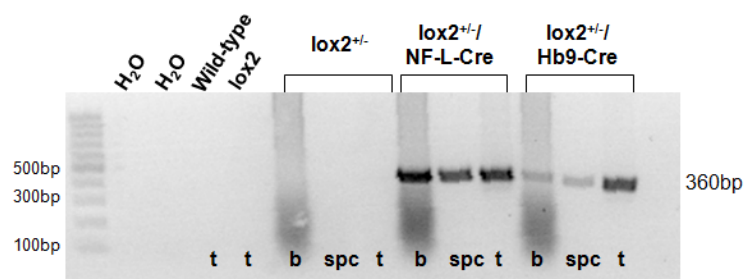


Figure 42: Cre-recombination on DNA level was analyzed by PCR of genomic DNA, isolated from brain, spinal cord and tail tissue of transgenic mice. Recombinant DNA yielded a product of 360 bp. t: tail, b: brain, spc: spinal cord.

Quantification of total PrP^C in double transgenic lox2^{+/-}/Hb9-Cre and lox2^{+/-}/NF-L-Cre mice was estimated by densitometric analysis of western blots. PrP^C was visualized by anti-PrP B2-43 (epitope aa 144-151), normalized to β -actin and signal intensities were measured using AIDA software and compared to signals of wild-type (*Prnp*^{+/+}) mice. In lox2^{+/-} a reduction in PrP^C of approximately 40% in brain and 60% in spinal cord was measured. A further reduction in PrP^C of about 20% was observed for lox2^{+/-}/NF-L-Cre in brain and spinal cord, respectively. The results were in good agreement with data obtained for Tg floxed LacZ-PrP^{Q167R}/NF-L-Cre.

In contrast lox2^{+/-}/Hb9-Cre mice did not exhibit any further reduction in PrP^C when compared to lox2^{+/-}, rather a slight enhancement in PrP^C was observed (Fig 43). These contradictory results may be due to the fact that Hb9-Cre is expressed only in a subset of MN and therefore alterations in PrP^C content are under detection limit.

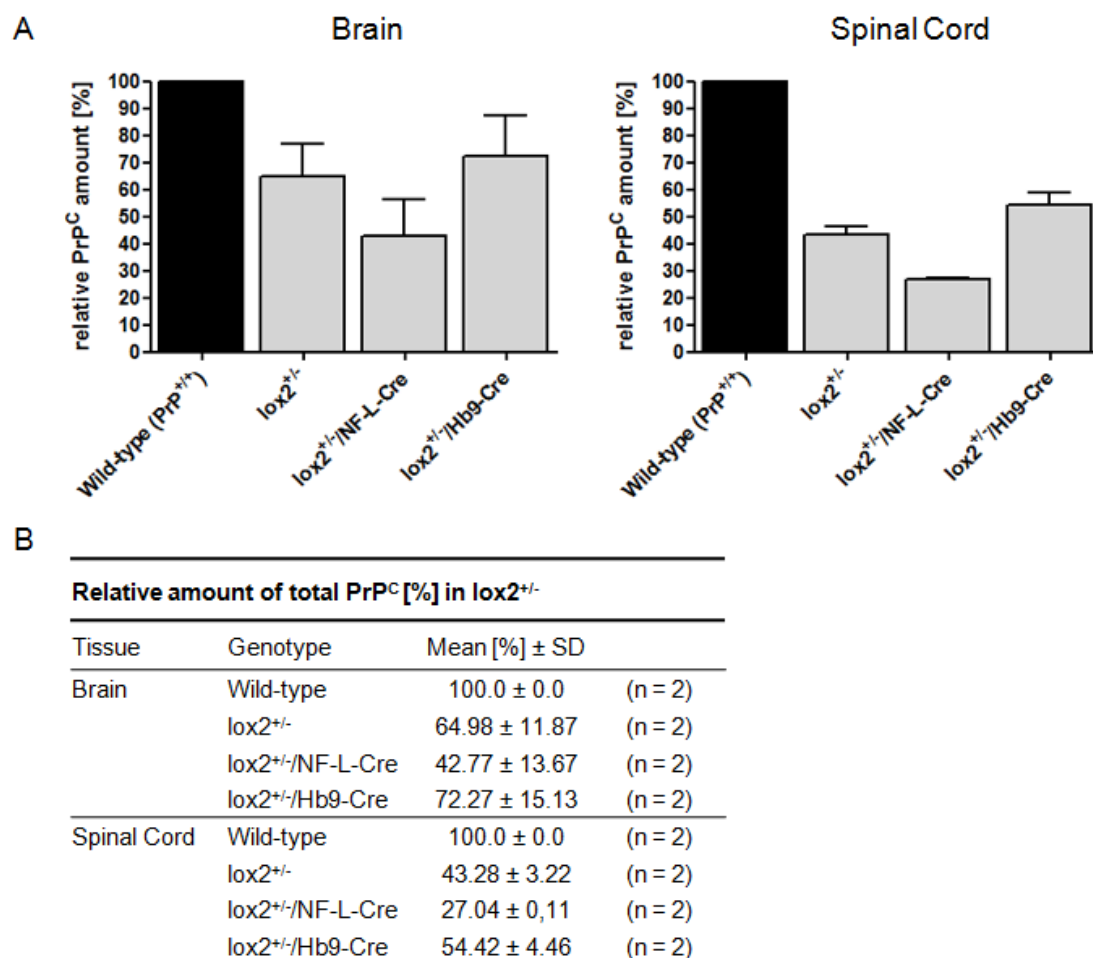


Figure 43: Quantification of PrP^C in lox2^{+/-}/Cre transgenic mice. (A) Comparison of relative PrP^C amounts in brain and spinal cord of different transgenic mice. PrP^C signals of wild-type (*Prnp*^{+/+}) mice were set as 100%. Columns display mean \pm standard deviation (SD) (B) Summary of relative PrP^C amounts in lox2^{+/-}/Cre transgenic mice in comparison to wild-type mice; n = number of measurements.

5.3.2 Accumulation of PrP^{Sc} in spleen and spinal cord of neuronal PrP deficient mice

To investigate PrP^{Sc} levels in spleen and spinal cord of lox2^{+/-}, lox2^{+/-}/Hb9-Cre and lox2^{+/-}/NF-L-Cre mice, age-matched littermates of each genotype were inoculated with RML prions [Chandler, 1961]. Mice were intracerebrally (i.c.) infected with a high dose of prions (3x10⁵LD₅₀). Intraperitoneal (i.p.) inoculation was performed using either a high dose or a low dose of prions (10⁶ or 10³ LD₅₀). At 50 days post inoculation (dpi), spleen and spinal cord tissue was collected and a sodium phosphotungstic acid (NaPTA) precipitation of PrP^{Sc} with subsequent PK-treatment and analysis by western blot was performed (Fig 44).

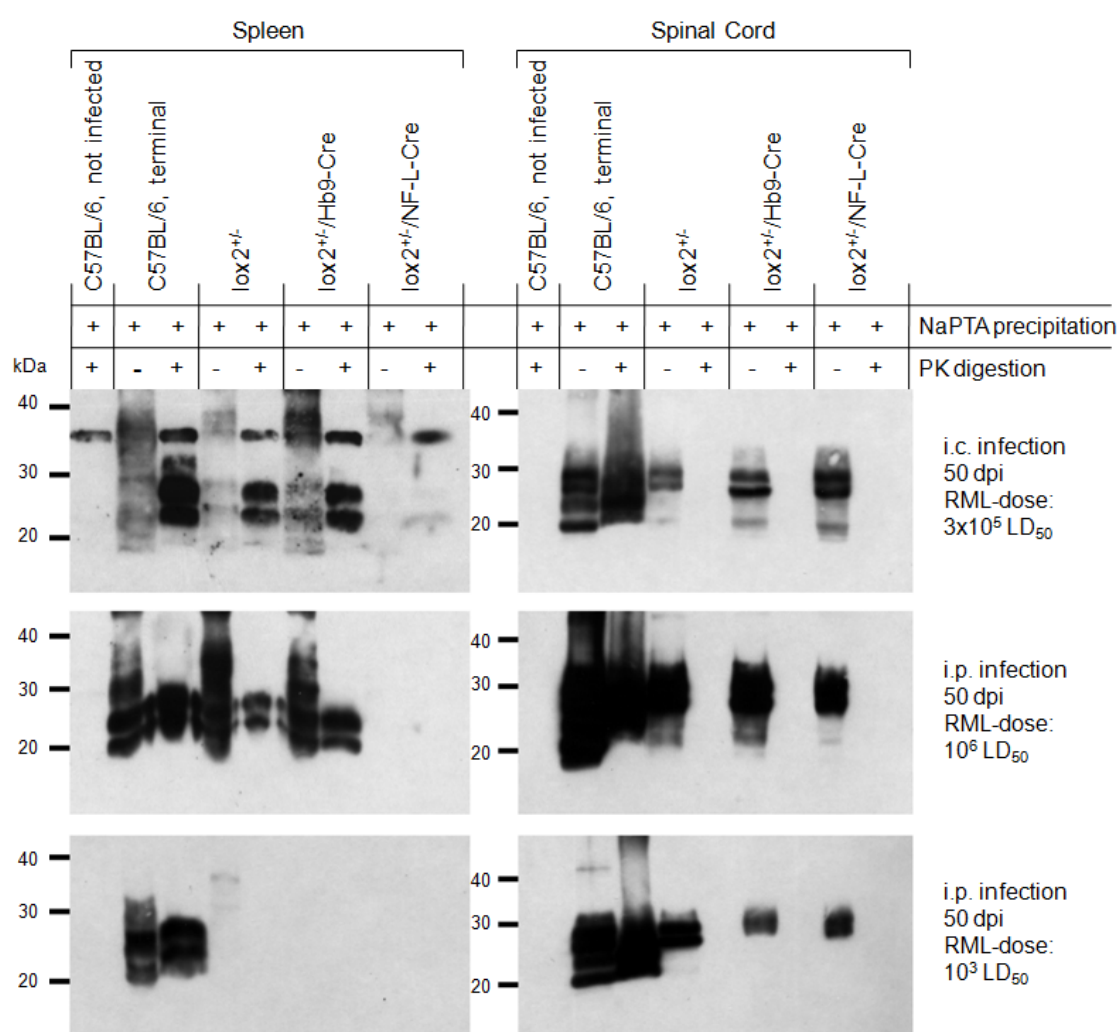


Figure 44: Sodium phosphotungstic acid (NaPTA) precipitation of PrP^{Sc} in spleen and spinal cord of lox2^{+/-}, lox2^{+/-}/Hb9-Cre and lox2^{+/-}/NF-L-Cre mice at 50 dpi. Mice were i.c. or i.p. inoculated with different RML doses as indicated. Protein amounts for NaPTA precipitation: 1000µg total protein for PK-treated samples; 200µg of total protein for samples without PK-digestion. Spleen and spinal cord material of uninfected and terminally scrapie-affected C57BL/6 mice served as controls.

At 50 dpi no PrP^{Sc} was detected in spinal cord tissue of lox2^{+/-}, lox2^{+/-}/Hb9-Cre and lox2^{+/-}/NF-L-Cre mice, independent on inoculation route and RML dose as indicated by PK digestion. Moreover, PK-untreated spinal cord samples of lox2^{+/-}, lox2^{+/-}/Hb9-Cre and lox2^{+/-}/NF-L-Cre mice exhibited comparable PrP amounts of about half the quantity of C57BL/6 (*Prnp*^{+/+}).

I.c. and i.p. inoculation with a high dose of RML resulted in PrP^{Sc} accumulation in spleens of lox2^{+/-} and lox2^{+/-}/Hb9-Cre but not in lox2^{+/-}/NF-L-Cre mice. In addition all mice that were i.p. inoculated with a low dose of RML, did not accumulate PrP^{Sc} in the spleen until 50 dpi (Fig 44).

The results suggest that PrP^{Sc} replication in the spleen is impaired in mice with pan-neuronal PrP^C-depletion such as lox2^{+/-}/NF-L-Cre. A PrP-knockout in subsets of MN does not influence the replication of PrP^{Sc} in spleen.

5.3.3 Determination of prion infectivity titers in spleen of neuronal PrP deficient mice

Prion infectivity titers in spleens of lox2^{+/-}, lox2^{+/-}/Hb9-Cre and lox2^{+/-}/NF-L-Cre mice were determined in a bioassay using Tga20 indicator mice. Therefore 1% spleen homogenates of lox2^{+/-}, lox2^{+/-}/Hb9-Cre and lox2^{+/-}/NF-L-Cre mice (previously i.c. or i.p. infected with either a high or a low dose of RML) were prepared and intracerebrally inoculated into Tga20 mice. The infectivity titer of each spleen homogenate was calculated from Tga20 incubation times [*Prusiner et al.*, 1982].

Lox2^{+/-}, lox2^{+/-}/Hb9-Cre and lox2^{+/-}/NF-L-Cre mice, inoculated with a high dose of RML, accumulated infectivity titers of 4-6 log LD₅₀ in the spleen until 50dpi. In these groups all Tga20 indicator animals developed terminal scrapie.

Spleens of low dose i.p. infected lox2^{+/-} mice exhibited infectivity titers of 4,3 log LD₅₀, which was sufficient to cause terminal scrapie in all Tga20 indicator mice. Spleens of lox2^{+/-}/Hb9-Cre mice with MN-specific PrP depletion showed a reduced infectivity titer of 2,44 log LD₅₀. In this group only 3 out of 4 Tga20 mice succumbed to terminal scrapie. The lowest infectivity titer of 1,56 log LD₅₀ was measured in spleens of lox2^{+/-}/NF-L-Cre mice. As the infectivity titer in spleens of lox2^{+/-}/NF-L-Cre mice was nearly under detection limit and only 2 out of 5 Tga20 mice developed scrapie, it seemed that pan-neuronal depletion of PrP inhibited the accumulation of prion infectivity in spleen at 50 dpi. Therefore the results suggest that accumulation of prions in the spleen is dependent on PrP^C expression in the nervous tissue (Fig 45).

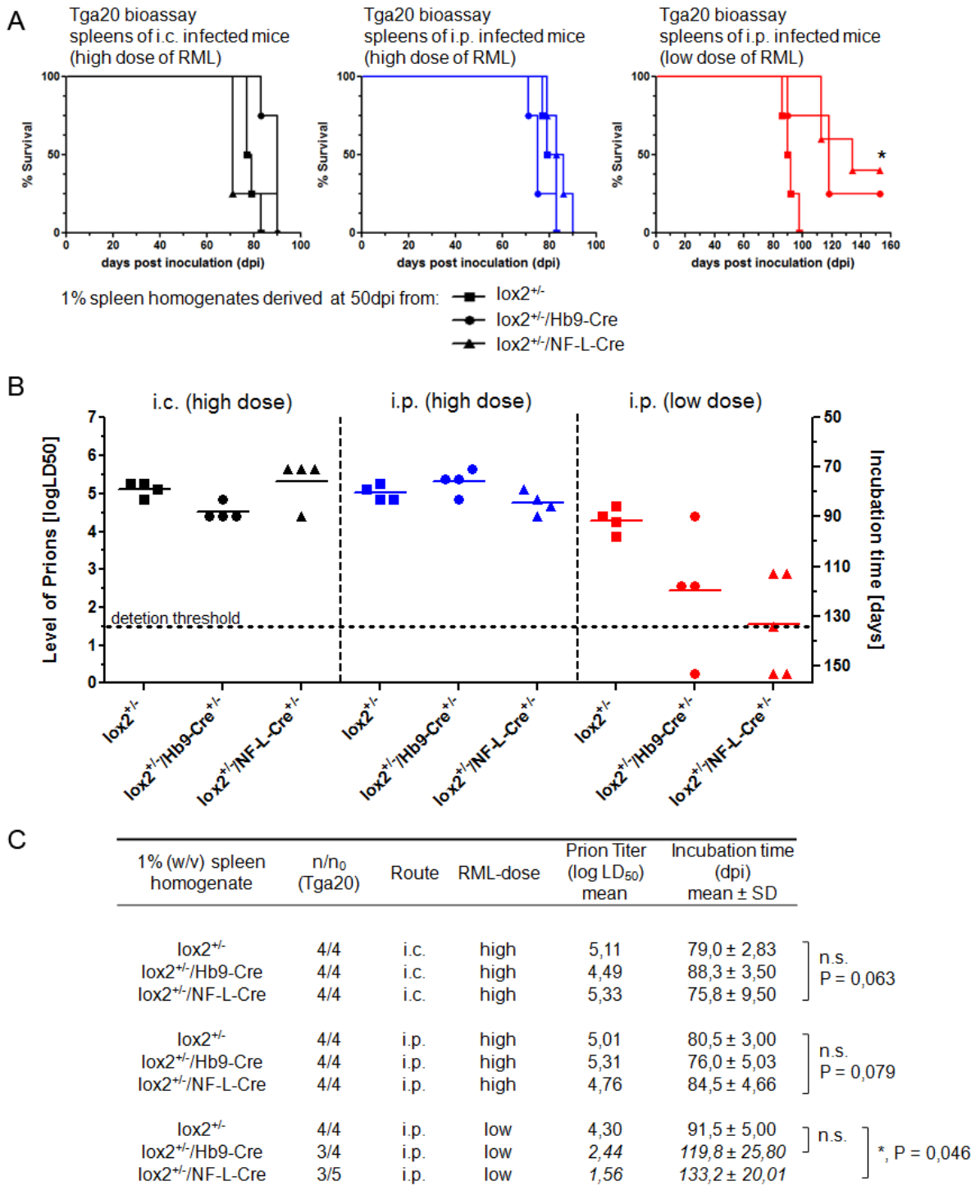


Figure 45: Tga20 bioassay. (A) Kaplan-Meier survival plots of Tga20 mice, inoculated with 1% spleen homogenates derived from i.c. (RML dose: $3 \times 10^5 LD_{50}$) or i.p. (RML dose: $10^6 LD_{50}$ or $10^3 LD_{50}$) infected $lox2^{+/-}$, $lox2^{+/-}/Hb9-Cre$ and $lox2^{+/-}/NF-L-Cre$ mice. *: $P < 0.01$. (B) Determination of prion infectivity titers of spleen homogenates. Symbols underneath the dotted line represent prion titers below the detection threshold (indicator mice did not develop scrapie). Each dot represents one individual. (C) Tabular overview of prion infectivity titers and mean survival time of Tga20 mice after prion infection with 1% spleen homogenates. n/n₀, number of scrapie affected mice / number of inoculated mice.

6 Discussion

6.1 Transgenic mice with inducible expression of dominant-negative PrP^{Q167R} in motor neurons

Several neurodegenerative diseases have been related to a selective impairment of distinct neuronal populations. In Parkinson's disease a selective loss of dopaminergic neurons is described [Beal, 2001] and selective degeneration of motor neurons (MN) is found in amyotrophic lateral sclerosis [Cleveland and Rothstein, 2001].

The identification of vulnerable cell populations in the nervous system, responsible for triggering the onset of clinical prion disease, is still elusive. Beside the typical clinical symptoms like trembling, paresis and finally severe ataxia, several studies point out a role for MN in the clinical manifestation of prion disease. Kimberlin and Walker first postulated clinical target areas (CTA), distinct neuronal populations in the brainstem and spinal cord in which prions have to access and replicate to a certain threshold to cause clinical prion disease [Kimberlin and Walker, 1986, 1988]. It was shown that early clinical symptoms are consistent with neuronal damage in brain areas that control motor functions [Bartz *et al.*, 2002] and recently we reported that impaired axonal transport in MN of nucleus ruber and motor cortex correlates with the onset of clinical prion disease [Ermolayev *et al.*, 2009a].

As an experimental approach to strengthen these points we developed a novel mouse model with Cre-mediated expression of dominant-negative PrP^{Q167R}. Mating of Tg floxed LacZ-PrP^{Q167R} to Hb9-Cre mice [Arber *et al.*, 1999; Yang *et al.*, 2001] led to the expression of PrP^{Q167R} in MN of the spinal cord while NF-L-Cre [Schweizer *et al.*, 2002] directed PrP^{Q167R} expression at a broader set of spinal MN as well as to several neuronal populations of the brain. The model takes advantage of the natural dominant-negative properties of a sheep PrP polymorphism [Goldmann *et al.*, 1994]. PrP^{Q167R} inhibits the conversion from PrP^C to PrP^{Sc} *in vitro* and *in vivo*, probably by a competitive interaction between PrP^{Q167R} and PrP^C for PrP^{Sc}, thus slowing down PrP^{Sc} accumulation and providing prolonged survival [Kaneko *et al.*, 1997b; Perrier *et al.*, 2002].

The transgenic DNA for nuclear injection consists of a UbiC promoter, a floxed LacZ marker gene followed by the dominant-negative *Prnp*^{Q167R} mutant, including a PvuI restriction site as well as a specific antibody epitope designated 3F4-tag. The specific characteristics of *Prnp*^{Q167R} enabled us to discriminate between endogenous wild-type PrP and PrP^{Q167R}, which was important as Tg floxed LacZ-PrP^{Q167R} mice were generated on a wild-type *Prnp*^{+/+} background to ensure normal prion propagation outside the cells of interest.

Experiments using PrP deficient 293T cells proofed the functionality of the trans-

genic DNA in cell culture. In the absence of Cre, enzymatically active β -galactosidase (β -gal) was expressed from the *LacZ* marker gene, while co-transfection with a Cre-expressing plasmid led to the expression of PrP^{Q167R} on the cell surface. PrP^{Q167R} was present in a di- mono- and unglycosylated form and detectable by several anti-PrP antibodies, including the specific anti-PrP-3F4. Therefore a correct processing and post-translational modification of PrP^{Q167R} can be assumed.

Microinjection of the transgenic DNA led to 22 founder lines that were efficiently identified by a PCR directed against *LacZ*. An additional PCR was performed to show the presence of dominant-negative *Prnp*^{Q167R}. The unique PvuI restriction site of *Prnp*^{Q167R} ensured a definite identification of Tg floxed *LacZ*-PrP^{Q167R} mice. Further analysis of transgenic offsprings by a X-gal screening assay revealed that only 6 out of 22 lines expressed β -gal in brain and spinal cord. This phenomenon can be explained by the integration characteristics of pronuclear injected transgenes.

Depending on the size of the transgene, each fertilized oocyte receives ten to several hundred DNA molecules. Those DNA molecules can recombine to large tandemly arranged concatamers before the DNA integrates into the host chromosome. Thus, multi-copy arrays can influence the expression of the transgene [Bishop and Smith, 1989]. Integration sites for transgenic DNA are randomly distributed [Brinster et al., 1989] and can cause severe side effects. For example integration of the transgene into oncogenes or tumor suppressor genes is a frequent observation in transgenic approaches. In this case, transgenic mice may be viable and fertile but develop tumors at a young age. Transgenic mice derived from line Tg119 tended to develop tumors at the age of 40 weeks and were therefore excluded from further experiments.

In addition position effects can influence the spatial and temporal expression characteristics of the transgene. Position effects can be caused by integration of the transgene into the direct vicinity of transcription control elements, a region of imprinting or a non-transcribed heterochromatin region as well as into X- and Y-chromosomes [Rülicke and Hübscher, 2000]. Frequently, an inactivation of transgenes by *de-novo* methylation of DNA has been observed for stable transfected cells as well as for transgenic mice [Li et al., 1993]. It has been reported that especially transgenes containing viral sequences are susceptible to this process, suggesting that *de-novo* methylation of DNA might be a defense mechanism against the activity of foreign genes in a host genome [Wienhues and Doerfler, 1985]. If multiple transgene insertion sites are located on different chromosomes, a segregation of the transgenic cluster upon breeding is possible, leading to different transgene expression patterns of the resulting offsprings [Rülicke and Hübscher, 2000]. To ensure a stable inheritance of the transgenic cluster and to identify multi-copy arrays, transgene copy numbers of each transgenic line were determined by quantitative real time PCR. Indeed, a transgenic line Tg136, carrying a double-insertion of transgenic DNA, was identified.

Further strategies to control integration events of transgenic DNA have been described. It was reported that position effects can be eliminated for transgenes harboring a cis-regulatory element called locus control region (LCR). LCRs are short stretches of DNA, characterized by stable DNase-I hypersensitive sites, which provide an open chromatin structure to neighboring sequences even when the transgene is integrated into heterochromatin regions of a chromosome [Grosveld *et al.*, 1987]. In addition to that, matrix/scaffold attachment regions are thought to be important for the organization of chromatin into functional genetic domains [Bode *et al.*, 1992] and an element from the cytosine-phosphate-guanine (CpG) island sequence of the hamster adenine phosphoribosyl transferase (APRT) locus was identified that may reduce *de-novo* methylation of flanking sequences [Siegfried *et al.*, 1999].

Finally, transgenic lines Tg117 and Tg127 were selected for further experiments, because they exhibited the strongest expression of β -gal in brain and spinal cord, displayed a normal phenotype and behavior and reproduced efficiently.

In detail, expression of the marker gene β -gal was found in the cerebellum, various regions of the midbrain, in the hippocampus and cortex. Further immunohistochemical (IHC) analysis exposed β -gal expression in neurons of the nucleus ruber and motor cortex as well as in the dorsal and ventral horn of the spinal cord. The results confirmed that transgene expression in Tg floxed LacZ-PrP^{Q167R} mice was present in the spinal cord as well as in brain regions essential for motor control.

While MN are predominately located in the ventral horn, the dorsal horn of the spinal cord mainly contains sensory neurons. MN are connected to higher brain centers either via the pyramidal or the extrapyramidal system. In contrast to humans and primates, where the pyramidal tract plays an important role in motor control, the extrapyramidal system is more important in other mammalian species such as rodents. Important brain regions for motor control are the motor cortex and nucleus ruber. The motor cortex is involved in the planning, control, and execution of voluntary motor functions and connected to various cranial nerve nuclei in the brain stem, such as oculomotor, trochlear, motor nucleus of the trigeminal nerve, abducens, facial, accessory and hypoglossal nucleus. In addition a majority of motor cortex fibers extends directly to the spinal cord. The nucleus ruber is an important member of the extrapyramidal tract in rodents that controls tonic and posture. Neurons of the nucleus ruber project to neurons in the spinal cord, which are involved in reflexes, locomotion, complex movements, and postural control. Lesions of nucleus ruber in non-primates have been related to contra-lateral paresis as well as to ataxia [Poirier, 1974; Armand, 1984].

Successful recombination of transgenic DNA in Tg floxed LacZ-PrP^{Q167R} mice mated to Cre-strains was demonstrated by PCR analysis. Moreover PrP^{Q167R} expression was detected in brain and spinal cord homogenates of Tg/NF-L-Cre mice, while transgenic mice carrying an additional Hb9-Cre allele exhibited PrP^{Q167R} expression exclusively

in the spinal cord. Beside this, IHC stainings confirmed the expression of PrP^{Q167R} after Cre-recombination. In contrast to β -gal, which was located inside the neuronal cytosol, PrP^{Q167R} showed a diffuse distribution. A diffuse distribution of PrP^C is also observed in Tg(SHaPrP) mice, overexpressing hamster PrP^C on a *Prnp*^{0/0} background and argues for the presence of PrP^{Q167R} on the neuronal cell surface (probably on axons). Taken together, the results show that the expression of PrP^{Q167R} is dependent on Cre-expression, which was controlled by the NF-L or Hb9 promoter.

To investigate whether the expression of PrP^{Q167R} had an effect on survival and pathogenesis, transgenic mice and age-matched control littermates were inoculated with mouse-adapted prions of the Rocky Mountain Laboratory strain (RML). In addition to an intracerebral (i.c.) prion infection, prions were also applied from the periphery by intraperitoneal (i.p.) or intranerval (i.n.) inoculation. In case of i.p. prion infection, two different doses of infectivity were used. After prion infection, all transgenic mice that succumbed to the disease displayed typical scrapie symptoms similar to those of wild-type mice and independent of the inoculation route.

Infection with a high dose of RML led to an unaltered susceptibility of Tg117/Cre and Tg127/Cre mice, suggesting that the expression levels of PrP^{Q167R} were too low to significantly slow down PrP^{Sc} replication. Several strategies could enhance PrP^{Q167R} expression levels. For instance an increase in Cre-expression by establishing homozygous Cre-strains would be possible. While NF-L-Cre mice are viable, homozygous Hb9-Cre mice die at or soon after birth. Therefore a second strategy would be the usage of different strains with stronger MN-specific Cre-expression, such as *Isl1*-Cre mice [Srinivas *et al.*, 2001], application of Cre-expressing viral vectors or a direct injection of Cre-RNA [Ahmed *et al.*, 2004].

In addition, expression levels of PrP^{Q167R} also dependent on the regulation of the UbiC promoter. In the literature it was reported that the human UbiC promoter directs high ubiquitous expression of transgenes in spleen, liver, heart, lung, ovary, stomach, intestine, kidney, brain, mammary gland, uterus and skin of mice [Schorpp *et al.*, 1996]. Although the activity of the UbiC promoter was impressively demonstrated in the X-gal screening assay, the expression strength may vary between distinct subsets of neurons. Therefore it might be that neurons exhibiting a strong expression of Cre shown only low UbiC promoter activity.

In contrast low dose i.p. prion infection resulted in a prolonged survival of Tg117/NF-L-Cre mice. Tg117/NF-L-Cre mice exhibited clinical symptoms at 265 dpi, showing a statistically significant delay of 33 dpi (15%) in incubation time when compared to Tg117 littermates (231 dpi). Moreover, a subset of these mice remained completely free of clinical symptoms and did not develop scrapie until 304 dpi, when the experimental observation was terminated and the mice were excluded from the statistic. Interestingly, Tg117/Hb9-Cre mice displayed only a slightly enhanced incubation time

and succumbed to clinical prion disease at 238 dpi, which was not significantly different from control groups. The limited protective effect of PrP^{Q167R} in Tg117/Hb9-Cre may be explained by the expression pattern of the Hb9 promoter.

In the mammalian spinal cord, the homeobox gene *Hb9* is expressed by developing embryonic MN, predominately during embryonic stage E9 - E9.5 until E10,5 - E11. Its encoded homeodomain protein Hb9 has an essential role in MN development and MN fate [Arber *et al.*, 1999; Thaler *et al.*, 1999]. Hb9 expression is present in cholinergic MN with ventral projections but has not been detected above the level of the abducens motor nucleus or in dorsal sensory neurons such as the spinal accessory or vagus nerve [Thaler *et al.*, 1999].

In contrast, the NF-L promoter targets a broader set of neurons as it regulates the expression of light chain neurofilament proteins. The expression of NF-L correlates with the development of the mouse CNS and PNS and continues in postmitotic neurons [Yazdanbakhsh *et al.*, 1993]. Thus, the NF-L promoter directs Cre expression to dorsal sensory as well as to ventral MN of the spinal cord. In the brain, NF-L-Cre expression is found e.g. in the cerebral cortex, the ammon's horn of the hippocampus as well as in several motor and sensory cranial nerve nuclei, including the trigeminal nerve nuclei, the facial nucleus, the ventral cochlear nucleus, the hypoglossal nucleus and the reticular nucleus [Schweizer *et al.*, 2002]. However, both promoters are inactive in interneurons and glia.

Moreover, prolonged survival was observed in Tg117/NF-L-Cre only after peripheral prion infection pointing out the relevance of prion neuroinvasion via parasympathetic nerve fibers (e.g. nervus vagus) [McBride *et al.*, 2001] as this route is "blocked" in Tg117/NF-L-Cre mice but not in Tg117/Hb9-Cre.

Surprisingly, Tg127/NF-L-Cre mice did not exhibit a prolonged survival upon low dose i.p. prion infection. In comparison to Tg117/NF-L-Cre, Tg127/NF-L-Cre mice exhibited a weaker expression of PrP^{Q167R} in the brain, while PrP^{Q167R} levels in the spinal cord were almost equal in both transgenic lines. If the protection of CTA in the brain would be more efficient than a protection of spinal cord MN, a diminished expression of PrP^{Q167R} in the brain of Tg127/NF-L-Cre could account for a limited effect on the survival of Tg127/NF-L-Cre mice.

In this context, an interesting time table was outlined in a previous study, that aimed to investigate the spread of TME prions from the sciatic nerve to the brain in a Syrian hamster model. It was reported that PrP^{Sc} was first detected in the spinal cord at 4 weeks post infection in those segments that correspond to the sciatic nerve. PrP^{Sc} was first detected in the brain at 6 weeks post infection in the nucleus ruber as well as in the lateral vestibular nucleus and interposed nucleus of the cerebellum. At 9 weeks post infection, PrP^{Sc} was present in the hind limb motor cortex [Bartz *et al.*, 2002]. It is remarkable that all of these structures are involved in the control of motor functions, in-

cluding balance and coordination. Recently, it was demonstrated that impaired axonal transport in MN correlated with the onset of clinical prion disease in different mouse models. After inoculation of prions into the sciatic nerve, 30-45% of neurons in the nucleus ruber and 94% of neurons in the motor cortex showed axonal transport defects at the onset of clinical prion disease [Ermolayev *et al.*, 2009a]. Both studies confirm that nucleus ruber is an early entry site of prions that may play an important role in the clinical manifestation of prion disease.

Despite different incubation times no differences in total PrP^{Sc} amounts and pathology in transgenic mice were obvious at the terminal stage of scrapie. In contrast, Tg/NF-L-Cre mice that remained free of clinical signs did not accumulate PrP^{Sc} in the CNS and did not display scrapie-typical neuropathological changes, such as astrogliosis or vacuolization. It can be assumed that in these mice the disease was blocked at a subclinical level, supporting the hypothesis that clinical signs appear when neuronal damage in the CTA reaches a certain threshold [Kimberlin and Walker, 1988].

In a previous study, transgenic mice with ubiquitous expression of dominant-negative PrP^{Q167R} were generated either on a *Prnp*^{0/0} and on a *Prnp*^{+/+} background. Upon i.c. prion infection, Tg (MoPrP, Q167R)/*Prnp*^{0/0} did not develop scrapie for more than 550 days, while Tg (MoPrP, Q167R)/*Prnp*^{+/+} mice succumbed to the disease at 447 dpi [Perrier *et al.*, 2002]. The fact that Tg (MoPrP, Q167R) mice exhibited ubiquitous expression of PrP^{Q167R} at the same level as wild-type PrP might explain the extended survival of these mice in comparison to our transgenic model.

In analogy to our conditional mouse model, terminal Tg (MoPrP, Q167R) /*Prnp*^{+/+} mice displayed widespread vacuolization and severe astrogliosis at the terminal stage of scrapie. In contrast Tg (MoPrP, Q167R)/*Prnp*^{0/0} mice did not display a typical scrapie pathology [Perrier *et al.*, 2002]. In conclusion neuropathological changes in terminal Tg floxed LacZ-PrP^{Q167R} mice can be attributed to the co-expression of PrP^{Q167R} and wild-type PrP.

Moreover it was reported that PrP^{Q167R} can not be converted into PrP^{Sc} [Kaneko *et al.*, 1997b], consequently we did not detect any PK-resistant PrP^{Q167R} in scrapie affected transgenic mice. Similar to our results no PK-resistant PrP was observed in Tg (MoPrP, Q167R)/*Prnp*^{0/0} mice, while Tg (MoPrP, Q167R) /*Prnp*^{+/+} mice exhibited PrP^{Sc} accumulation in the brain at the late stage of the disease [Perrier *et al.*, 2002]. Transgenic PrP^{Q167R} in Tg (MoPrP, Q167R) mice did not contain a specific antibody epitope. Therefore it was not distinguishable from wild-type PrP^C but it is likely that also in these mice PrP^{Q167R} did not contribute to PrP^{Sc} levels. Recently, several new dominant-negative PrP mutants, such as S221P and Y217C, were identified by generation of a PrP library. These new dominant-negative PrP mutants were capable to inhibit prion replication in prion infected murine neuroblastoma cells (N2a) [Ott *et al.*, 2008] and it will be of interest to investigate the properties of these new PrP mutants *in*

vivo.

In summary, our findings demonstrate that the protection of neurons inside brain areas that are responsible for motor control delays the appearance of clinical symptoms after low dose peripheral prion infection. Expression of protective PrP^{Q167R} exclusively in a subset of spinal MN did not influence the clinical course of scrapie. Therefore the results suggest CTA upstream of the abducens motor nucleus, e.g. in nucleus ruber, which is in agreement with other studies [Flechsig *et al.*, 2000; Bartz *et al.*, 2002; Ermolayev *et al.*, 2009a]. Furthermore our data confirms earlier results, showing that neuronal depletion of PrP^C in prion infected mice prevented progression to clinical prion disease [Mallucci *et al.*, 2003].

A detailed characterization of brain centers and neuronal populations that are involved in prion accumulation and pathogenesis has important implications for the development of therapeutical concepts. Considering the various possibilities of the Cre/loxP technology, the new mouse model with inducible expression of PrP^{Q167R} offers a great potential to identify new CTA responsible for the manifestation of clinical prion disease. After identification of such defined vulnerable cell populations, therapeutical strategies can be applied in a more focused and therefore more effective way. Moreover an advance in therapeutics can only be achieved, when intervention occurs at an early stage of infection before massive replication and accumulation of the infectious agent and clinical signs are obvious. A successful gene therapy approach in a mouse-model of prion disease has already been published. In this study a lentiviral gene transfer was used to deliver PrP^{Q167R} into prion infected wild-type mice resulting in a prolonged lifespan of the treated mice [Toupet *et al.*, 2008]. In addition several approaches using RNA interference techniques as well as antibody-based immunotherapies and attempts aiming at the identification of new anti-prion molecules are under investigation [Sakaguchi, 2009; White and Mallucci, 2009; Relación-Ginés *et al.*, 2009]. Thus, a detailed knowledge of CTA might contribute to the development of promising strategies against prion diseases.

6.2 Transfer of Cre-recombinase into Tg floxed LacZ-PrP^{Q167R} mice by adeno-associated viral vectors (AAV-Cre)

A strategy to enhance expression levels of protective PrP^{Q167R} in the spinal cord of Tg floxed-LacZ-PrP^{Q167R} mice is the transfer of Cre by adeno-associated virus vectors (dsAAV2-Cre). It was reported that AAV2 vectors efficiently spread retrogradly from muscle tissue via muscle-innervating neurons into the spinal cord and from there proceed to connected brain centers, where the encoded transgene is efficiently expressed [Kaspar *et al.*, 2003].

Therefore dsAAV2-Cre was injected into the hind-limb muscles of Tg floxed-LacZ-

PrP^{Q167R} mice. At different time points after dsAAV2-Cre application, brain, spinal cord and muscle tissue of transgenic mice was collected and analyzed for Cre-recombination and expression of PrP^{Q167R} by PCR and western blot. Moreover, two different dsAAV2-Cre batches, exhibiting different viral titers were used.

In a number of previous studies a toxic effect of Cre-expression was observed in cell culture as well as in transgenic mice. Cells lacking ectopic loxP sites died after application of lenti-Cre vectors, while a massive tissue damage was found 3 weeks after viral transfer of Cre into the brain of reporter mice. It was concluded that the mammalian genome contains pseudo loxP sites, which serve as functional recognition sites for Cre. As a consequence, recombination of these pseudo-loxP sites leads to chromosome rearrangements [Silver and Livingston, 2001; Pfeifer et al., 2001]. In this study, the application of dsAAV2-Cre had no deleterious effect on behavior and fitness of Tg floxed-LacZ-PrP^{Q167R} mice until 107 dpi. Thus, the results do not confirm recent reports of Cre-toxicity.

In Tg floxed-LacZ-PrP^{Q167R} mice, treated with dsAAV2-Cre of batch 1, no recombinant DNA and consequently no expression of PrP^{Q167R} was observed. Therefore a second batch of dsAAV2-Cre, providing a higher virus titer of 5×10^{10} genomic particles per ml (GP/ml) was used. In addition to that, mice treated with dsAAV2-Cre of batch 2 were sacrificed at an earlier time point. In these mice, recombinant DNA as well as viral Cre DNA was detected in the muscle tissue. No recombinant DNA was found in the spinal cord or in the brain. The results confirm that functional Cre was expressed at least at the site of virus application. Unfortunately, no expression of PrP^{Q167R} protein was observed in muscle, spinal cord or brain. The results suggest that even a virus titer of 5×10^{10} GP/ml was not sufficient to induce the expression of PrP^{Q167R}. Although expression of PrP^{Q167R} under control of the UbiC promoter was observed in brain and spinal cord as discussed before, it remains elusive if UbiC directs expression to skeletal muscle.

Several hypothesis may explain the poor efficiency of dsAAV2-Cre vectors to induce recombination in Tg floxed-LacZ-PrP^{Q167R} mice. It has to be considered that the virus titer of both batches was calculated from quantitative real time PCR analysis. Therefore the virus titer is only a physical titer and does not characterize the ability of dsAAV2-Cre to infect cells *in vivo*. Thus, the biological titer of both dsAAV2-Cre batches may be clearly lower than 5×10^{10} GP/ml.

However, it was reported that a dose of 1×10^{10} viral particles (vp) of single-stranded AAV-GFP was sufficient to achieve transport of AAV from the hind limb quadriceps to the lumbar spinal cord [Kaspar et al., 2003] and application of 0,8 μ l of ssAAV2-Cre (biological titer: 1×10^8 vp/ml) into the brain of transgenic mice induced Cre-recombination [Ahmed et al., 2004]. Furthermore, several studies proofed a superior and accelerated transduction of dsAAV *in vitro* and *in vivo* as well as an increase in transgene expres-

sion as compared to ssAAV vectors [Wang *et al.*, 2003; Chen *et al.*, 2007]. A stable and efficient expression of dsAAV-GFP after i.m. injection of a 30 μ l volume, exhibiting a virus titer of 1×10^{11} GP/ml, resulted in strong expression of GFP already at 7 dpi [Wang *et al.*, 2003].

The total packaging capacity of AAV is about 5 kb [Gonçalves, 2005]. Consequently it was suggested that in case of dsAAV vectors, the entire AAV vector genome should not exceed 2,5 kb so that a dimer molecule can be packed within the viral capsid [Wang *et al.*, 2003]. As the size of dsAAV2-Cre was 5,135 kb a correct packaging of Cre-DNA into the AAV capsid can not be assured and may lead to defective viral particles.

The fact that dsAAV2-Cre was expressed in muscle tissue but not in the spinal cord or brain may also be related to an inefficient dsAAV2-Cre transport. It is possible that AAV particles were not able to enter muscle innervating nerve fibers. As a consequence, dsAAV2-Cre was not transported into MN of the spinal cord or to spinal cord projecting neurons of the brain. In order to enhance the uptake of AAV into nerve fibers and to improve retrograde transport of viral particles, a modification of capsid proteins would be required. Alteration of the virus tropism can be achieved by chemical, immunological or genetic means. For example a chemical modification of the AAV capsid using bispecific antibodies with specificity for the virion of AAV2 and the cell surface receptor $\alpha_{IIb} \beta_3$ enabled AAV2 to transduce human megakaryoblast cells [Bartlett *et al.*, 1999]. In addition, insertion of foreign epitopes that mediate binding to specific cell receptors into the capsid coding region may be an approach to enhance virus uptake into distinct cell populations [Rabinowitz and Samulski, 2000].

To summarize, the results suggest that the current dsAAV2-Cre vector system needs further improvement to achieve efficient transport from the site of application to the CNS and to induce expression of PrP^{Q167R} in Tg floxed LacZ-PrP^{Q167R} mice. In general, an efficient dsAAV2-Cre vector system would be desirable as it could avoid time-consuming breeding of transgenic mice to Cre-strains.

6.3 Accumulation of PrP^{Sc} and prion infectivity in splenic tissue of neuronal PrP deficient mice

The lethal journey of prions through the body of infected individuals involves numerous cell types and tissues. After oral uptake prion spread from the intestine to lymphoid organs from where they ascend to the CNS, most likely by traveling along tissue innervating fibers that are connected to neurons of the spinal cord or directly to neurons of the brain [Beekes and McBride, 2007]. An accumulation of prions in the lymphoreticular system (LRS) seems to be essential for an efficient delivery of prions to the CNS. In particular the spleen was identified as an early site of prion replication [Fraser and Dickinson, 1970; Mould *et al.*, 1970; Kimberlin and Walker, 1989]. However, it remains

unclear if splenic lymphocytes or follicular dendritic cells (FDC) themselves are capable to replicate the infectious agent or if other PrP-expressing cell types, such as neurons innervating the LRS are involved.

To answer this question and investigate if such neurons and in particular MN are involved in the accumulation of prions in splenic tissue, we established a double transgenic mouse model, carrying one allele of floxed *Prnp* ($lox2^{+/-}$) [Rossi *et al.*, 2001] and either one allele of Hb9-Cre or NF-L-Cre on a *Prnp*^{0/0} background. The recombination of transgenic DNA was demonstrated by PCR, while quantification of western blots revealed diminished PrP levels in brain and spinal cord of double- transgenic mice, suggesting that the expression of Cre in these mice led to a conditional PrP knockout in a subset of MN of the spinal cord (Hb9-Cre) [Arber *et al.*, 1999; Yang *et al.*, 2001] or in various neuronal populations of brain and spinal cord (NF-L-Cre) [Schweizer *et al.*, 2002].

Lox2 mice originate from a cloning strategy that aimed to generate a *Prnp* knockout strain called *Prnp*^{0/0} Zürich II. Cre-mediated deletion of loxP flanked *Prnp* alleles, led to a knockout of the entire PrP encoding region and its flanking sequences in *Prnp*^{0/0} Zürich II mice. It is known that these mice develop a cerebellar syndrome, which is attributed to a severe loss of Purkinje cells starting at the age of ~ 6 month. Symptoms of this cerebellar syndrome include tremor and a trembling gait [Rossi *et al.*, 2001]. Although Cre-mediated recombination in neurons of $lox2^{+/-}$ /NF-L-Cre and $lox2^{+/-}$ /Hb9-Cre mice established a PrP knockout similar to *Prnp*^{0/0} Zürich II, the phenotype and behavior of double-transgenic mice was not distinguishable from wild-type mice.

After intracerebral (i.c.) and intraperitoneal (i.p.) inoculation of double-transgenic mice with prions, the accumulation of PrP^{Sc} and prion infectivity in splenic tissue and in the spinal cord was investigated at 50 days post inoculation (dpi). No accumulation of PrP^{Sc} was detected in the spinal cord in any of the inoculated mice, confirming that 50 dpi represents indeed an early time point of the infection before the CNS is affected.

While PrP^{Sc} accumulation in the spleen was unaltered in PrP heterozygous ($lox2^{+/-}$) and MN-specific PrP deficient mice ($lox2^{+/-}$ /Hb9-Cre mice), mice with PrP depletion in spinal cord and brain ($lox2^{+/-}$ /NF-L-Cre) failed to replicate PrP^{Sc} in splenic tissue. In addition, these mice exhibited a clearly reduced prion infectivity titer in comparison to $lox2^{+/-}$ and $lox2^{+/-}$ /Hb9-Cre mice as shown in a bioassay using PrP overexpressing Tga20 indicator mice.

Therefore the results demonstrate that PrP^{Sc} accumulation as well as the accumulation of prion infectivity titers in the spleen at an early time point of prion infection is dependent on pan-neuronal PrP expression. In contrast a MN-specific PrP depletion did not influence splenic PrP^{Sc} replication, suggesting that nerve fibers located in the direct vicinity of splenic tissues are responsible. Therefore it might be possible that after prion infection the agent multiplies in neuronal tissue, which segregates PrP^{Sc}

and prion infectivity to lymphoid components. In those components such as follicular dendritic cells (FDC) or B- and T-lymphocytes, prions can be stored and accumulate to a certain threshold.

It was reported that the expression of light neurofilaments, which is controlled by the NF-L promoter, occurs in the mouse central and in the peripheral nervous system (PNS) [Cochard and Paulin, 1984]. In addition to that it was shown that the NF-L promoter can also initiate muscle-specific transgene expression [Yaworsky *et al.*, 1997]. So far no direct evidence for NF-L promoter activity in splenic tissue or in spleen innervating neurons was found, raising the question how NF-L positive nerve fibers can influence prion accumulation in the spleen. Therefore a detailed mapping of the NF-L promoter activity using highly sensitive approaches such as real time PCR, hybridization or high resolution microscopy should be carried out.

Nevertheless, our results are in good agreement with previous studies investigating neuron-specific PrP expression in prion pathogenesis. It is clear that PrP^C is required for prion replication as *Prnp*^{0/0} mice are resistant to prion infection [Büeler *et al.*, 1993]. PrP expression is also necessary for the transfer of prions from the periphery to the CNS [Blättler *et al.*, 1997]. Moreover, neuron-specific expression of hamster PrP in transgenic mice was sufficient to render mice susceptible to hamster scrapie [Race *et al.*, 1995]. Another conditional PrP knockout model was described in 2002 [Mallucci *et al.*, 2002]. Similar to lox2, MloxP mice possess floxed *Prnp* alleles on a *Prnp*^{0/0} background. Upon breeding of MloxP to a strain with Cre expression under control of the neurofilament heavy chain (NF-H) promoter, a neuronal PrP depletion was achieved and it turned out that these mice were resistant to scrapie infection. Later it was demonstrated that depletion of neuronal PrP^C in mice with established prion infection even reversed early spongiform changes and prevented neuronal loss as well as progression to clinical disease [Mallucci *et al.*, 2003]. However, if these mice accumulate PrP^{Sc} and prion infectivity in the spleen was not investigated.

Although neuronal expression of PrP^C seems to be crucial to sustain scrapie infection, non-neuronal cells may also contribute to the disease development as expression of hamster PrP exclusively in astrocytes rendered *Prnp*^{0/0} mice susceptible to hamster scrapie [Raeber *et al.*, 1997]. Furthermore a hematogenous spread of prions cannot be excluded since vCJD-cases have been described, in which transmission probably occurred after blood transfusion [Llewelyn *et al.*, 2004; Peden and Ironside, 2004].

As peripheral prion accumulation occurs at an early phase of the disease progression before neuronal damage and clinical signs become obvious, the involvement of non-neuronal cells has been studied extensively. It was shown that in splenic tissue prion infectivity is associated with B- and T-lymphocytes as well as with the stroma [Raeber *et al.*, 1999] and prion replication in the spleen seems to depend on PrP^C expressing FDCs [Montrasio *et al.*, 2000; Mabbott *et al.*, 2003]. In contrast, prion in-

oculation experiments with mice lacking FDCs revealed that other cell types were also capable of replicating prions [Prinz *et al.*, 2002], but it remains unclear which other lymphoreticular cells are involved. Furthermore it is still elusive, how prions proceed from FDCs to the PNS. Because of the microarchitecture of lymphoid organs, a direct transfer from FDCs to peripheral nerve fibers seems to be unlikely as both are located in separated compartments [Felten, 1993; Defaweux *et al.*, 2005]. In this context motile dendritic cells (DC) as well as exosomes have been proposed as prion transport vehicles [Février *et al.*, 2005]. It was already demonstrated that FDCs are able to bind as well as to secrete exosomes [Denzer *et al.*, 2000a, b]. Whether those exosomes contain prion infectivity and if they are capable to fuse with the neuronal membrane of peripheral nerves remains to be investigated. In addition it would be very interesting to study if peripheral nerves are able to secrete exosomes that contain prion infectivity.

Prion disease show up with very long incubation periods. During the course of the disease clinical signs appear at a late stage of the disease, when neuronal damage is already widespread and non-reversible. Therefore the mechanisms of early prion accumulation, which precede neuronal dysfunctions have to be studied extensively in order to develop effective diagnostic tools as well as new strategies against prion replication and spread. In contrast to the CNS, which is separated by the blood-brain barrier, peripheral sites such as lymphoreticular organs are much easier accessible. In this context peripheral sites are of outstanding interest for the development of anti-prion therapies.

7 Summary

Prion diseases such as scrapie in sheep, bovine spongiform encephalopathy (BSE) in cattle or Creutzfeldt-Jakob disease (CJD) in humans are fatal neurodegenerative disorders characterized by brain lesions and the accumulation of a disease-associated protein, designated PrP^{Sc}. How prions proceed to damage neurons and whether all or only subsets of neurons have to be affected for the onset of the clinical disease is still elusive. The manifestation of clinical prion disease is characterized by motor dysfunctions, dementia and death. Furthermore loss of motor neurons (MN) in the spinal cord is a constant finding in different mouse models of prion disease, suggesting that MN are vulnerable cells for triggering the onset of clinical symptoms.

To determine whether the protection of MN against prion induced dysfunctions is an approach for holding the disease at the sub-clinical level, we established a novel conditional model for Cre-mediated expression of a dominant-negative PrP mutant (PrP^{Q167R}) in the cells of interest. Dominant-negative PrP mutants provide protection of prion induced dysfunctions by inhibiting prion replication. Transgenic mice were generated carrying a floxed *LacZ* marker gene followed by the coding sequence of PrP^{Q167R} under control of the human ubiquitin C promoter. Two Cre strains have been used to direct PrP^{Q167R} expression either to a subset of MN of the spinal cord (Hb9-Cre) or to various neuronal cell populations of the spinal cord and brain (NF-L-Cre). Transgenic mice were infected with mouse-adapted prions via different inoculation routes (intranerval, intracerebral and intraperitoneal) and monitored for effects on incubation time and pathology. Tg floxed LacZ-PrP^{Q167R}/NF-L-Cre mice showed about 15% prolonged survival upon intraperitoneal low dose prion infection, whereas survival of Tg floxed LacZ-PrP^{Q167R}/Hb9-Cre mice was comparable to control littermates. The results suggest that the protection of spinal MN prolongs the incubation period but is not sufficient to completely inhibit clinical prion disease.

In a second approach, Cre was transferred into the hind limb muscles of transgenic mice via a double-stranded adeno-associated virus vector (dsAAV2-Cre). The goal of this strategy was to target a broader cell population and thus to enhance expression levels of protective PrP^{Q167R} in the spinal cord of Tg floxed-LacZ-PrP^{Q167R} mice.

After intramuscular (i.m.) application of dsAAV2-Cre, exhibiting a physical titer of 5×10^{10} GP/ml, recombinant transgenic DNA was detected only in the muscle tissue, pointing out that functional Cre-recombinase was expressed at the side of virus application. However, dsAAV2-Cre did neither induce recombination of transgenic DNA in the spinal cord or brain nor expression of dominant-negative PrP^{Q167R}. In conclusion the dsAAV2-Cre vectors system needs further improvement to achieve efficient transport from muscle tissue to the central nervous system (CNS).

The lymphoreticular system (LRS) is an early site of prion replication. In splenic tissue prion infectivity is associated with follicular dendritic cells (FDC) as well as with B- and T-lymphocytes. However, it is still unknown if those cell types are able to replicate the infectious agent or if other PrP-expressing cell types are engaged.

To investigate if neurons and in particular MN are involved, transgenic mice carrying one allele of floxed *Prnp* ($lox2^{+/-}$) and either one allele of Hb9-Cre or NF-L-Cre were generated on a *Prnp*^{0/0} background. Therefore a conditional PrP knockout was established in a subset of MN of the spinal cord (Hb9-Cre) or in various neuronal populations of the spinal cord and brain (NF-L-Cre). Transgenic mice were inoculated with prions to study the accumulation of PrP^{Sc} and prion infectivity in spleen and spinal cord at an early time point after infection.

The findings show that PrP^{Sc} accumulation in mice with MN-specific PrP depletion ($lox2^{+/-}$ /Hb9-Cre) was comparable to control littermates, while pan-neuronal PrP deficient mice ($lox2^{+/-}$ /NF-L-Cre) were not able to accumulate PrP^{Sc} in splenic tissue until 50 days post inoculation. Moreover spleens of $lox2^{+/-}$ /NF-L-Cre mice exhibited a clearly reduced prion infectivity titer, suggesting that accumulation of prions in the spleen is dependent on PrP expression in the nervous tissue.

8 Zusammenfassung

Prionenerkrankungen, wie Scrapie beim Schaf, die bovine spongiforme Enzephalopathie (BSE) beim Rind oder die Creutzfeldt-Jakob-Krankheit (CJD) beim Menschen sind letale, neurodegenerative Erkrankungen des zentralen Nervensystems (ZNS). Typische Merkmale der Erkrankung sind neben Neuronenverlust die Akkumulation des mit der Krankheit assoziierten Proteins PrP^{Sc} im Gehirn infizierter Individuen. Wie die Akkumulation von Prionen zu Neurodegeneration führt und welche Regionen des ZNS für die klinische Erkrankung verantwortlich sind, ist bisher unbekannt. Charakteristische, klinische Symptome von Prionenkrankheiten sind motorische Störungen sowie Demenz in einem späten Stadium der Erkrankung. Außerdem ist der Verlust von Motoneuronen (MN) im Rückenmark ein konstanter Befund im Tiermodell, was eine Rolle des motorischen Nervensystems bei der Prionpathogenese vermuten lässt.

In dieser Arbeit sollte daher untersucht werden, ob der Schutz von MN vor Prionen induzierten Dysfunktionen den Ausbruch der klinischen Erkrankung verzögern kann. Dazu wurde ein konditionales Mausmodell mit Cre-induzierbarer Expression einer dominant-negativen PrP-Mutante (PrP^{Q167R}) hergestellt. Dominant-negative PrP Mutanten schützen vor Prionen induzierten Schädigungen, indem sie die Replikation von Prionen inhibieren. Das Transgen besteht aus dem humanen Ubiquitin C Promoter, einem „gefloxten“ *LacZ* Markergen und der kodierenden Sequenz von PrP^{Q167R}. Die Kreuzung von Tg floxed *LacZ-PrP^{Q167R}* Mäusen mit der Hb9-Cre Linie bewirkt eine MN-spezifische Expression von PrP^{Q167R} im Rückenmark, während das Einkreuzen eines NF-L-Cre Allels die Expression von PrP^{Q167R} in den meisten Neuronen des Rückenmarks sowie in verschiedenen motorischen Kerngebieten des Gehirns zur Folge hat. Transgenen Mäuse wurden auf verschiedenen Routen (intranerval, intrazerebral und intraperitoneal) mit Maus-adaptierten Prionen infiziert und der Effekt von PrP^{Q167R} auf die Inkubationszeit und Pathologie der Tiere untersucht. Während Tg floxed *LacZ-PrP^{Q167R}/NF-L-Cre* Mäuse eine um 15% verlängerte Inkubationszeit aufwiesen, war bei Tg floxed *LacZ-PrP^{Q167R}/Hb9-Cre* Mäusen kein Überlebensvorteil zu beobachten. Somit verlängert der Schutz von MN des Rückenmarks zwar die Inkubationszeit, ist aber nicht ausreichend, um den klinischen Ausbruch der Erkrankung zu verhindern.

Um eine größere Zellpopulation im Rückenmark von Tg floxed *LacZ-PrP^{Q167R}* Mäusen und so eine stärkere Expression von PrP^{Q167R} zu erreichen, wurde ein viraler Gentransfer von Cre-Rekombinase durchgeführt. Dazu wurden doppelsträngige, Cre-exprimierende Adeno-assoziierte Virus Vektoren (dsAAV2-Cre) bilateral in die Muskulatur der Hinterbeine von Tg floxed *LacZ-PrP^{Q167R}* Mäusen injiziert.

Die Applikation von dsAAV2-Cre, mit einem physikalischen Virus-Titer von 5×10^{10} GP/ml, führte ausschließlich im Muskelgewebe zur Expression von enzymatisch aktiver Cre-Rekombinase und folglich zur Rekombination der transgenen DNA. Im Rücken-

mark oder Gehirn war keine rekombinante DNA detektierbar. Auch auf Protein-Ebene konnte die Expression von PrP^{Q167R} weder im Muskel noch im Rückenmark oder Gehirn nachgewiesen werden. Um den Transport von dsAAV2-Cre vom Applikationsort bis in das ZNS zu gewährleisten und Cre stabil zu exprimieren, ist demnach eine weitere Optimierung des dsAAV2-Cre Vektorsystems notwendig.

Prionen replizieren im lymphoretikulären System (LRS) bereits in einem frühen Stadium der Erkrankung. In der Milz ist Prionen-Infektiosität in follikulär dendritischen Zellen (FDC) sowie in B- und T-Lymphozyten lokalisiert. Ob noch andere PrP exprimierende Zellen an der Prionen-Replikation im LRS beteiligt sind, ist unklar.

Um die Beteiligung von Neuronen und MN an der Akkumulation von Prionen im LRS zu untersuchen, wurden transgene, neuronal PrP defiziente Mäuse generiert. Ein Neuronen-spezifischer bzw. MN-spezifischer Knockout von PrP wurde durch Kreuzung von transgenen lox2^{+/-} Mäusen, welche ein „gefloxtes“ *Prnp* Allel *Prnp* auf einem *Prnp*^{0/0} Hintergrund tragen, mit NF-L-Cre oder Hb9-Cre Mäusen erreicht. Nach Prionen-Infektion von lox2^{+/-}/NF-L-Cre und lox2^{+/-}/Hb9-Cre Mäusen wurde die Akkumulation von PrP^{Sc} und Prionen-Infektiosität in der Milz und im Rückenmark am Tag 50 nach der Infektion analysiert.

Während die Replikation von PrP^{Sc} in der Milz von Mäusen mit MN-spezifischem PrP Knockout (lox2^{+/-}/Hb9-Cre) nicht beeinträchtigt war, war in pan-neuronal PrP defizienten Mäusen (lox2^{+/-}/NF-L-Cre) keine Akkumulation von PrP^{Sc} nachweisbar. Zudem war die Prionen-Infektiosität in der Milz von lox2^{+/-}/NF-L-Cre Mäusen deutlich reduziert. Die Ergebnisse weisen darauf hin, dass die Akkumulation von PrP^{Sc} und Prionen-Infektiosität in der Milz abhängig von neuronaler PrP Expression ist.

References

- Aguzzi, A., and M. Polymenidou, Mammalian prion biology: one century of evolving concepts., *Cell*, 116(2), 313–327, 2004.
- Aguzzi, A., M. Heikenwalder, and M. Polymenidou, Insights into prion strains and neurotoxicity., *Nat Rev Mol Cell Biol*, 8(7), 552–561, 2007.
- Ahmed, B. Y., et al., Efficient delivery of cre-recombinase to neurons in vivo and stable transduction of neurons using adeno-associated and lentiviral vectors., *BMC Neurosci*, 5, 4, 2004.
- Alper, T., D. A. Haig, and M. C. Clarke, The exceptionally small size of the scrapie agent., *Biochem Biophys Res Commun*, 22(3), 278–284, 1966.
- Alper, T., W. A. Cramp, D. A. Haig, and M. C. Clarke, Does the agent of scrapie replicate without nucleic acid?, *Nature*, 214(5090), 764–766, 1967.
- Alpers, M., and L. Rail, Kuru and creutzfeldt-jakob disease: clinical and aetiological aspects., *Proc Aust Assoc Neurol*, 8, 7–15, 1971.
- Araki, K., T. Imaizumi, K. Okuyama, Y. Oike, and K. Yamamura, Efficiency of recombination by cre transient expression in embryonic stem cells: comparison of various promoters., *J Biochem*, 122(5), 977–982, 1997.
- Arber, S., B. Han, M. Mendelsohn, M. Smith, T. M. Jessell, and S. Sockanathan, Requirement for the homeobox gene hb9 in the consolidation of motor neuron identity., *Neuron*, 23(4), 659–674, 1999.
- Armand, J., [the pyramidal tract. recent anatomic and physiologic findings], *Rev Neurol (Paris)*, 140(5), 309–329, 1984.
- Arnold, J. E., C. Tipler, L. Laszlo, J. Hope, M. Landon, and R. J. Mayer, The abnormal isoform of the prion protein accumulates in late-endosome-like organelles in scrapie-infected mouse brain., *J Pathol*, 176(4), 403–411, 1995.
- Atchison, R. W., B. C. Casto, and W. M. Hammon, Adenovirus-associated defective virus particles., *Science*, 149, 754–756, 1965.
- Baldwin, M. A., et al., Spectroscopic characterization of conformational differences between prpc and prpsc: an alpha-helix to beta-sheet transition., *Philos Trans R Soc Lond B Biol Sci*, 343(1306), 435–441, 1994.
- Baron, G. S., and B. Caughey, Effect of glycosylphosphatidylinositol anchor-dependent and -independent prion protein association with model raft membranes on conversion to the protease-resistant isoform., *J Biol Chem*, 278(17), 14,883–14,892, 2003.
- Bartlett, J. S., R. J. Samulski, and T. J. McCown, Selective and rapid uptake of adeno-associated virus type 2 in brain., *Hum Gene Ther*, 9(8), 1181–1186, 1998.
- Bartlett, J. S., J. Kleinschmidt, R. C. Boucher, and R. J. Samulski, Targeted adeno-associated virus vector transduction of nonpermissive cells mediated by a bispecific f(ab'gamma)2 antibody., *Nat Biotechnol*, 17(2), 181–186, 1999.
- Bartz, J. C., A. E. Kincaid, and R. A. Bessen, Retrograde transport of transmissible mink encephalopathy within descending motor tracts., *J Virol*, 76(11), 5759–5768, 2002.
- Basler, K., B. Oesch, M. Scott, D. Westaway, M. Wälchli, D. F. Groth, M. P. McKinley, S. B. Prusiner, and C. Weissmann, Scrapie and cellular prp isoforms are encoded by the same chromosomal gene., *Cell*, 46(3), 417–428, 1986.
- Beal, M. F., Experimental models of parkinson's disease., *Nat Rev Neurosci*, 2(5), 325–334, 2001.
- Beekes, M., and P. A. McBride, Early accumulation of pathological prp in the enteric nervous system and gut-associated lymphoid tissue of hamsters orally infected with scrapie., *Neurosci Lett*, 278(3), 181–184, 2000.

- Beekes, M., and P. A. McBride, The spread of prions through the body in naturally acquired transmissible spongiform encephalopathies., *FEBS J*, 274(3), 588–605, 2007.
- Büeler, H., M. Fischer, Y. Lang, H. Bluethmann, H. P. Lipp, S. J. DeArmond, S. B. Prusiner, M. Aguet, and C. Weissmann, Normal development and behaviour of mice lacking the neuronal cell-surface prp protein., *Nature*, 356(6370), 577–582, 1992.
- Büeler, H., A. Aguzzi, A. Sailer, R. A. Greiner, P. Autenried, M. Aguet, and C. Weissmann, Mice devoid of prp are resistant to scrapie., *Cell*, 73(7), 1339–1347, 1993.
- Büeler, H., A. Raeber, A. Sailer, M. Fischer, A. Aguzzi, and C. Weissmann, High prion and prpsc levels but delayed onset of disease in scrapie-inoculated mice heterozygous for a disrupted prp gene., *Mol Med*, 1(1), 19–30, 1994.
- Bellinger-Kawahara, C., J. E. Cleaver, T. O. Diener, and S. B. Prusiner, Purified scrapie prions resist inactivation by uv irradiation., *J Virol*, 61(1), 159–166, 1987a.
- Bellinger-Kawahara, C., T. O. Diener, M. P. McKinley, D. F. Groth, D. R. Smith, and S. B. Prusiner, Purified scrapie prions resist inactivation by procedures that hydrolyze, modify, or shear nucleic acids., *Virology*, 160(1), 271–274, 1987b.
- Bellworthy, S. J., et al., Tissue distribution of bovine spongiform encephalopathy infectivity in romney sheep up to the onset of clinical disease after oral challenge., *Vet Rec*, 156(7), 197–202, 2005.
- Belt, P. B., I. H. Muileman, B. E. Schreuder, J. B. de Ruijter, A. L. Gielkens, and M. A. Smits, Identification of five allelic variants of the sheep prp gene and their association with natural scrapie., *J Gen Virol*, 76 (Pt 3), 509–517, 1995.
- Bernoulli, C., J. Siegfried, G. Baumgartner, F. Regli, T. Rabinowicz, D. C. Gajdusek, and C. J. Gibbs, Danger of accidental person-to-person transmission of creutzfeldt-jakob disease by surgery., *Lancet*, 1(8009), 478–479, 1977.
- Bessen, R. A., D. A. Kocisko, G. J. Raymond, S. Nandan, P. T. Lansbury, and B. Caughey, Non-genetic propagation of strain-specific properties of scrapie prion protein., *Nature*, 375(6533), 698–700, 1995.
- Bishop, J. O., and P. Smith, Mechanism of chromosomal integration of microinjected dna., *Mol Biol Med*, 6(4), 283–298, 1989.
- Blanquet-Grossard, F., N. M. Thielens, C. Vendrely, M. Jamin, and G. J. Arlaud, Complement protein c1q recognizes a conformationally modified form of the prion protein., *Biochemistry*, 44(11), 4349–4356, 2005.
- Blättler, T., S. Brandner, A. J. Raeber, M. A. Klein, T. Voigtländer, C. Weissmann, and A. Aguzzi, Prp-expressing tissue required for transfer of scrapie infectivity from spleen to brain., *Nature*, 389(6646), 69–73, 1997.
- Bode, J., Y. Kohwi, L. Dickinson, T. Joh, D. Klehr, C. Mielke, and T. Kohwi-Shigematsu, Biological significance of unwinding capability of nuclear matrix-associating dnas., *Science*, 255(5041), 195–197, 1992.
- Bolton, D. C., M. P. McKinley, and S. B. Prusiner, Identification of a protein that purifies with the scrapie prion., *Science*, 218(4579), 1309–1311, 1982.
- Bons, N., N. Mestre-Frances, P. Belli, F. Cathala, D. C. Gajdusek, and P. Brown, Natural and experimental oral infection of nonhuman primates by bovine spongiform encephalopathy agents., *Proc Natl Acad Sci U S A*, 96(7), 4046–4051, 1999.
- Botto, L., M. Masserini, A. Cassetti, and P. Palestini, Immunoseparation of prion protein-enriched domains from other detergent-resistant membrane fractions, isolated from neuronal cells., *FEBS Lett*, 557(1-3), 143–147, 2004.
- Bradford, M. M., A rapid and sensitive method for the quantitation of microgram quantities of protein utilizing the principle of protein-dye binding., *Anal Biochem*, 72, 248–254, 1976.
- Brückner, G., A. Bringmann, G. Köppe, W. Härtig, and K. Brauer, In vivo and in vitro labelling of perineuronal nets in rat brain., *Brain Res*, 720(1-2), 84–92, 1996.

- Brinster, R. L., R. E. Braun, D. Lo, M. R. Avarbock, F. Oram, and R. D. Palmiter, Targeted correction of a major histocompatibility class ii e alpha gene by dna microinjected into mouse eggs., *Proc Natl Acad Sci U S A*, 86(18), 7087–7091, 1989.
- Brown, D. R., B. Schmidt, M. H. Groschup, and H. A. Kretzschmar, Prion protein expression in muscle cells and toxicity of a prion protein fragment., *Eur J Cell Biol*, 75(1), 29–37, 1998.
- Brown, D. R., B. S. Wong, F. Hafiz, C. Clive, S. J. Haswell, and I. M. Jones, Normal prion protein has an activity like that of superoxide dismutase., *Biochem J*, 344 Pt 1, 1–5, 1999a.
- Brown, D. R., et al., The cellular prion protein binds copper in vivo., *Nature*, 390(6661), 684–687, 1997.
- Brown, K. L., K. Stewart, D. L. Ritchie, N. A. Mabbott, A. Williams, H. Fraser, W. I. Morrison, and M. E. Bruce, Scrapie replication in lymphoid tissues depends on prion protein-expressing follicular dendritic cells., *Nat Med*, 5(11), 1308–1312, 1999b.
- Brown, P., The clinical neurology and epidemiology of creutzfeldt-jakob disease, with special reference to iatrogenic cases., *Ciba Found Symp*, 135, 3–23, 1988.
- Brown, P., et al., Iatrogenic creutzfeldt-jakob disease at the millennium., *Neurology*, 55(8), 1075–1081, 2000.
- Browning, S. R., et al., Transmission of prions from mule deer and elk with chronic wasting disease to transgenic mice expressing cervid prp., *J Virol*, 78(23), 13,345–13,350, 2004.
- Bruce, M. E., et al., Transmissions to mice indicate that 'new variant' cjd is caused by the bse agent., *Nature*, 389(6650), 498–501, 1997.
- Bull, L. B., and D. Murnane, An outbreak of scrapie in british sheep imported into victoria., *Aust Vet J*, 34, 213–215, 1958.
- Burthem, J., B. Urban, A. Pain, and D. J. Roberts, The normal cellular prion protein is strongly expressed by myeloid dendritic cells., *Blood*, 98(13), 3733–3738, 2001.
- Carlson, G. A., D. T. Kingsbury, P. A. Goodman, S. Coleman, S. T. Marshall, S. DeArmond, D. Westaway, and S. B. Prusiner, Linkage of prion protein and scrapie incubation time genes., *Cell*, 46(4), 503–511, 1986.
- Carter, B. J., Adeno-associated virus vectors in clinical trials., *Hum Gene Ther*, 16(5), 541–550, 2005.
- Caughey, B., In vitro expression and biosynthesis of prion protein., *Curr Top Microbiol Immunol*, 172, 93–107, 1991.
- Caughey, B., Interactions between prion protein isoforms: the kiss of death?, *Trends Biochem Sci*, 26(4), 235–242, 2001.
- Caughey, B., and G. J. Raymond, The scrapie-associated form of prp is made from a cell surface precursor that is both protease- and phospholipase-sensitive., *J Biol Chem*, 266(27), 18,217–18,223, 1991.
- Caughey, B., D. A. Kocisko, G. J. Raymond, and P. T. Lansbury, Aggregates of scrapie-associated prion protein induce the cell-free conversion of protease-sensitive prion protein to the protease-resistant state., *Chem Biol*, 2(12), 807–817, 1995.
- Chandler, R. L., Encephalopathy in mice produced by inoculation with scrapie brain material., *Lancet*, 1(7191), 1378–1379, 1961.
- Chen, S. L., H. I. Ma, J. M. Han, P. L. Tao, P. Y. Law, and H. H. Loh, dsav type 2-mediated gene transfer of mors196a-egfp into spinal cord as a pain management paradigm., *Proc Natl Acad Sci U S A*, 104(50), 20,096–20,101, 2007.
- Chesebro, B., et al., Identification of scrapie prion protein-specific mrna in scrapie-infected and uninfected brain., *Nature*, 315(6017), 331–333, 1985.
- Cleveland, D. W., and J. D. Rothstein, From charcot to lou gehrig: deciphering selective motor neuron death in als., *Nat Rev Neurosci*, 2(11), 806–819, 2001.
- Clinton, J., C. Forsyth, M. C. Royston, and G. W. Roberts, Synaptic degeneration is the primary neuropathological feature in prion disease: a preliminary study., *Neuroreport*, 4(1), 65–68, 1993.

- Cochard, P., and D. Paulin, Initial expression of neurofilaments and vimentin in the central and peripheral nervous system of the mouse embryo in vivo., *J Neurosci*, 4(8), 2080–2094, 1984.
- Cohen, F. E., and S. B. Prusiner, Pathologic conformations of prion proteins., *Annu Rev Biochem*, 67, 793–819, 1998.
- Cohen, F. E., K. M. Pan, Z. Huang, M. Baldwin, R. J. Fletterick, and S. B. Prusiner, Structural clues to prion replication., *Science*, 264(5158), 530–531, 1994.
- Coitinho, A. S., R. Roesler, V. R. Martins, R. R. Brentani, and I. Izquierdo, Cellular prion protein ablation impairs behavior as a function of age., *Neuroreport*, 14(10), 1375–1379, 2003.
- Colling, S. B., J. Collinge, and J. G. Jefferys, Hippocampal slices from prion protein null mice: disrupted Ca^{2+} -activated K^+ currents., *Neurosci Lett*, 209(1), 49–52, 1996.
- Collinge, J., Prion diseases of humans and animals: their causes and molecular basis., *Annu Rev Neurosci*, 24, 519–550, 2001.
- Collinge, J., M. A. Whittington, K. C. Sidle, C. J. Smith, M. S. Palmer, A. R. Clarke, and J. G. Jefferys, Prion protein is necessary for normal synaptic function., *Nature*, 370(6487), 295–297, 1994.
- Collinge, J., J. Beck, T. Campbell, K. Estibeiro, and R. G. Will, Prion protein gene analysis in new variant cases of creutzfeldt-jakob disease., *Lancet*, 348(9019), 56, 1996.
- Collinge, J., J. Whitfield, E. McKintosh, J. Beck, S. Mead, D. J. Thomas, and M. P. Alpers, Kuru in the 21st century—an acquired human prion disease with very long incubation periods., *Lancet*, 367(9528), 2068–2074, 2006.
- Come, J. H., P. E. Fraser, and P. T. Lansbury, A kinetic model for amyloid formation in the prion diseases: importance of seeding., *Proc Natl Acad Sci U S A*, 90(13), 5959–5963, 1993.
- Creutzfeldt, H. G., Über eine eigenartige herdförmige Erkrankung des zentralnervensystems., *Z Ges Neurol Psychiat*, 57, 1–18, 1920.
- Criado, J. R., et al., Mice devoid of prion protein have cognitive deficits that are rescued by reconstitution of prp in neurons., *Neurobiol Dis*, 19(1-2), 255–265, 2005.
- Crozet, C., Y.-L. Lin, C. Mettling, C. Mourton-Gilles, P. Corbeau, S. Lehmann, and V. Perrier, Inhibition of prpsc formation by lentiviral gene transfer of prp containing dominant negative mutations., *J Cell Sci*, 117(Pt 23), 5591–5597, 2004.
- Cuillé, J., and P. L. Chelle, Pathologie animale. la maladie dite de la tremblante du mouton est-elle inoculable, *Comptes Rendus de l'Académie des Sciences*, 26, 1552–1554, 1936.
- Dawson, M., G. A. Wells, B. N. Parker, and A. C. Scott, Primary parenteral transmission of bovine spongiform encephalopathy to the pig., *Vet Rec*, 127(13), 338, 1990.
- Díaz, C., Z. G. Vitezica, R. Rupp, O. Andréoletti, and J. M. Elsen, Polygenic variation and transmission factors involved in the resistance/susceptibility to scrapie in a romanov flock., *J Gen Virol*, 86(Pt 3), 849–857, 2005.
- DeArmond, S. J., M. P. McKinley, R. A. Barry, M. B. Braunfeld, J. R. McColloch, and S. B. Prusiner, Identification of prion amyloid filaments in scrapie-infected brain., *Cell*, 41(1), 221–235, 1985.
- Defaweux, V., G. Dorban, C. Demonceau, J. Piret, O. Jolois, O. Thellin, C. Thielen, E. Heinen, and N. Antoine, Interfaces between dendritic cells, other immune cells, and nerve fibres in mouse peyer's patches: potential sites for neuroinvasion in prion diseases., *Microsc Res Tech*, 66(1), 1–9, 2005.
- Deleault, N. R., B. T. Harris, J. R. Rees, and S. Supattapone, Formation of native prions from minimal components in vitro., *Proc Natl Acad Sci U S A*, 104(23), 9741–9746, 2007.
- Denzer, K., M. J. Kleijmeer, H. F. Heijnen, W. Stoorvogel, and H. J. Geuze, Exosome: from internal vesicle of the multivesicular body to intercellular signaling device., *J Cell Sci*, 113 Pt 19, 3365–3374, 2000a.
- Denzer, K., M. van Eijk, M. J. Kleijmeer, E. Jakobson, C. de Groot, and H. J. Geuze, Follicular dendritic cells carry mhc class ii-expressing microvesicles at their surface., *J Immunol*, 165(3), 1259–1265, 2000b.

- Duffy, P., J. Wolf, G. Collins, A. G. DeVoe, B. Streeten, and D. Cowen, Letter: Possible person-to-person transmission of creutzfeldt-jakob disease., *N Engl J Med*, 290(12), 692–693, 1974.
- Edenhofer, F., R. Rieger, M. Famulok, W. Wendler, S. Weiss, and E. L. Winnacker, Prion protein prp^c interacts with molecular chaperones of the hsp60 family., *J Virol*, 70(7), 4724–4728, 1996.
- Eghiaian, F., Structuring the puzzle of prion propagation., *Curr Opin Struct Biol*, 15(6), 724–730, 2005.
- Ermolayev, V., T. Cathomen, J. Merk, M. Friedrich, W. Härtig, G. S. Harms, M. A. Klein, and E. Flechsig, Impaired axonal transport in motor neurons correlates with clinical prion disease., *PLoS Pathog*, 5(8), e1000558, 2009a.
- Ermolayev, V., M. Friedrich, R. Nozadze, T. Cathomen, M. A. Klein, G. S. Harms, and E. Flechsig, Ultramicroscopy reveals axonal transport impairments in cortical motor neurons at prion disease., *Biophys J*, 96(8), 3390–3398, 2009b.
- Felten, D. L., Direct innervation of lymphoid organs: substrate for neurotransmitter signaling of cells of the immune system., *Neuropsychobiology*, 28(1-2), 110–112, 1993.
- Ferreira, I. D., V. E. do Rosário, and P. V. L. Cravo, Real-time quantitative pcr with sybr green i detection for estimating copy numbers of nine drug resistance candidate genes in plasmodium falciparum., *Malar J*, 5, 1, 2006.
- Fevrier, B., D. Vilette, F. Archer, D. Loew, W. Faigle, M. Vidal, H. Laude, and G. Raposo, Cells release prions in association with exosomes., *Proc Natl Acad Sci U S A*, 101(26), 9683–9688, 2004.
- Fischer, M., T. Rüllicke, A. Raeber, A. Sailer, M. Moser, B. Oesch, S. Brandner, A. Aguzzi, and C. Weissmann, Prion protein (prp) with amino-proximal deletions restoring susceptibility of prp knockout mice to scrapie., *EMBO J*, 15(6), 1255–1264, 1996.
- Flechsig, E., and C. Weissmann, The role of prp in health and disease., *Curr Mol Med*, 4(4), 337–353, 2004.
- Flechsig, E., D. Shmerling, I. Hegyi, A. J. Raeber, M. Fischer, A. Cozzio, C. von Mering, A. Aguzzi, and C. Weissmann, Prion protein devoid of the octapeptide repeat region restores susceptibility to scrapie in prp knockout mice., *Neuron*, 27(2), 399–408, 2000.
- Fraser, H., and A. G. Dickinson, Pathogenesis of scrapie in the mouse: the role of the spleen., *Nature*, 226(5244), 462–463, 1970.
- Frigg, R., M. A. Klein, I. Hegyi, R. M. Zinkernagel, and A. Aguzzi, Scrapie pathogenesis in subclinically infected b-cell-deficient mice., *J Virol*, 73(11), 9584–9588, 1999.
- Février, B., D. Vilette, H. Laude, and G. Raposo, Exosomes: a bubble ride for prions?, *Traffic*, 6(1), 10–17, 2005.
- Gabizon, R., M. P. McKinley, D. Groth, and S. B. Prusiner, Immunoaffinity purification and neutralization of scrapie prion infectivity., *Proc Natl Acad Sci U S A*, 85(18), 6617–6621, 1988.
- Gaiger, S., Scrapie., *J Comp Path*, 37, 259–277, 1924.
- Gajdusek, D. C., Unconventional viruses and the origin and disappearance of kuru., *Science*, 197(4307), 943–960, 1977.
- Gajdusek, D. C., and V. Zigas, Degenerative disease of the central nervous system in new guinea; the endemic occurrence of kuru in the native population., *N Engl J Med*, 257(20), 974–978, 1957.
- Gajdusek, D. C., C. J. Gibbs, and M. Alpers, Experimental transmission of a kuru-like syndrome to chimpanzees., *Nature*, 209(5025), 794–796, 1966.
- Gambetti, P., et al., A novel human disease with abnormal prion protein sensitive to protease., *Ann Neurol*, 63(6), 697–708, 2008.
- Gasset, M., M. A. Baldwin, R. J. Fletterick, and S. B. Prusiner, Perturbation of the secondary structure of the scrapie prion protein under conditions that alter infectivity., *Proc Natl Acad Sci U S A*, 90(1), 1–5, 1993.

- Gauczynski, S., D. Nikles, S. El-Gogo, D. Papy-Garcia, C. Rey, S. Alban, D. Barritault, C. I. Lasmezas, and S. Weiss, The 37-kda/67-kda laminin receptor acts as a receptor for infectious prions and is inhibited by polysulfated glycanes., *J Infect Dis*, 194(5), 702–709, 2006.
- Gibbs, C. J., D. C. Gajdusek, D. M. Asher, M. P. Alpers, E. Beck, P. M. Daniel, and W. B. Matthews, Creutzfeldt-jakob disease (spongiform encephalopathy): transmission to the chimpanzee., *Science*, 161(839), 388–389, 1968.
- Giese, A., M. H. Groschup, B. Hess, and H. A. Kretzschmar, Neuronal cell death in scrapie-infected mice is due to apoptosis., *Brain Pathol*, 5(3), 213–221, 1995.
- Glatzel, M., and A. Aguzzi, Prp(c) expression in the peripheral nervous system is a determinant of prion neuroinvasion., *J Gen Virol*, 81(Pt 11), 2813–2821, 2000.
- Glatzel, M., and A. Aguzzi, The shifting biology of prions., *Brain Res Brain Res Rev*, 36(2-3), 241–248, 2001.
- Goldfarb, L. G., et al., Fatal familial insomnia and familial creutzfeldt-jakob disease: disease phenotype determined by a dna polymorphism., *Science*, 258(5083), 806–808, 1992.
- Goldmann, W., N. Hunter, G. Smith, J. Foster, and J. Hope, Prp genotype and agent effects in scrapie: change in allelic interaction with different isolates of agent in sheep, a natural host of scrapie., *J Gen Virol*, 75 (Pt 5), 989–995, 1994.
- Gonçalves, M. A. F. V., Adeno-associated virus: from defective virus to effective vector., *Virology*, 2, 43, 2005.
- Govaerts, C., H. Wille, S. B. Prusiner, and F. E. Cohen, Evidence for assembly of prions with left-handed beta-helices into trimers., *Proc Natl Acad Sci U S A*, 101(22), 8342–8347, 2004.
- Graham, F. L., J. Smiley, W. C. Russell, and R. Nairn, Characteristics of a human cell line transformed by dna from human adenovirus type 5., *J Gen Virol*, 36(1), 59–74, 1977.
- Graner, E., et al., Cellular prion protein binds laminin and mediates neuriteogenesis., *Brain Res Mol Brain Res*, 76(1), 85–92, 2000.
- Grieger, J. C., and R. J. Samulski, Adeno-associated virus as a gene therapy vector: vector development, production and clinical applications., *Adv Biochem Eng Biotechnol*, 99, 119–145, 2005.
- Griffith, J. S., Self-replication and scrapie., *Nature*, 215(5105), 1043–1044, 1967.
- Grosveld, F., M. Antoniou, G. B. van Assendelft, E. de Boer, J. Hurst, G. Kollias, F. MacFarlane, and N. Wrighton, The regulation of expression of human beta-globin genes., *Prog Clin Biol Res*, 251, 133–144, 1987.
- Gu, H., Y. R. Zou, and K. Rajewsky, Independent control of immunoglobulin switch recombination at individual switch regions evidenced through cre-loxp-mediated gene targeting., *Cell*, 73(6), 1155–1164, 1993.
- Haltia, M., J. Kovanen, H. V. Crevel, G. T. Bots, and S. Stefanko, Familial creutzfeldt-jakob disease., *J Neurol Sci*, 42(3), 381–389, 1979.
- Handa, H., and B. J. Carter, Adeno-associated virus dna replication complexes in herpes simplex virus or adenovirus-infected cells., *J Biol Chem*, 254(14), 6603–6610, 1979.
- Haraguchi, T., et al., Asparagine-linked glycosylation of the scrapie and cellular prion proteins., *Arch Biochem Biophys*, 274(1), 1–13, 1989.
- Hepner, F. L., A. D. Christ, M. A. Klein, M. Prinz, M. Fried, J. P. Kraehenbuhl, and A. Aguzzi, Transendothelial prion transport by m cells., *Nat Med*, 7(9), 976–977, 2001.
- Hetz, C., K. Maundrell, and C. Soto, Is loss of function of the prion protein the cause of prion disorders?, *Trends Mol Med*, 9(6), 237–243, 2003.
- Higuchi, R., C. Fockler, G. Dollinger, and R. Watson, Kinetic pcr analysis: real-time monitoring of dna amplification reactions., *Biotechnology (N Y)*, 11(9), 1026–1030, 1993.
- Hill, A. F., M. Desbruslais, S. Joiner, K. C. Sidle, I. Gowland, J. Collinge, L. J. Doey, and P. Lantos, The same prion strain causes vscj and bse., *Nature*, 389(6650), 448–50, 526, 1997.

- Hill, A. F., et al., Investigation of variant creutzfeldt-jakob disease and other human prion diseases with tonsil biopsy samples., *Lancet*, 353(9148), 183–189, 1999.
- Hope, J., L. J. Morton, C. F. Farquhar, G. Multhaup, K. Beyreuther, and R. H. Kimberlin, The major polypeptide of scrapie-associated fibrils (saf) has the same size, charge distribution and n-terminal protein sequence as predicted for the normal brain protein (prp)., *EMBO J*, 5(10), 2591–2597, 1986.
- Horiuchi, M., S. A. Priola, J. Chabry, and B. Caughey, Interactions between heterologous forms of prion protein: binding, inhibition of conversion, and species barriers., *Proc Natl Acad Sci U S A*, 97(11), 5836–5841, 2000.
- Hornemann, S., C. Korth, B. Oesch, R. Riek, G. Wider, K. Wüthrich, and R. Glockshuber, Recombinant full-length murine prion protein, mprp(23-231): purification and spectroscopic characterization., *FEBS Lett*, 413(2), 277–281, 1997.
- Houston, E. F., and M. B. Gravenor, Clinical signs in sheep experimentally infected with scrapie and bse., *Vet Rec*, 152(11), 333–334, 2003.
- Hsiao, K., H. F. Baker, T. J. Crow, M. Poulter, F. Owen, J. D. Terwilliger, D. Westaway, J. Ott, and S. B. Prusiner, Linkage of a prion protein missense variant to gerstmann-sträussler syndrome., *Nature*, 338(6213), 342–345, 1989.
- Huang, F.-P., C. F. Farquhar, N. A. Mabbott, M. E. Bruce, and G. G. MacPherson, Migrating intestinal dendritic cells transport prp(sc) from the gut., *J Gen Virol*, 83(Pt 1), 267–271, 2002.
- Huang, Z., S. B. Prusiner, and F. E. Cohen, Scrapie prions: a three-dimensional model of an infectious fragment., *Fold Des*, 1(1), 13–19, 1996.
- Hunter, N., J. D. Foster, W. Goldmann, M. J. Stear, J. Hope, and C. Bostock, Natural scrapie in a closed flock of cheviot sheep occurs only in specific prp genotypes., *Arch Virol*, 141(5), 809–824, 1996.
- Hutter, G., F. L. Heppner, and A. Aguzzi, No superoxide dismutase activity of cellular prion protein in vivo., *Biol Chem*, 384(9), 1279–1285, 2003.
- J. Gerstmann, I. S., E. Sträussler, Über eine eigenartige hereditär-familiäre erkrankung des zentralnervensystems., *Z ges Neurol Psychiat*, 154, 736–762, 1936.
- Jackson, G. S., I. Murray, L. L. Hosszu, N. Gibbs, J. P. Waltho, A. R. Clarke, and J. Collinge, Location and properties of metal-binding sites on the human prion protein., *Proc Natl Acad Sci U S A*, 98(15), 8531–8535, 2001.
- Jakob, A., Über eine eigenartige erkrankung des zentralnervensystems mit bemerkenswerten anatomischen befunde (spastische pseudosklerose mit disseminierten degenerationsherden)., *Dtsch Z Nervenheilk*, 70, 132–146, 1921.
- Jeffrey, M., and G. A. Wells, Spongiform encephalopathy in a nyala (tragelaphus angasi)., *Vet Pathol*, 25(5), 398–399, 1988.
- Jeffrey, M., G. McGovern, C. M. Goodsir, K. L. Brown, and M. E. Bruce, Sites of prion protein accumulation in scrapie-infected mouse spleen revealed by immuno-electron microscopy., *J Pathol*, 191(3), 323–332, 2000.
- Jeffrey, M., S. Ryder, S. Martin, S. A. Hawkins, L. Terry, C. Berthelin-Baker, and S. J. Bellworthy, Oral inoculation of sheep with the agent of bovine spongiform encephalopathy (bse). 1. onset and distribution of disease-specific prp accumulation in brain and viscera., *J Comp Pathol*, 124(4), 280–289, 2001.
- Jones, C. E., S. R. Abdelraheim, D. R. Brown, and J. H. Viles, Preferential cu²⁺ coordination by his96 and his111 induces beta-sheet formation in the unstructured amyloidogenic region of the prion protein., *J Biol Chem*, 279(31), 32,018–32,027, 2004.
- Kaneko, K., M. Vey, M. Scott, S. Pilkuhn, F. E. Cohen, and S. B. Prusiner, CooH-terminal sequence of the cellular prion protein directs subcellular trafficking and controls conversion into the scrapie isoform., *Proc Natl Acad Sci U S A*, 94(6), 2333–2338, 1997a.
- Kaneko, K., L. Zulianello, M. Scott, C. M. Cooper, A. C. Wallace, T. L. James, F. E. Cohen, and S. B. Prusiner, Evidence for protein x binding to a discontinuous epitope on the cellular prion protein during scrapie prion propagation., *Proc Natl Acad Sci U S A*, 94(19), 10,069–10,074, 1997b.

- Kaplitt, M. G., et al., Safety and tolerability of gene therapy with an adeno-associated virus (aav) borne gad gene for parkinson's disease: an open label, phase i trial., *Lancet*, 369(9579), 2097–2105, 2007.
- Kascsak, R. J., R. Rubenstein, P. A. Merz, M. Tonna-DeMasi, R. Fersko, R. I. Carp, H. M. Wisniewski, and H. Diringer, Mouse polyclonal and monoclonal antibody to scrapie-associated fibril proteins., *J Virol*, 61(12), 3688–3693, 1987.
- Kashiwakura, Y., et al., Hepatocyte growth factor receptor is a coreceptor for adeno-associated virus type 2 infection., *J Virol*, 79(1), 609–614, 2005.
- Kaspar, B. K., J. Lladó, N. Sherkat, J. D. Rothstein, and F. H. Gage, Retrograde viral delivery of igf-1 prolongs survival in a mouse als model., *Science*, 301(5634), 839–842, 2003.
- Kaspar, B. K., et al., Adeno-associated virus effectively mediates conditional gene modification in the brain., *Proc Natl Acad Sci U S A*, 99(4), 2320–2325, 2002.
- Kimberlin, R. H., and C. A. Walker, Pathogenesis of scrapie (strain 263k) in hamsters infected intracerebrally, intraperitoneally or intraocularly., *J Gen Virol*, 67 (Pt 2), 255–263, 1986.
- Kimberlin, R. H., and C. A. Walker, Pathogenesis of experimental scrapie., *Ciba Found Symp*, 135, 37–62, 1988.
- Kimberlin, R. H., and C. A. Walker, The role of the spleen in the neuroinvasion of scrapie in mice., *Virus Res*, 12(3), 201–211, 1989.
- Kirkwood, J. K., G. A. Wells, J. W. Wilesmith, A. A. Cunningham, and S. I. Jackson, Spongiform encephalopathy in an arabian oryx (*oryx leucoryx*) and a greater kudu (*tragelaphus strepsiceros*), *Vet Rec*, 127(17), 418–420, 1990.
- Kitamoto, T., T. Muramoto, S. Mohri, K. Doh-Ura, and J. Tateishi, Abnormal isoform of prion protein accumulates in follicular dendritic cells in mice with creutzfeldt-jakob disease., *J Virol*, 65(11), 6292–6295, 1991.
- Klein, M. A., et al., A crucial role for b cells in neuroinvasive scrapie., *Nature*, 390(6661), 687–690, 1997.
- Klein, M. A., et al., Complement facilitates early prion pathogenesis., *Nat Med*, 7(4), 488–492, 2001.
- Kocisko, D. A., J. H. Come, S. A. Priola, B. Chesebro, G. J. Raymond, P. T. Lansbury, and B. Caughey, Cell-free formation of protease-resistant prion protein., *Nature*, 370(6489), 471–474, 1994.
- Koeberl, D. D., I. E. Alexander, C. L. Halbert, D. W. Russell, and A. D. Miller, Persistent expression of human clotting factor ix from mouse liver after intravenous injection of adeno-associated virus vectors., *Proc Natl Acad Sci U S A*, 94(4), 1426–1431, 1997.
- Kovács, G. G., G. Trabattoni, J. A. Hainfellner, J. W. Ironside, R. S. G. Knight, and H. Budka, Mutations of the prion protein gene phenotypic spectrum., *J Neurol*, 249(11), 1567–1582, 2002.
- Kovács, G. G., M. Preusser, M. Strohschneider, and H. Budka, Subcellular localization of disease-associated prion protein in the human brain., *Am J Pathol*, 166(1), 287–294, 2005.
- Kretzschmar, H. A., S. B. Prusiner, L. E. Stowring, and S. J. DeArmond, Scrapie prion proteins are synthesized in neurons., *Am J Pathol*, 122(1), 1–5, 1986.
- Kurschner, C., and J. I. Morgan, The cellular prion protein (prp) selectively binds to bcl-2 in the yeast two-hybrid system., *Brain Res Mol Brain Res*, 30(1), 165–168, 1995.
- Laemmli, U. K., Cleavage of structural proteins during the assembly of the head of bacteriophage t4., *Nature*, 227(5259), 680–685, 1970.
- Landolt, H.-P., et al., Sleep-wake disturbances in sporadic creutzfeldt-jakob disease., *Neurology*, 66(9), 1418–1424, 2006.
- Lasmézas, C. I., et al., Transmission of the bse agent to mice in the absence of detectable abnormal prion protein., *Science*, 275(5298), 402–405, 1997.
- Laurén, J., D. A. Gimbel, H. B. Nygaard, J. W. Gilbert, and S. M. Strittmatter, Cellular prion protein mediates impairment of synaptic plasticity by amyloid-beta oligomers., *Nature*, 457(7233), 1128–1132, 2009.

- Leclerc, E., H. Serban, S. B. Prusiner, D. R. Burton, and R. A. Williamson, Copper induces conformational changes in the n-terminal part of cell-surface prpc., *Arch Virol*, 151(11), 2103–2109, 2006.
- Lee, C. I., Q. Yang, V. Perrier, and I. V. Baskakov, The dominant-negative effect of the q218k variant of the prion protein does not require protein x., *Protein Sci*, 16(10), 2166–2173, 2007.
- Lee, H. S., P. Brown, L. Cervenáková, R. M. Garruto, M. P. Alpers, D. C. Gajdusek, and L. G. Goldfarb, Increased susceptibility to kuru of carriers of the prnp 129 methionine/methionine genotype., *J Infect Dis*, 183(2), 192–196, 2001.
- Legname, G., I. V. Baskakov, H.-O. B. Nguyen, D. Riesner, F. E. Cohen, S. J. DeArmond, and S. B. Prusiner, Synthetic mammalian prions., *Science*, 305(5684), 673–676, 2004.
- Lewandoski, M., and G. R. Martin, Cre-mediated chromosome loss in mice., *Nat Genet*, 17(2), 223–225, 1997.
- Li, E., C. Beard, and R. Jaenisch, Role for dna methylation in genomic imprinting., *Nature*, 366(6453), 362–365, 1993.
- Linden, R., V. R. Martins, M. A. M. Prado, M. Cammarota, I. Izquierdo, and R. R. Brentani, Physiology of the prion protein., *Physiol Rev*, 88(2), 673–728, 2008.
- Liu, T., R. Li, B. S. Wong, D. Liu, T. Pan, R. B. Petersen, P. Gambetti, and M. S. Sy, Normal cellular prion protein is preferentially expressed on subpopulations of murine hemopoietic cells., *J Immunol*, 166(6), 3733–3742, 2001.
- Livak, K. J., and T. D. Schmittgen, Analysis of relative gene expression data using real-time quantitative pcr and the 2(-delta delta c(t)) method., *Methods*, 25(4), 402–408, 2001.
- Llewelyn, C. A., P. E. Hewitt, R. S. G. Knight, K. Amar, S. Cousens, J. Mackenzie, and R. G. Will, Possible transmission of variant creutzfeldt-jakob disease by blood transfusion., *Lancet*, 363(9407), 417–421, 2004.
- Lois, C., E. J. Hong, S. Pease, E. J. Brown, and D. Baltimore, Germline transmission and tissue-specific expression of transgenes delivered by lentiviral vectors., *Science*, 295(5556), 868–872, 2002.
- Lugaresi, E., I. Tobler, P. Gambetti, and P. Montagna, The pathophysiology of fatal familial insomnia., *Brain Pathol*, 8(3), 521–526, 1998.
- Mabbott, N. A., and G. G. MacPherson, Prions and their lethal journey to the brain., *Nat Rev Microbiol*, 4(3), 201–211, 2006.
- Mabbott, N. A., A. Williams, C. F. Farquhar, M. Pasparakis, G. Kollias, and M. E. Bruce, Tumor necrosis factor alpha-deficient, but not interleukin-6-deficient, mice resist peripheral infection with scrapie., *J Virol*, 74(7), 3338–3344, 2000.
- Mabbott, N. A., M. E. Bruce, M. Botto, M. J. Walport, and M. B. Pepys, Temporary depletion of complement component c3 or genetic deficiency of c1q significantly delays onset of scrapie., *Nat Med*, 7(4), 485–487, 2001.
- Mabbott, N. A., J. Young, I. McConnell, and M. E. Bruce, Follicular dendritic cell dedifferentiation by treatment with an inhibitor of the lymphotoxin pathway dramatically reduces scrapie susceptibility., *J Virol*, 77(12), 6845–6854, 2003.
- Maignien, T., C. I. Lasmézas, V. Beringue, D. Dormont, and J. P. Deslys, Pathogenesis of the oral route of infection of mice with scrapie and bovine spongiform encephalopathy agents., *J Gen Virol*, 80 (Pt 11), 3035–3042, 1999.
- Maignien, T., M. Shakweh, P. Calvo, D. Marcé, N. Salès, E. Fattal, J.-P. Deslys, P. Couvreur, and C. I. Lasmézas, Role of gut macrophages in mice orally contaminated with scrapie or bse., *Int J Pharm*, 298(2), 293–304, 2005.
- Mallucci, G., A. Dickinson, J. Linehan, P.-C. Klöhn, S. Brandner, and J. Collinge, Depleting neuronal prp in prion infection prevents disease and reverses spongiosis., *Science*, 302(5646), 871–874, 2003.
- Mallucci, G. R., S. Ratté, E. A. Asante, J. Linehan, I. Gowland, J. G. R. Jefferys, and J. Collinge, Post-natal knockout of prion protein alters hippocampal ca1 properties, but does not result in neurodegeneration., *EMBO J*, 21(3), 202–210, 2002.

- Manno, C. S., et al., Aav-mediated factor ix gene transfer to skeletal muscle in patients with severe hemophilia b., *Blood*, 101(8), 2963–2972, 2003.
- Marijanovic, Z., A. Caputo, V. Campana, and C. Zurzolo, Identification of an intracellular site of prion conversion., *PLoS Pathog*, 5(5), e1000426, 2009.
- Marsh, R. F., and W. J. Hadlow, Transmissible mink encephalopathy., *Rev Sci Tech*, 11(2), 539–550, 1992.
- Masters, C. L., J. O. Harris, D. C. Gajdusek, C. J. Gibbs, C. Bernoulli, and D. M. Asher, Creutzfeldt-jakob disease: patterns of worldwide occurrence and the significance of familial and sporadic clustering., *Ann Neurol*, 5(2), 177–188, 1979.
- Masters, C. L., D. C. Gajdusek, and C. J. Gibbs, Creutzfeldt-jakob disease virus isolations from the gerstmann-sträussler syndrome with an analysis of the various forms of amyloid plaque deposition in the virus-induced spongiform encephalopathies., *Brain*, 104(3), 559–588, 1981.
- Matsushita, T., S. Elliger, C. Elliger, G. Podsakoff, L. Villarreal, G. J. Kurtzman, Y. Iwaki, and P. Colosi, Adeno-associated virus vectors can be efficiently produced without helper virus., *Gene Ther*, 5(7), 938–945, 1998.
- Matthews, D., and B. C. Cooke, The potential for transmissible spongiform encephalopathies in non-ruminant livestock and fish., *Rev Sci Tech*, 22(1), 283–296, 2003.
- Mayer, R. J., M. Landon, L. Laszlo, G. Lennox, and J. Lowe, Protein processing in lysosomes: the new therapeutic target in neurodegenerative disease., *Lancet*, 340(8812), 156–159, 1992.
- McBride, P. A., W. J. Schulz-Schaeffer, M. Donaldson, M. Bruce, H. Diringer, H. A. Kretschmar, and M. Beekes, Early spread of scrapie from the gastrointestinal tract to the central nervous system involves autonomic fibers of the splanchnic and vagus nerves., *J Virol*, 75(19), 9320–9327, 2001.
- McGowan, J. P., Scrapie in sheep., *Scottish J. Agric.*, 5, 365–375, 1922.
- McKinley, M. P., D. C. Bolton, and S. B. Prusiner, A protease-resistant protein is a structural component of the scrapie prion., *Cell*, 35(1), 57–62, 1983.
- McKinley, M. P., R. K. Meyer, L. Kenaga, F. Rahbar, R. Cotter, A. Serban, and S. B. Prusiner, Scrapie prion rod formation in vitro requires both detergent extraction and limited proteolysis., *J Virol*, 65(3), 1340–1351, 1991.
- Mead, S., Prion disease genetics., *Eur J Hum Genet*, 14(3), 273–281, 2006.
- Medori, R., P. Montagna, H. J. Tritschler, A. LeBlanc, P. Cortelli, P. Tinuper, E. Lugaresi, and P. Gambetti, Fatal familial insomnia: a second kindred with mutation of prion protein gene at codon 178., *Neurology*, 42(3 Pt 1), 669–670, 1992.
- Medrano, A. Z., S. J. Barmada, E. Biasini, and D. A. Harris, Gfp-tagged mutant prion protein forms intra-axonal aggregates in transgenic mice., *Neurobiol Dis*, 31(1), 20–32, 2008.
- Meyer, R. K., M. P. McKinley, K. A. Bowman, M. B. Braunfeld, R. A. Barry, and S. B. Prusiner, Separation and properties of cellular and scrapie prion proteins., *Proc Natl Acad Sci U S A*, 83(8), 2310–2314, 1986.
- Mähönen, A. J., K. J. Airene, M. M. Lind, H. P. Lesch, and S. Ylä-Herttuala, Optimized self-excising cre-expression cassette for mammalian cells., *Biochem Biophys Res Commun*, 320(2), 366–371, 2004.
- Mishra, R. S., et al., Protease-resistant human prion protein and ferritin are cotransported across caco-2 epithelial cells: implications for species barrier in prion uptake from the intestine., *J Neurosci*, 24(50), 11,280–11,290, 2004.
- Montrasio, F., R. Frigg, M. Glatzel, M. A. Klein, F. Mackay, A. Aguzzi, and C. Weissmann, Impaired prion replication in spleens of mice lacking functional follicular dendritic cells., *Science*, 288(5469), 1257–1259, 2000.
- Morel, E., S. Fouquet, D. Chateau, L. Yvernault, Y. Frobert, M. Pincon-Raymond, J. Chambaz, T. Pilot, and M. Rousset, The cellular prion protein prpc is expressed in human enterocytes in cell-cell junctional domains., *J Biol Chem*, 279(2), 1499–1505, 2004.

- Mori, S., L. Wang, T. Takeuchi, and T. Kanda, Two novel adeno-associated viruses from cynomolgus monkey: pseudotyping characterization of capsid protein., *Virology*, 330(2), 375–383, 2004.
- Moser, M., R. J. Colello, U. Pott, and B. Oesch, Developmental expression of the prion protein gene in glial cells., *Neuron*, 14(3), 509–517, 1995.
- Mouillet-Richard, S., M. Ermonval, C. Chebassier, J. L. Laplanche, S. Lehmann, J. M. Launay, and O. Kellermann, Signal transduction through prion protein., *Science*, 289(5486), 1925–1928, 2000.
- Mould, D. L., A. M. Dawson, and J. C. Rennie, Very early replication of scrapie in lymphocytic tissue., *Nature*, 228(5273), 779–780, 1970.
- Nagy, A., Cre recombinase: the universal reagent for genome tailoring., *Genesis*, 26(2), 99–109, 2000.
- Nakahara, D. H., V. R. Lingappa, and S. L. Chuck, Translocational pausing is a common step in the biogenesis of unconventional integral membrane and secretory proteins., *J Biol Chem*, 269(10), 7617–7622, 1994.
- Nico, P. B. C., et al., Altered behavioural response to acute stress in mice lacking cellular prion protein., *Behav Brain Res*, 162(2), 173–181, 2005.
- Novitskaya, V., N. Makarava, I. Sylvester, I. B. Bronstein, and I. V. Baskakov, Amyloid fibrils of mammalian prion protein induce axonal degeneration in ntera2-derived terminally differentiated neurons., *J Neurochem*, 2007.
- Nunziante, M., S. Gilch, and H. M. Schätzl, Prion diseases: from molecular biology to intervention strategies., *ChemBiochem*, 4(12), 1268–1284, 2003.
- Oesch, B., et al., A cellular gene encodes scrapie prp 27-30 protein., *Cell*, 40(4), 735–746, 1985.
- O'Rourke, K. I., G. R. Holyoak, W. W. Clark, J. R. Mickelson, S. Wang, R. P. Melco, T. E. Besser, and W. C. Foote, Prp genotypes and experimental scrapie in orally inoculated suffolk sheep in the united states., *J Gen Virol*, 78 (Pt 4), 975–978, 1997.
- Ott, D., C. Taraborrelli, and A. Aguzzi, Novel dominant-negative prion protein mutants identified from a randomized library., *Protein Eng Des Sel*, 21(10), 623–629, 2008.
- Pan, K. M., et al., Conversion of alpha-helices into beta-sheets features in the formation of the scrapie prion proteins., *Proc Natl Acad Sci U S A*, 90(23), 10,962–10,966, 1993.
- Park, S. K., S. I. Choi, J. K. Jin, E. K. Choi, J. I. Kim, R. I. Carp, and Y. S. Kim, Differential expression of bax and bcl-2 in the brains of hamsters infected with 263k scrapie agent., *Neuroreport*, 11(8), 1677–1682, 2000.
- Parry, H., *Scrapie disease in sheep*, London: Academic Press, 1983.
- Parry, H. B., Scrapie: a transmissible and hereditary disease of sheep., *Heredity*, 17, 75–105, 1962.
- Pauly, P. C., and D. A. Harris, Copper stimulates endocytosis of the prion protein., *J Biol Chem*, 273(50), 33,107–33,110, 1998.
- Peden, A. H., and J. W. Ironside, Review: pathology of variant creutzfeldt-jakob disease., *Folia Neuropathol*, 42 Suppl A, 85–91, 2004.
- Peden, A. H., M. W. Head, D. L. Ritchie, J. E. Bell, and J. W. Ironside, Preclinical vcd after blood transfusion in a prnp codon 129 heterozygous patient., *Lancet*, 364(9433), 527–529, 2004.
- Pergami, P., H. Jaffe, and J. Safar, Semipreparative chromatographic method to purify the normal cellular isoform of the prion protein in nondenatured form., *Anal Biochem*, 236(1), 63–73, 1996.
- Perrier, V., K. Kaneko, J. Safar, J. Vergara, P. Tremblay, S. J. DeArmond, F. E. Cohen, S. B. Prusiner, and A. C. Wallace, Dominant-negative inhibition of prion replication in transgenic mice., *Proc Natl Acad Sci U S A*, 99(20), 13,079–13,084, 2002.
- Pfeifer, A., E. P. Brandon, N. Kootstra, F. H. Gage, and I. M. Verma, Delivery of the cre recombinase by a self-deleting lentiviral vector: efficient gene targeting in vivo., *Proc Natl Acad Sci U S A*, 98(20), 11,450–11,455, 2001.

- Pichon, C. E. L., M. T. Valley, M. Polymenidou, A. T. Chesler, B. T. Sagdullaev, A. Aguzzi, and S. Firestein, Olfactory behavior and physiology are disrupted in prion protein knockout mice., *Nat Neurosci*, 12(1), 60–69, 2009.
- Poirier, L. J., Nervous mechanisms involved in experimentally induced extrapyramidal disturbances., *Confin Neurol*, 36(4-6), 223–236, 1974.
- Prinz, M., F. Montrasio, M. A. Klein, P. Schwarz, J. Priller, B. Odermatt, K. Pfeffer, and A. Aguzzi, Lymph nodal prion replication and neuroinvasion in mice devoid of follicular dendritic cells., *Proc Natl Acad Sci U S A*, 99(2), 919–924, 2002.
- Prinz, M., G. Huber, A. J. S. Macpherson, F. L. Heppner, M. Glatzel, H.-P. Eugster, N. Wagner, and A. Aguzzi, Oral prion infection requires normal numbers of peyer's patches but not of enteric lymphocytes., *Am J Pathol*, 162(4), 1103–1111, 2003.
- Priola, S. A., B. Caughey, G. J. Raymond, and B. Chesebro, Prion protein and the scrapie agent: in vitro studies in infected neuroblastoma cells., *Infect Agents Dis*, 3(2-3), 54–58, 1994.
- Prusiner, S. B., Novel proteinaceous infectious particles cause scrapie., *Science*, 216(4542), 136–144, 1982.
- Prusiner, S. B., Scrapie prions., *Annu Rev Microbiol*, 43, 345–374, 1989.
- Prusiner, S. B., Molecular biology of prion diseases., *Science*, 252(5012), 1515–1522, 1991.
- Prusiner, S. B., Shattuck lecture—neurodegenerative diseases and prions., *N Engl J Med*, 344(20), 1516–1526, 2001.
- Prusiner, S. B., D. F. Groth, M. P. McKinley, S. P. Cochran, K. A. Bowman, and K. C. Kasper, Thiocyanate and hydroxyl ions inactivate the scrapie agent., *Proc Natl Acad Sci U S A*, 78(7), 4606–4610, 1981.
- Prusiner, S. B., S. P. Cochran, D. F. Groth, D. E. Downey, K. A. Bowman, and H. M. Martinez, Measurement of the scrapie agent using an incubation time interval assay., *Ann Neurol*, 11(4), 353–358, 1982.
- Prusiner, S. B., D. F. Groth, D. C. Bolton, S. B. Kent, and L. E. Hood, Purification and structural studies of a major scrapie prion protein., *Cell*, 38(1), 127–134, 1984.
- Qing, K., C. Mah, J. Hansen, S. Zhou, V. Dwarki, and A. Srivastava, Human fibroblast growth factor receptor 1 is a co-receptor for infection by adeno-associated virus 2., *Nat Med*, 5(1), 71–77, 1999.
- Rabinowitz, J. E., and R. J. Samulski, Building a better vector: the manipulation of aav virions., *Virology*, 278(2), 301–308, 2000.
- Race, R., M. Oldstone, and B. Chesebro, Entry versus blockade of brain infection following oral or intraperitoneal scrapie administration: role of prion protein expression in peripheral nerves and spleen., *J Virol*, 74(2), 828–833, 2000.
- Race, R. E., S. A. Priola, R. A. Bessen, D. Ernst, J. Dockter, G. F. Rall, L. Mucke, B. Chesebro, and M. B. Oldstone, Neuron-specific expression of a hamster prion protein minigene in transgenic mice induces susceptibility to hamster scrapie agent., *Neuron*, 15(5), 1183–1191, 1995.
- Raeber, A. J., M. A. Klein, R. Frigg, E. Flechsig, A. Aguzzi, and C. Weissmann, Prp-dependent association of prions with splenic but not circulating lymphocytes of scrapie-infected mice., *EMBO J*, 18(10), 2702–2706, 1999.
- Raeber, A. J., et al., Astrocyte-specific expression of hamster prion protein (prp) renders prp knockout mice susceptible to hamster scrapie., *EMBO J*, 16(20), 6057–6065, 1997.
- Relaño-Ginés, A., A. Gabelle, S. Lehmann, O. Milhavel, and C. Crozet, Gene and cell therapy for prion diseases., *Infect Disord Drug Targets*, 9(1), 58–68, 2009.
- Rescigno, M., M. Urbano, B. Valzasina, M. Francolini, G. Rotta, R. Bonasio, F. Granucci, J. P. Kraehenbuhl, and P. Ricciardi-Castagnoli, Dendritic cells express tight junction proteins and penetrate gut epithelial monolayers to sample bacteria., *Nat Immunol*, 2(4), 361–367, 2001.
- Richter, M., A. Iwata, J. Nyhuis, Y. Nitta, A. D. Miller, C. L. Halbert, and M. D. Allen, Adeno-associated virus vector transduction of vascular smooth muscle cells in vivo., *Physiol Genomics*, 2(3), 117–127, 2000.

- Ridley, R. M., and H. F. Baker, Oral transmission of bse to primates., *Lancet*, 348(9035), 1174, 1996.
- Rieger, R., F. Edenhofer, C. I. Lasmézas, and S. Weiss, The human 37-kda laminin receptor precursor interacts with the prion protein in eukaryotic cells., *Nat Med*, 3(12), 1383–1388, 1997.
- Riek, R., S. Hornemann, G. Wider, R. Glockshuber, and K. Wüthrich, Nmr characterization of the full-length recombinant murine prion protein, mprp(23-231)., *FEBS Lett*, 413(2), 282–288, 1997.
- Rülicke, T., and U. Hübscher, Germ line transformation of mammals by pronuclear microinjection., *Exp Physiol*, 85(6), 589–601, 2000.
- Roberts, R. J., Restriction endonucleases., *CRC Crit Rev Biochem*, 4(2), 123–164, 1976.
- Roesler, R., R. Walz, J. Quevedo, F. de Paris, S. M. Zanata, E. Graner, I. Izquierdo, V. R. Martins, and R. R. Brentani, Normal inhibitory avoidance learning and anxiety, but increased locomotor activity in mice devoid of prp(c)., *Brain Res Mol Brain Res*, 71(2), 349–353, 1999.
- Rossi, D., A. Cozzio, E. Flechsig, M. A. Klein, T. Rülicke, A. Aguzzi, and C. Weissmann, Onset of ataxia and purkinje cell loss in prp null mice inversely correlated with dpl level in brain., *EMBO J*, 20(4), 694–702, 2001.
- Rubinson, D. A., et al., A lentivirus-based system to functionally silence genes in primary mammalian cells, stem cells and transgenic mice by rna interference., *Nat Genet*, 33(3), 401–406, 2003.
- Saam, J. R., and J. I. Gordon, Inducible gene knockouts in the small intestinal and colonic epithelium., *J Biol Chem*, 274(53), 38,071–38,082, 1999.
- Saborio, G. P., B. Permanne, and C. Soto, Sensitive detection of pathological prion protein by cyclic amplification of protein misfolding., *Nature*, 411(6839), 810–813, 2001.
- Safar, J., P. P. Roller, D. C. Gajdusek, and C. J. Gibbs, Conformational transitions, dissociation, and unfolding of scrapie amyloid (prion) protein., *J Biol Chem*, 268(27), 20,276–20,284, 1993.
- Safar, J., H. Wille, V. Itri, D. Groth, H. Serban, M. Torchia, F. E. Cohen, and S. B. Prusiner, Eight prion strains have prp(sc) molecules with different conformations., *Nat Med*, 4(10), 1157–1165, 1998.
- Saiki, R. K., D. H. Gelfand, S. Stoffel, S. J. Scharf, R. Higuchi, G. T. Horn, K. B. Mullis, and H. A. Erlich, Primer-directed enzymatic amplification of dna with a thermostable dna polymerase., *Science*, 239(4839), 487–491, 1988.
- Sailer, A., H. Büeler, M. Fischer, A. Aguzzi, and C. Weissmann, No propagation of prions in mice devoid of prp., *Cell*, 77(7), 967–968, 1994.
- Sakaguchi, S., [a systematic review of the therapeutics for prion diseases], *Brain Nerve*, 61(8), 929–938, 2009.
- Sales, N., What can we learn from the oral intake of prions by sheep?, *J Pathol*, 209(1), 1–3, 2006.
- Santuccione, A., V. Sytnyk, I. Leshchyns'ka, and M. Schachner, Prion protein recruits its neuronal receptor ncam to lipid rafts to activate p59fyn and to enhance neurite outgrowth., *J Cell Biol*, 169(2), 341–354, 2005.
- Sauer, B., and N. Henderson, Site-specific dna recombination in mammalian cells by the cre recombinase of bacteriophage p1., *Proc Natl Acad Sci U S A*, 85(14), 5166–5170, 1988.
- Schmidt-Suppran, M., and K. Rajewsky, Vagaries of conditional gene targeting., *Nat Immunol*, 8(7), 665–668, 2007.
- Schmitt-Ulms, G., et al., Binding of neural cell adhesion molecules (n-cams) to the cellular prion protein., *J Mol Biol*, 314(5), 1209–1225, 2001.
- Schorpp, M., R. Jäger, K. Schellander, J. Schenkel, E. F. Wagner, H. Weiher, and P. Angel, The human ubiquitin c promoter directs high ubiquitous expression of transgenes in mice., *Nucleic Acids Res*, 24(9), 1787–1788, 1996.
- Schätzl, H. M., M. D. Costa, L. Taylor, F. E. Cohen, and S. B. Prusiner, Prion protein gene variation among primates., *J Mol Biol*, 245(4), 362–374, 1995.

- Schweizer, U., J. Gunnarsen, C. Karch, S. Wiese, B. Holtmann, K. Takeda, S. Akira, and M. Sendtner, Conditional gene ablation of stat3 reveals differential signaling requirements for survival of motoneurons during development and after nerve injury in the adult., *J Cell Biol*, 156(2), 287–297, 2002.
- Scott, M., et al., Transgenic mice expressing hamster prion protein produce species-specific scrapie infectivity and amyloid plaques., *Cell*, 59(5), 847–857, 1989.
- Scott, M. R., R. Will, J. Ironside, H. O. Nguyen, P. Tremblay, S. J. DeArmond, and S. B. Prusiner, Compelling transgenetic evidence for transmission of bovine spongiform encephalopathy prions to humans., *Proc Natl Acad Sci U S A*, 96(26), 15,137–15,142, 1999.
- Shibuya, S., J. Higuchi, R. W. Shin, J. Tateishi, and T. Kitamoto, Protective prion protein polymorphisms against sporadic creutzfeldt-jakob disease., *Lancet*, 351(9100), 419, 1998.
- Shyng, S. L., M. T. Huber, and D. A. Harris, A prion protein cycles between the cell surface and an endocytic compartment in cultured neuroblastoma cells., *J Biol Chem*, 268(21), 15,922–15,928, 1993.
- Shyng, S. L., J. E. Heuser, and D. A. Harris, A glycolipid-anchored prion protein is endocytosed via clathrin-coated pits., *J Cell Biol*, 125(6), 1239–1250, 1994.
- Siegfried, Z., S. Eden, M. Mendelsohn, X. Feng, B. Z. Tsuberi, and H. Cedar, Dna methylation represses transcription in vivo., *Nat Genet*, 22(2), 203–206, 1999.
- Sigurdson, C. J., C. Barillas-Mury, M. W. Miller, B. Oesch, L. J. M. van Keulen, J. P. M. Langeveld, and E. A. Hoover, Prp(cwd) lymphoid cell targets in early and advanced chronic wasting disease of mule deer., *J Gen Virol*, 83(Pt 10), 2617–2628, 2002.
- Sigurdsson, B., Observation on three slow virus infections of sheep. maedi. paratuberculosis. rida, a chronic encephalitis of sheep with general remarks on infections, which develop slowly, and some of their special characteristics., *British Veterinary Journal*, 110, 225–270, 307–322, 341–354, 1954.
- Silver, D. P., and D. M. Livingston, Self-excising retroviral vectors encoding the cre recombinase overcome cre-mediated cellular toxicity., *Mol Cell*, 8(1), 233–243, 2001.
- Simons, K., and E. Ikonen, Functional rafts in cell membranes., *Nature*, 387(6633), 569–572, 1997.
- Sparkes, R. S., et al., Assignment of the human and mouse prion protein genes to homologous chromosomes., *Proc Natl Acad Sci U S A*, 83(19), 7358–7362, 1986.
- Srinivas, S., T. Watanabe, C. S. Lin, C. M. William, Y. Tanabe, T. M. Jessell, and F. Costantini, Cre reporter strains produced by targeted insertion of eyfp and ecfp into the rosa26 locus., *BMC Dev Biol*, 1, 4, 2001.
- Stahl, N., D. R. Borchelt, K. Hsiao, and S. B. Prusiner, Scrapie prion protein contains a phosphatidylinositol glycolipid., *Cell*, 51(2), 229–240, 1987.
- Steele, A. D., J. G. Emsley, P. H. Ozdinler, S. Lindquist, and J. D. Macklis, Prion protein (prpc) positively regulates neural precursor proliferation during developmental and adult mammalian neurogenesis., *Proc Natl Acad Sci U S A*, 103(9), 3416–3421, 2006.
- Sternberg, N., D. Hamilton, and R. Hoess, Bacteriophage p1 site-specific recombination. ii. recombination between loxp and the bacterial chromosome., *J Mol Biol*, 150(4), 487–507, 1981.
- Summerford, C., and R. J. Samulski, Membrane-associated heparan sulfate proteoglycan is a receptor for adeno-associated virus type 2 virions., *J Virol*, 72(2), 1438–1445, 1998.
- Summerford, C., J. S. Bartlett, and R. J. Samulski, Alphavbeta5 integrin: a co-receptor for adeno-associated virus type 2 infection., *Nat Med*, 5(1), 78–82, 1999.
- Surosky, R. T., M. Urabe, S. G. Godwin, S. A. McQuiston, G. J. Kurtzman, K. Ozawa, and G. Natsoulis, Adeno-associated virus rep proteins target dna sequences to a unique locus in the human genome., *J Virol*, 71(10), 7951–7959, 1997.
- Tateishi, J., T. Kitamoto, M. Z. Hoque, and H. Furukawa, Experimental transmission of creutzfeldt-jakob disease and related diseases to rodents., *Neurology*, 46(2), 532–537, 1996.
- Telling, G. C., M. Scott, J. Mastrianni, R. Gabizon, M. Torchia, F. E. Cohen, S. J. DeArmond, and S. B. Prusiner, Prion propagation in mice expressing human and chimeric prp transgenes implicates the interaction of cellular prp with another protein., *Cell*, 83(1), 79–90, 1995.

- Thaler, J., K. Harrison, K. Sharma, K. Lettieri, J. Kehrl, and S. L. Pfaff, Active suppression of interneuron programs within developing motor neurons revealed by analysis of homeodomain factor hb9., *Neuron*, 23(4), 675–687, 1999.
- Tobler, I., T. Deboer, and M. Fischer, Sleep and sleep regulation in normal and prion protein-deficient mice., *J Neurosci*, 17(5), 1869–1879, 1997.
- Tobler, I., et al., Altered circadian activity rhythms and sleep in mice devoid of prion protein., *Nature*, 380(6575), 639–642, 1996.
- Toupet, K., V. Compan, C. Crozet, C. Mourton-Gilles, N. Mestre-Francés, F. Ibos, P. Corbeau, J.-M. Verdier, and V. Perrier, Effective gene therapy in a mouse model of prion diseases., *PLoS One*, 3(7), e2773, 2008.
- Towbin, H., T. Staehelin, and J. Gordon, Electrophoretic transfer of proteins from polyacrylamide gels to nitrocellulose sheets: procedure and some applications., *Proc Natl Acad Sci U S A*, 76(9), 4350–4354, 1979.
- Tuo, W., K. I. O'Rourke, D. Zhuang, W. P. Cheevers, T. R. Spraker, and D. P. Knowles, Pregnancy status and fetal prion genetics determine prpsc accumulation in placentomes of scrapie-infected sheep., *Proc Natl Acad Sci U S A*, 99(9), 6310–6315, 2002.
- Vey, M., S. Pilkuhn, H. Wille, R. Nixon, S. J. DeArmond, E. J. Smart, R. G. Anderson, A. Taraboulos, and S. B. Prusiner, Subcellular colocalization of the cellular and scrapie prion proteins in caveolae-like membranous domains., *Proc Natl Acad Sci U S A*, 93(25), 14,945–14,949, 1996.
- Voziyanov, Y., S. Pathania, and M. Jayaram, A general model for site-specific recombination by the integrase family recombinases., *Nucleic Acids Res*, 27(4), 930–941, 1999.
- Waggoner, D. J., B. Drisaldi, T. B. Bartnikas, R. L. Casareno, J. R. Prohaska, J. D. Gitlin, and D. A. Harris, Brain copper content and cuproenzyme activity do not vary with prion protein expression level., *J Biol Chem*, 275(11), 7455–7458, 2000.
- Walz, R., O. B. Amaral, I. C. Rockenbach, R. Roesler, I. Izquierdo, E. A. Cavalheiro, V. R. Martins, and R. R. Brentani, Increased sensitivity to seizures in mice lacking cellular prion protein., *Epilepsia*, 40(12), 1679–1682, 1999.
- Wang, Z., H.-I. Ma, J. Li, L. Sun, J. Zhang, and X. Xiao, Rapid and highly efficient transduction by double-stranded adeno-associated virus vectors in vitro and in vivo., *Gene Ther*, 10(26), 2105–2111, 2003.
- Weissmann, C., and E. Flechsig, Prp knock-out and prp transgenic mice in prion research., *Br Med Bull*, 66, 43–60, 2003.
- Wells, G. A., A. C. Scott, C. T. Johnson, R. F. Gunning, R. D. Hancock, M. Jeffrey, M. Dawson, and R. Bradley, A novel progressive spongiform encephalopathy in cattle., *Vet Rec*, 121(18), 419–420, 1987.
- Wells, G. A. H., S. A. C. Hawkins, A. R. Austin, S. J. Ryder, S. H. Done, R. B. Green, I. Dexter, M. Dawson, and R. H. Kimberlin, Studies of the transmissibility of the agent of bovine spongiform encephalopathy to pigs., *J Gen Virol*, 84(Pt 4), 1021–1031, 2003.
- Westaway, D., V. Zuliani, C. M. Cooper, M. D. Costa, S. Neuman, A. L. Jenny, L. Detwiler, and S. B. Prusiner, Homozygosity for prion protein alleles encoding glutamine-171 renders sheep susceptible to natural scrapie., *Genes Dev*, 8(8), 959–969, 1994.
- Westergard, L., H. M. Christensen, and D. A. Harris, The cellular prion protein (prp(c)): its physiological function and role in disease., *Biochim Biophys Acta*, 1772(6), 629–644, 2007.
- White, M. D., and G. R. Mallucci, Rnai for the treatment of prion disease: A window for intervention in neurodegeneration?, *CNS Neurol Disord Drug Targets*, 2009.
- Whittington, M. A., K. C. Sidle, I. Gowland, J. Meads, A. F. Hill, M. S. Palmer, J. G. Jefferys, and J. Collinge, Rescue of neurophysiological phenotype seen in prp null mice by transgene encoding human prion protein., *Nat Genet*, 9(2), 197–201, 1995.
- Wienhues, U., and W. Doerfler, Lack of evidence for methylation of parental and newly synthesized adenovirus type 2 dna in productive infections., *J Virol*, 56(1), 320–324, 1985.

- Wigler, M., R. Sweet, G. K. Sim, B. Wold, A. Pellicer, E. Lacy, T. Maniatis, S. Silverstein, and R. Axel, Transformation of mammalian cells with genes from procaryotes and eucaryotes., *Cell*, 16(4), 777–785, 1979.
- Wilesmith, J. W., G. A. Wells, M. P. Cranwell, and J. B. Ryan, Bovine spongiform encephalopathy: epidemiological studies., *Vet Rec*, 123(25), 638–644, 1988.
- Wilesmith, J. W., J. B. Ryan, and M. J. Atkinson, Bovine spongiform encephalopathy: epidemiological studies on the origin., *Vet Rec*, 128(9), 199–203, 1991.
- Will, R. G., et al., A new variant of creutzfeldt-jakob disease in the uk., *Lancet*, 347(9006), 921–925, 1996.
- Wille, H., M. D. Michelitsch, V. Guenebaut, S. Supattapone, A. Serban, F. E. Cohen, D. A. Agard, and S. B. Prusiner, Structural studies of the scrapie prion protein by electron crystallography., *Proc Natl Acad Sci U S A*, 99(6), 3563–3568, 2002.
- Williams, E. S., and S. Young, Chronic wasting disease of captive mule deer: a spongiform encephalopathy., *J Wildl Dis*, 16(1), 89–98, 1980.
- Windl, O., et al., Genetic basis of creutzfeldt-jakob disease in the united kingdom: a systematic analysis of predisposing mutations and allelic variation in the prnp gene., *Hum Genet*, 98(3), 259–264, 1996.
- Wong, B. S., et al., Increased levels of oxidative stress markers detected in the brains of mice devoid of prion protein., *J Neurochem*, 76(2), 565–572, 2001.
- Woolhouse, M. E., P. Coen, L. Matthews, J. D. Foster, J. M. Elsen, R. M. Lewis, D. T. Haydon, and N. Hunter, A centuries-long epidemic of scrapie in british sheep?, *Trends Microbiol*, 9(2), 67–70, 2001.
- Wopfner, F., G. Weidenhöfer, R. Schneider, A. von Brunn, S. Gilch, T. F. Schwarz, T. Werner, and H. M. Schätzl, Analysis of 27 mammalian and 9 avian prps reveals high conservation of flexible regions of the prion protein., *J Mol Biol*, 289(5), 1163–1178, 1999.
- Wyatt, J. M., G. R. Pearson, T. N. Smerdon, T. J. Gruffydd-Jones, G. A. Wells, and J. W. Wilesmith, Naturally occurring scrapie-like spongiform encephalopathy in five domestic cats., *Vet Rec*, 129(11), 233–236, 1991.
- Yang, X., S. Arber, C. William, L. Li, Y. Tanabe, T. M. Jessell, C. Birchmeier, and S. J. Burden, Patterning of muscle acetylcholine receptor gene expression in the absence of motor innervation., *Neuron*, 30(2), 399–410, 2001.
- Yaworsky, P. J., D. P. Gardner, and C. Kappen, Transgenic analyses reveal developmentally regulated neuron- and muscle-specific elements in the murine neurofilament light chain gene promoter., *J Biol Chem*, 272(40), 25,112–25,120, 1997.
- Yazdanbakhsh, K., P. Fraser, D. Kioussis, M. Vidal, F. Grosveld, and M. Lindenbaum, Functional analysis of the human neurofilament light chain gene promoter., *Nucleic Acids Res*, 21(3), 455–461, 1993.
- Zanata, S. M., et al., Stress-inducible protein 1 is a cell surface ligand for cellular prion that triggers neuroprotection., *EMBO J*, 21(13), 3307–3316, 2002.
- Zeidler, M., et al., New variant creutzfeldt-jakob disease: psychiatric features., *Lancet*, 350(9082), 908–910, 1997a.
- Zeidler, M., et al., New variant creutzfeldt-jakob disease: neurological features and diagnostic tests., *Lancet*, 350(9082), 903–907, 1997b.
- Zhang, C. C., A. D. Steele, S. Lindquist, and H. F. Lodish, Prion protein is expressed on long-term repopulating hematopoietic stem cells and is important for their self-renewal., *Proc Natl Acad Sci U S A*, 103(7), 2184–2189, 2006.
- Zulianello, L., K. Kaneko, M. Scott, S. Erpel, D. Han, F. E. Cohen, and S. B. Prusiner, Dominant-negative inhibition of prion formation diminished by deletion mutagenesis of the prion protein., *J Virol*, 74(9), 4351–4360, 2000.

9 Supplement

9.1 Abbreviations

aa	Amino acid	HSV	Herpes simplex virus
AAV	Adeno-associated virus	i.c.	Intracerebral
Ad	Adeno virus	i.m.	Intramuscular
A β	Alzheimer's peptide	i.n.	Intranerval
β -gal	β -galactosidase	i.p.	Intraperitoneal
BSE	Bovine spongiform encephalopathies	IHC	Immunohistochemistry
CJD	Creutzfeldt-Jakob disease	iCJD	Iatrogenic CJD
CMV	Cytomegalo virus	ITR	Inverted terminal repeat
CNS	Central nervous system	LCR	Locus control region
Cre	Cre-recombinase	LRS	Lymphoreticular system
CTA	Clinical target area	LTP	Long term potentiation
CWD	Chronic wasting disease	MBM	Meat-and-bone-meal
DC	Dendritic cell	MN	Motor neuron
DNA	Deoxyribonucleic acid	n	Number of measurements
dpi	Days post inoculation	N2a	Neuroblastoma cells
ds	Double stranded	neo	Neomycin
E	Embryonic stage	NeuN	Neuronal neuclei
e.g.	for example (Latin: <i>exempli gratia</i>)	NF-L	Neurofilament light chain
ER	Endoplasmatic reticulum	NLS	Nuclear localization signal
FACS	Fluorescence activated cell sorting	NMR	Nuclear magnetic resonance
fCJD	Familiar Creutzfeldt-Jakob disease	NTP	Nucleotide triphosphate
FDC	Follicular dendritic cell	OD	Optical density
FFI	Fatal familiar insomnia	PAGE	Polyacrylamide gel electrophoresis
FSE	Feline spongiform encephalopathies	PCR	Polymerase chain reaction
GALT	Gut-associated lymphoid tissue	PK	Proteinase K
GFAP	Glial fibrillary acidic protein	PMCA	Protein misfolding cyclic amplification
GFP	Green fluorescent protein	PNS	Peripheral nervous system
GPI	Glycophosphatidylinositol anchor	prion	Proteinaceous infectious particles
GSS	Gerstmann-Sträussler-Scheinker syndrome	<i>Prnp</i>	PrP gene
HA	Haemagglutinin tag	PrP	Prion protein
Hb9	Homeobox gene	PrP ^C	cellular form of PrP
HE	Hematoxylin-eosin	PrP ^{Sc}	infectious form of PrP, PrP-scrapie
		PSPr	Protease-sensitive prionopathy
		PVDF	Polyvinylidene difluoride membrane
		qrt	Quantitative real time

HEK	Human embryonic kidney cells	RML	Rocky mountain laboratory
HRP	Horse radish Peroxidase	RNA	Ribonucleic acid
sCJD	Sporadic CJD	TME	Transmissible mink encephalopathies
SD	Standard deviation	trs	Terminal resolution site
SDS	Sodium dodecyl sulfate	TSE	Transmissible spongiform encephalopathies
SOD	Superoxide dismutase	UbiC	Human ubiquitin C promoter
ss	Single stranded	UK	United Kingdom
STE	Stop transfer region	vCJD	Variant CJD
Tg	Trangenic	WFA	Wisteria floribunda agglutinin
TM	Transmembrane sequence		

9.2 Units

SI Base quantity	Name	Symbol	SI base unit
length	meter	m	m
mass	kilogram	kg	kg
time	second	s	s
electric current	ampere	A	A
thermodynamic temperature	kelvin	K	K
amount of substance	mole	mol	mol
luminous intensity	candela	cd	cd
SI Derived quantity			
electric potential difference	volt	V	$\text{m}^2 \text{kg s}^{-3} \text{A}^{-1}$
Celsius temperature	degree Celsius	°C	K
Non SI quantity			
minute		min	1 min = 60 s
hour		h	1 h = 60 min = 3600 s
day		d	1 d = 24 h = 86400 s
liter		L	1 L = 1 dm ⁻³ = 10 ⁻³ m ³
Molarity (concentration)		M (c)	mol L ⁻¹
Mass-volume percentage		% (w/v)	
Volume-volume percentage		% (v/v)	

SI prefixes

Factor	Name	Symbol	Factor	Name	Symbol
10^{24}	yotta	Y	10^{-1}	deci	d
10^{21}	zetta	Z	10^{-2}	centi	c
10^{18}	exa	E	10^{-3}	milli	m
10^{15}	peta	P	10^{-6}	micro	μ
10^{12}	tera	T	10^{-9}	nano	n
10^9	giga	G	10^{-12}	pico	p
10^6	mega	M	10^{-15}	femto	f
10^3	kilo	k	10^{-18}	atto	a
10^2	hecto	h	10^{-21}	zepto	z
10^1	deka	da	10^{-24}	yocto	y

9.3 Resume

Personal Information

Day of birth	16th February 1981 in Melle
Nationality	German
Family status	Unmarried, no children

Dissertation

06/2006 – 09/2009	Institute of Virology and Immunobiology, working group of Prof. Dr. Klein <i>"Cre-loxP based mouse models to study prion pathogenesis in the motor nervous system."</i>
-------------------	--

Diploma thesis

03/2005 – 12/2005	Institute of Biotechnology, University of Würzburg, working group of Prof. Benz and Laboratoire de Chimie de Coordination, Toulouse, working group of Prof. Faller <i>"Interaction of the Alzheimer's Aβ-Peptide with Model Membranes."</i> (Grade: 1.0)
-------------------	--

Course of Studies

10/2000 – 12/2005	Study of Biology, Julius-Maximilians University of Würzburg Main subject: Biotechnology (Grade 1.0) Minor subjects: Organic Chemistry (Grade 1.0) Biochemistry (Grade 1.0)
02/2004 – 07/2004	Participation in the ERASMUS students exchange program at the Paul Sabatier University Toulouse III, France; practical training in the working group of Prof. Faller. <i>"Interaction of the Alzheimer's Aβ-Peptide with Metal Ions (Zn/Cd) and Methallothionein."</i>

Education

07/2000	A-Level at Hoffmann-von-Fallersleben Gymnasium, Germany (Grade: 1.8)
---------	--

9.4 Publications

Mekmouche Y, Coppel Y, Hochgräfe K, Guilloreau L, Talmard C, Mazarguil H, Faller P.

Characterization of the Zn^{II} binding to the peptide amyloid-beta1-16 linked to Alzheimer's disease.

Chembiochem. 2005 Sep; 6(9):1663-71.

Hochgraefe K, Ermolayev V, Rüllicke T, Flechsig E and Klein MA

Conditional transgenic mice carrying dominant-negative PrP in the nervous system display prolonged survival.

submitted to Journal of Neuroscience Research

Ermolayev V, Hochgraefe K, Klein MA and Flechsig E.

Transgenic mice expressing truncated p75NTR receptor demonstrate prolonged incubation time upon intraperitoneal prion challenge.

manuscript in preparation

9.5 Erklärung

Hiermit erkläre ich ehrenwörtlich, dass ich diese Dissertation selbstständig angefertigt und keine anderen als die von mir angegebenen Hilfsmittel und Quellen benutzt habe.

Zudem erkläre ich, dass diese Dissertation weder in gleicher noch in anderer Form bereits in einem Prüfungsverfahren vorgelegen hat.

Ich habe früher, außer den mit dem Zulassungsgesuch urkundlichen Graden, keine weiteren akademischen Grade erworben oder zu erwerben versucht.

Würzburg,

Katja Hochgräfe

9.6 Danksagung

Mein Dank gilt vor allem Prof. Dr. Michael Klein sowie Dr. Eckhard Flechsig für die Vergabe des interessanten Themas, die hervorragende Betreuung sowie für die Unterstützung und Förderung während der gesamten Arbeit.

Ich danke Prof. Dr. Erich Buchner für die Übernahme der Zweitkorrektur.

Dr. Vladimir Ermolayev möchte ich besonders für seine Unterstützung und Hilfe bei sämtlichen Tierexperimenten danken.

Herzlich möchte ich mich auch bei den restlichen, mittlerweile leider ehemaligen Mitgliedern der AG Klein/Flechsig – Julia Merck, Nele Lindner, Angela Bahlo, Jan Springer, Tanja Hoffmann, Patrick Porps und Cindy Nitschke – bedanken. Ihr seid die besten Kollegen, die man sich vorstellen kann und mir auch privat ans Herz gewachsen. Außerdem danke ich allen anderen Kollegen der Virologie Würzburg, die mich vor allem im letzten Jahr meiner Arbeit praktischerweise adoptiert haben.

Außerdem danke ich allen Freunden - besonders den Würzburgern, ohne die die Zeit hier nur halb so schön gewesen wäre.

Einen besonderen Dank möchte ich natürlich meiner Familie und Ingo aussprechen, die mich stets in allem begleitet und unterstützt haben.